Horizon-Layered Cosmology: From Black Hole Gravitational Collapse to Holographic Hierarchies

Anđelko Đermek

Abstract

We present *horizon-layered cosmology*, a theoretical framework that reinterprets black hole gravitational collapse as the origin of an emergent cosmological spacetime. In this model, the classical singularity is replaced by a hierarchy of null-ordered, redshift-frozen matter layers that accumulate causally on the event horizon. Each infalling quantum is holographically encoded at the Planck scale through discrete *causal incorporation* events, rendering the horizon a dynamic information-processing surface governed by a finite causal throughput fixed by gravitational time dilation. Lateral coherence across the horizon sustains a null-synchronized code whose internal holographic projection constitutes an expanding cosmological domain. The interior of the black hole corresponds to a topological causal void bounded by the event horizon, the external manifold's terminal surface, whose continued growth through information incorporation manifests internally as cosmic expansion.

The framework operationalizes the holographic principle and exhibits deep parallels with discrete causal and cellular automaton models of spacetime. Quantized horizon dynamics naturally reproduce the observed cosmic fractions of vacuum, baryonic, and dark matter without invoking an external dark-energy term, yielding an internal cosmic age of about **13.4** Gyr and predicting that the observable Hubble domain contains roughly half of the total internal mass. When the parent black hole possesses angular momentum, Kerr rotation induces an azimuthal phase gradient across the horizon code, generating a small matter–antimatter asymmetry and defining a preferred cosmic axis preserved through inflation. The binary spin structure of Planck-scale horizon quanta provides the geometric basis for fermionic spin-$\frac{1}{2}$ behavior, the Pauli exclusion principle, and the large-scale alignment of CMB and galactic spins, thereby linking quantum spin, baryon asymmetry, and cosmic anisotropy to a single holographic–causal origin.

This work was developed in collaboration with AI tools for linguistic and structural refinement. The theoretical constructs, physical reasoning, and mathematical development are original to the author.

Keywords: black hole; Schwarzschild geometry; holography; cosmology, cellular automaton

1 Introduction

Black holes mark the most profound intersection of general relativity and quantum theory, exposing a persistent tension between geometric determinism and informational completeness. Classically, the collapse of a massive star leads to a singularity enclosed by an event horizon, a surface beyond which no causal signals escape. While mathematically consistent within general relativity, this picture generates deep paradoxes: the fate of information, the physical status of the singularity, and the nature of spacetime regions beyond external causal reach.

Horizon-layered cosmology offers a new interpretation grounded in the external observer's frame. In this view, gravitational time dilation near the Schwarzschild radius halts the apparent infall of matter in external coordinate time. Although the infalling observer crosses the horizon in finite proper time, these two timescales are not independent but represent complementary aspects of one causal structure linked through extreme dilation. From the external frame, the infaller's clock slows without bound; from the infaller's frame, the external universe accelerates without limit. The crossing therefore never truly completes: matter asymptotically approaches the horizon, becoming encoded as successive null layers that evolve only as the black hole itself evolves. The "forward motion" toward the center proceeds in synchrony with the gradual evaporation and contraction of the horizon, so that when the encoded matter reaches the center in its own causal sequence, the external black hole has already evaporated. The event horizon thus functions not as a spatial surface to be crossed, but as a temporally dynamic causal boundary whose null layering defines the joint evolution of the black hole and its internal universe.

Collapse appears, in this picture, not as volumetric contraction toward a singularity but as a surface process of *causal incorporation*: infalling matter and radiation progressively redshift and become null-ordered onto the horizon as discrete, information-bearing strata. The event horizon is elevated from a passive mathematical boundary to an active, Planck-scale encoding surface, a dynamically layered quantum code that holographically generates the internal spacetime.

Since its inception, the holographic principle has been interpreted primarily as an informational bound rather than a physical mechanism. In the early formulations by 't Hooft [1] and Susskind [2], entropy was proposed to scale with boundary area rather than volume. Maldacena's AdS/CFT correspondence [3] provided an exact duality between gravitational and non-gravitational theories, yet left open the dynamical question of how infalling information is physically encoded. Even the membrane paradigm [4], which ascribed viscosity and conductivity to a stretched horizon, remained a heuristic model rather than a microphysical one. Later quantum-informational approaches using error-correction codes and tensor networks [5–7] clarified the algebraic structure of holography but not the causal dynamics of real spacetime encoding.

The horizon-layered model provides precisely this missing dynamical mechanism. Each infalling quantum becomes transcribed into the stretched horizon as a dipolar excitation within a discrete geometric lattice. These *causal incorporation* events occur at the finite information-throughput rate set by gravitational time dilation and the Planck time, establishing a one-to-one correspondence between external infall

and internal time generation. Lateral coherence across the null surface ensures global causal consistency, producing a self-updating, layered membrane that stores the complete history of collapse. The internal universe then emerges as the holographic projection of this evolving boundary state. An icosahedral–dodecahedral quantization of dipoles provides a natural discretization scheme distinguishing baryonic, dark, and vacuum sectors through specific geometric symmetries.

Within this picture, cosmological time is not a pre-existing parameter but a sequence of null-ordered horizon updates. Each incorporation event increases entropy and advances the internal causal order, unifying the arrow of time, entropy growth, and quantum state reduction. Wavefunction collapse corresponds to boundary-state updates, deterministic from the external perspective yet probabilistic internally. The model thus bridges quantum measurement, horizon thermodynamics, and cosmic evolution through a single principle of causal holography.

The resulting cosmology preserves unitarity, removes singularities, and defines an internally expanding universe bounded by the information capacity of the parent black hole. Black holes emerge as recursive, self-contained information systems whose internal spacetimes evolve through horizon-layered dynamics. Relating internal time to the locally measured Hubble constant yields an internal age of approximately 13.4 billion years and predicts that the observable Hubble patch contains roughly 50% of the total internal mass. Cosmic expansion thus results from the growth of holographic boundary area rather than an external dark-energy term, providing a natural resolution of the Hubble tension and a geometric foundation for large-scale structure formation.

A central conceptual advance of the horizon-layered cosmology concerns the very origin of the event horizon itself. From the early Oppenheimer–Snyder collapse models through modern holographic and quantum-gravity formulations, the horizon has been treated as a pre-existing or globally defined boundary enclosing an interior spacetime. In the present framework, this picture is replaced by a local, causal, and dynamically generated process. The event horizon is born at the Planck scale as a minimal quantum-defined seed, the first surface to satisfy the compactness condition, beyond which no classical description of spacetime persists. From this seed, the horizon grows outward through sequential Planck-time incorporations of redshift-frozen matter, each layer advancing the null-ordered causal structure of spacetime itself. The interior does not pre-exist this process but represents a causal excision: a topological void bounded by the expanding holographic surface. Spacetime, in this sense, is constructed from the outside inward, emerging through the continual self-assembly of the horizon's null layers. This *Planck-seed horizon growth* paradigm closes a conceptual gap that has persisted since the earliest collapse models, reinterpreting the event horizon not as the endpoint of gravitational collapse but as the generative frontier of spacetime and information.

When the parent black hole possesses angular momentum, Kerr rotation introduces an azimuthal phase gradient across the horizon code. This global spin field biases co-rotating and counter-rotating quanta, producing a small but cumulative matter–antimatter asymmetry and defining a preferred cosmic axis preserved through inflation. The binary spin structure of Planck-scale horizon quanta yields the geometric origin of fermionic spin-$\frac{1}{2}$ behavior, the Pauli exclusion principle, and large-scale

alignments of cosmic microwave background and galactic spins. Baryon asymmetry, spin quantization, and cosmic anisotropy thereby emerge as unified consequences of a single holographic–causal mechanism operating at the rotating horizon.

Some editorial refinements and structural adjustments were assisted by AI language models (GPT-5, OpenAI). All theoretical constructs, physical reasoning, and mathematical development are original to the author.

Unifying Postulates of the Horizon-Layered Cosmology

Since the advent of general relativity, spacetime and gravitation have been treated as continuous and geometric, while quantum theory has regarded energy and information as discrete and probabilistic. This divide has long obscured a unified view of cosmic evolution and black hole dynamics. The horizon-layered framework reconciles these domains by positing that spacetime geometry emerges from a discrete causal information process operating on null horizons. Just as Einstein's postulates of special relativity redefined motion through the invariance of light speed, the following principles redefine mass, time, and gravity through the invariance of the holographic information bound. They establish a consistent informational foundation from which both relativity and quantum mechanics arise as complementary limits of a deeper causal dynamics.

P1. Causal Horizon Encoding. All physically real information resides on null-synchronized horizons. The event horizon functions as an active, tension-bearing membrane that incorporates infalling energy in discrete Planck-scale steps. Each incorporation updates the universal quantum code and advances causal order by one Planck-time increment, making spacetime itself a record of sequential boundary-state updates.

P2. Emergent Internal Spacetime. The black hole interior is not a pre-existing domain but an emergent, holographically projected volume generated by the ordered layering of information on the horizon. Spacetime geometry, causal structure, and local vacuum properties arise collectively from coherence and correlation patterns within this evolving horizon code.

P3. Information–Mass Equivalence. Information and mass–energy are dual manifestations of a single conserved quantity encoded on the holographic boundary. The total information content scales with the horizon area,

$$I \propto A \propto M^2,$$

so that the growth of mass, area, and encoded information represents one unified causal process. The expansion of the internal universe thus corresponds to the quadratic accumulation of information-energy on the horizon.

P4. Causal Throughput Constraint. Gravitational time dilation near the horizon expresses a universal limit on the rate at which new information can be

incorporated into spacetime. This limit equals the invariant *Planck power*,

$$P_{\max} = \frac{c^5}{G},$$

the maximum causal bandwidth allowed by nature. Each horizon update transmits one Planck mass of energy in one Planck time, defining the finite causal rate of spacetime evolution. Because time dilates asymmetrically across the horizon, external observers perceive collapse as frozen, while internal observers experience this process as the fastest possible progression of physical events. Newton's constant G thus quantifies the causal compliance of spacetime, the conversion efficiency between mass incorporation and geometric reconfiguration.

P5. Informational Zeno Principle. Apparent motion and temporal flow emerge from the interplay of two synchronized processes on the horizon lattice. Each Planck-time update reconfigures the relational geometry of the stationary causal code, extending the lattice radially through the incorporation of new cells while preserving global causal order. Simultaneously, neighboring cells exchange information laterally through null-compatible tunnelling along the horizon surface, maintaining local coherence and enabling the propagation of radiation and interaction. Together, these two operations, global relational remapping and local lateral communication, generate the appearance of continuous motion and temporal evolution within a fundamentally discrete structure. A residual instantaneous equilibration within each tick preserves unitarity and holographic consistency, ensuring that no information is lost or duplicated. Thus, the flow of time, the propagation of light, and the dynamics of matter all arise as emergent patterns within a still but perpetually reconfigured causal network, resolving Zeno's paradox as the sequencing of stationary yet relationally evolving states.

P6. Holographic Completeness. No region of spacetime contains more independent information than permitted by the area of its boundary. Cosmic expansion represents the geometric increase of boundary area required to preserve holographic saturation as new information is incorporated. When this informational equilibrium is maintained, energy, geometry, and causality remain mutually consistent.

P7. Kerr-Induced Causal Orientation. Rotation of the parent black hole imposes a global azimuthal phase gradient across the horizon, characterized by the Kerr parameter

$$a = \frac{J}{m_{\mathrm{bh}} c}.$$

This phase structure breaks local isotropy and establishes a preferred orientation in the causal lattice, coupling the sense of horizon rotation to the handedness of encoded quantum modes. Co-rotating and counter-rotating excitations experience differential redshift and phase bias, generating chiral asymmetries in the internal field correlations. The Kerr-induced phase gradient organizes causal linkages within each horizon layer into a globally coherent chiral pattern, defining a cosmic axis inherited from the parent rotation. Reversing the spin reverses spatial parity and field handedness but leaves causal ordering and entropy growth

unchanged. Thus, rotation unifies microscopic spin orientation and macroscopic anisotropy as manifestations of a single geometric polarity imprinted by the causal structure of the rotating horizon.

P8. Objective Decoherence. Quantum measurement and wavefunction collapse correspond to deterministic boundary updates seen from the external frame but probabilistic transitions within the internal frame. Each update enforces global consistency between internal quantum amplitudes and the new boundary state, rendering decoherence a real physical process rather than a subjective act of observation.

P9. Gravitation as Spacetime Excision. Mass–energy corresponds to localized deficits in causal connectivity across the holographic membrane. Gravitational attraction emerges from the reconfiguration of null-synchronized horizons around these excisions: trajectories curve because spacetime geometry continuously readjusts to restore holographic consistency.

Together these postulates portray the universe as a self-updating causal code. Spacetime, gravitation, quantum coherence, and cosmic evolution are not separate mechanisms but complementary manifestations of one discrete informational process operating at the Planck scale. The classical continuum of general relativity arises as the macroscopic limit of this null-ordered, holographic computation.

The model thus unites gravitation, thermodynamics, and quantum theory within a single principle of causal incorporation, offering a coherent alternative to both singular classical cosmology and purely probabilistic quantum ontology.
In the following sections, we develop the theoretical basis of this framework beginning from the Schwarzschild solution and the contrasting perspectives of the external and infalling observers. By reexamining gravitational time dilation, redshift, and horizon formation, we replace the classical notion of matter crossing an event horizon with a physically discrete process of causal incorporation. The event horizon thereby becomes a real, information-bearing surface through which the holographic principle attains concrete dynamical expression. This shift transforms the horizon from a mathematical boundary into a physically active encoding interface that generates, layer by layer, the internal spacetime of the emergent universe.

2 Schwarzschild Black Hole

2.1 Current Black Hole Theories

The classical theory of gravitational collapse derives from the prediction of general relativity that sufficiently massive stars, once they have exhausted all pressure support, inevitably experience a continuous contraction. In classical general relativity, the Schwarzschild solution extended to radius $r = 0$ implies a singularity [8]. Infalling matter in its frame of reference crosses the horizon in a finite time, but the time required for any particle of a collapsing star to reach the event horizon for a distant external observer diverges to infinity due to gravitational time dilation. Nevertheless, the generally accepted understanding is that the particle *„must clearly pass to a smaller radius unless it is destroyed... Since we have already decided that... particles*

reach the horizon at finite proper time and encounter a perfectly well-behaved geometry there" [9]. To justify this, a special coordinate systems have been invented, such as the Kruskal-Szekeres coordinate system, which mathematically removes the singularity at Schwarzschild radius, suggesting a smooth crossing of the event horizon [9]. The Kruskal-Szekeres coordinate system reparameterizes the trajectory to be finite in T/R coordinates, but an external observer clock tied to Schwarzschild time still sees the particle asymptotically approaching the event horizon, never crossing it in a finite time. The ability to extend the geodesic system inside event horizon is mathematically elegant but irrelevant to physics that should be based only on what is possible to observe.

Contrary to the belief of crossing the event horizon in a finite time, all observable quantities such as photons or gravitational waves reach external observers in Schwarzschild time with redshift and dilation of time that diverges to infinity. The time dilation of the general theory of relativity has been empirically confirmed, as demonstrated by experiments such as the Hafele-Keating experiment [10], GPS correction [11], experiments with an atomic clock [12]. However, currently accepted theories reject measurable phenomena such as time dilation observed in the reference system of an external observer as a coordinate effect. Measurements confirm the physical reality of time dilation, supporting its application in models of gravitational collapse and black hole event horizons. The physical reality of the event horizon is indicated by the entropy of the black hole because Bekenstein-Hawking formula shows that it depends on the area of the event horizon, not the interior volume [13]. Additionally, Hawking radiation [14] suggests a slow loss of information and gradual black hole evaporation.

2.2 Radial Free Fall

In Schwarzschild geometry, the motion of falling objects towards the event horizon is determined by radial, temporal and angular metric components [15]. The Schwarzschild equation for a non-rotating, uncharged black hole of mass M, expressed in geometric units ($G = c = 1$), is:

$$ds^2 = -\left(1 - \frac{2M}{r}\right) dt^2 + \left(1 - \frac{2M}{r}\right)^{-1} dr^2 + r^2 \left(d\theta^2 + \sin^2\theta \, d\phi^2\right) \tag{1}$$

Although the radial and time components diverge as the object approaches the event horizon located at $r_s = 2M$, the angular part of the metric remains active. This asymmetry between the radial and angular behavior near the event horizon is a key observation that supports the central argument of this paper and will be revisited in the following sections.

Let us now examine the behavior of a freely falling object [15]. For an observer falling radially starting from rest at a large radius r_0, the proper time elapsed as the object falls towards the radius r is given by:

$$\tau - \tau_0 = \frac{2}{3\sqrt{2M}} \left(r_0^{3/2} - r^{3/2}\right) \tag{2}$$

In contrast, a distant observer measures the corresponding Schwarzschild coordinate time interval as:

$$t - t_0 = -\frac{2}{3\sqrt{2M}}\left[r^{3/2} - r_0^{3/2} + 6M(\sqrt{r} - \sqrt{r_0})\right] + 2M \ln\left(\frac{(\sqrt{r} + \sqrt{2M})(\sqrt{r_0} - \sqrt{2M})}{(\sqrt{r_0} + \sqrt{2M})(\sqrt{r} - \sqrt{2M})}\right) \tag{3}$$

Near the event horizon, where $r = 2M + u$ and $u \ll 2M$, the logarithmic term in Equation (3) diverges to infinity due to the denominator approaching zero as $\sqrt{r} \to \sqrt{2M}$. By defining $u = r - 2M$, we can approximate this term as:

$$\sqrt{r} - \sqrt{2M} \approx \frac{u}{2\sqrt{2M}} \tag{4}$$

This divergence indicates that from the perspective of a distant observer, an object falling into a black hole cannot cross the event horizon in a finite coordinate time. However, for an observer falling into a black hole, the time it takes to cross the event horizon remains finite. This difference between observers in the external and internal reference systems constitutes a fundamental paradox of black hole physics and motivates the need to revise the current causal-geometric interpretation.

In Schwarzschild geometry near the event horizon, where $r = 2M+u$ and $u \ll 2M$, the radial length is:

$$ds = \frac{dr}{\sqrt{1 - \frac{2M}{r}}} \approx \sqrt{\frac{2M}{u}}\, dr \tag{5}$$

For a body of fixed proper length in the radial direction equal to l_0, the corresponding coordinate radial length Δr is shortened according to the formula:

$$l_0 \approx \sqrt{\frac{2M}{u}}\,\Delta r \quad \Rightarrow \quad \Delta r \approx l_0\sqrt{\frac{u}{2M}} \tag{6}$$

Consider the case in which the corresponding radial distance from the horizon is halved: $u_2 = u_1/2$. Then:

$$\frac{\Delta r_2}{\Delta r_1} = \sqrt{\frac{u_2}{u_1}} = \frac{\sqrt{2}}{2} \tag{7}$$

So, as $r \to 2M$, the radial length Δr measured by a distant observer is shortened proportionally to $\sqrt{u}$ diverging to zero. This contraction is independent of the black hole mass M.

Let us derive a formula for the Schwarzschild coordinate time interval Δt that measures a distant observer when a falling particle falls from u_1 to u_2. From the geodesic equations [16], the radial coordinate velocity of a freely falling particle near the horizon is:

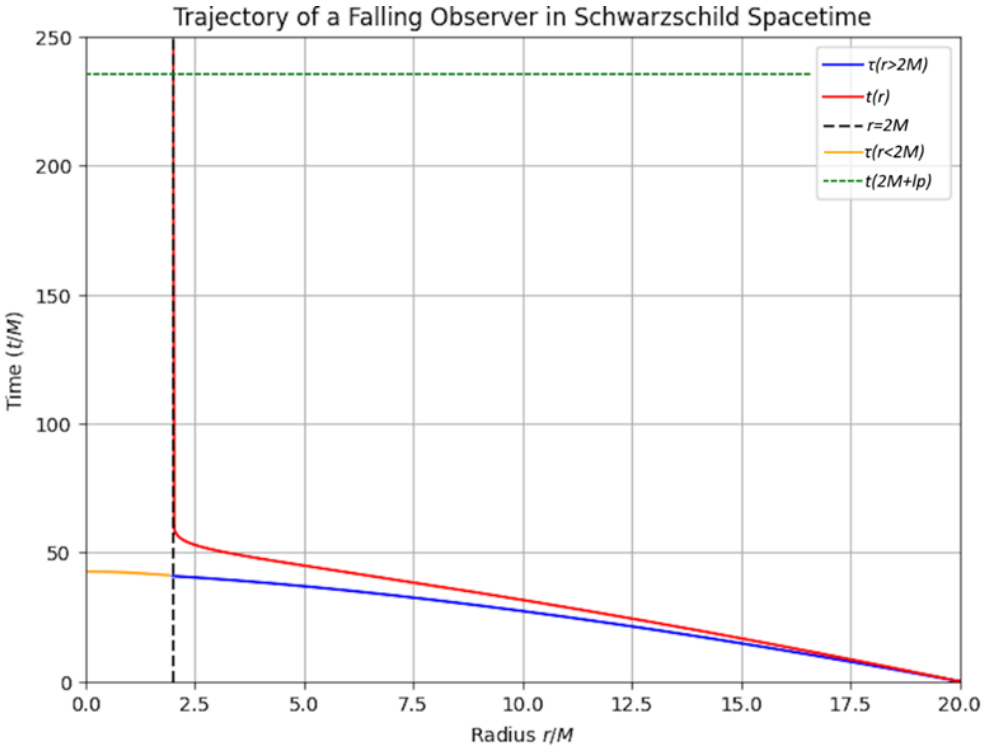

Fig. 1 The trajectory of a radially infalling observer in Schwarzschild spacetime plotted in terms of both proper time τ (equation (2)) and Schwarzschild coordinate time t (equation (3)). Both trajectories begin at $r_0 = 20M$, with $t_0 = \tau_0 = 0$. The orange segment represents a hypothetical continuation of the proper time trajectory past the horizon. The green line indicates the coordinate time at which the infaller reaches a Planck-length distance from the horizon. Adapted from [15].

$$\frac{dr}{dt} = -\sqrt{\frac{2M}{r}}\left(1 - \frac{2M}{r}\right) \approx -\frac{u}{2M} \quad \Rightarrow \quad \frac{du}{dt} \approx -\frac{u}{2M} \tag{8}$$

Integrating both sides:

$$\int_{u_1}^{u_2} \frac{du}{u} = -\frac{1}{2M}\int_{t_1}^{t_2} dt \quad \Rightarrow \quad \ln\left(\frac{u_2}{u_1}\right) = -\frac{\Delta t}{2M} \tag{9}$$

For a halving of the radial distance, $u_2 = u_1/2$, the result becomes as follows:

$$\Delta t = 2M \cdot \ln\left(\frac{u_1}{u_2}\right) = 2M \cdot \ln 2 \tag{10}$$

This implies $\Delta t \propto M$, with concrete values as follows:

$$M = 100 M_\odot \quad (M \approx 1.48 \times 10^5\,\mathrm{m}): \quad \Delta t \approx 682.6\,\mu\mathrm{s} \tag{11}$$

$$M = 1M_\odot \quad (M \approx 1.48 \times 10^3\,\mathrm{m}): \quad \Delta t \approx 6.826\,\mu\mathrm{s} \tag{12}$$

Thus, the Schwarzschild coordinate time required for a fixed fractional displacement u, such as halving the radial distance to the horizon, scales linearly with the black hole mass M. This is an expression of the logarithmic divergence that occurs near the horizon in all Schwarzschild geometries.

This behavior is exactly analogous to Zeno's paradox: *"That which is in locomotion must arrive at the half-way stage before it arrives at the goal"* [17]. An infinite number of halvings, each requiring a fixed interval of coordinate time, implies an unattainable limit, suggesting that, from an external perspective, the crossing of the event horizon is never actually completed.

However, the total time experienced by a falling observer, as given by equation (2), remains finite. **The steep divergence of the coordinate time in equation (3) occurs only within an extremely narrow range just before the horizon, at a distance much smaller than the Planck length.** This means that, viewed from an external reference frame, the entire stellar mass effectively reaches one Planck length above the horizon relatively quickly, although it never crosses it.(Fig. 1).

2.3 External Observer versus Infalling Observer Experience

Let us compare the experience of a particle falling towards the center of a black hole with that of an external stationary observer.

From the perspective of an external observer, according to equation (3) the particle approaches the horizon asymptotically and cannot reach it in finite coordinate time t, not even after billions of years. An extreme redshift occurs, and gravitational length contraction compresses the particle's radial length. This well-known divergence is more than a coordinate artifact, it is a physically significant manifestation of gravitational time dilation, confirmed by numerous experimental results. Moreover, when the black hole finally evaporates, the particle will still be floating at an infinitesimal distance above the then vanishing horizon.

From the point of view of a falling particle system, classical general relativity predicts a smooth crossing of the horizon in finite proper time τ. However, this classical picture must be revised if horizon thermodynamics and gravitational time dilation are to be taken seriously. Near the horizon, the relationship between the proper time of the falling particle and the coordinate time of the distant observer is the following:

$$\frac{d\tau}{dt} = \sqrt{1 - \frac{2M}{r}} \to 0 \quad \text{as} \quad r \to 2M \tag{13}$$

The standard interpretation treats this relationship as a coordinate singularity, assuming that proper time and coordinate time can decouple and that the particle crosses the horizon smoothly. In the present model, we reject that decoupling: equation (13) enforces a causal synchronization between t and τ and expresses an exact coupling between the two clocks: the local proper time cannot advance independently of the global coordinate time. If the external coordinate time has not reached infinity, then the proper time cannot advance beyond the horizon, meaning that $r(\tau) < r_s$

is physically disallowed. **The relation $dt/d\tau$ is a causal synchronization law, not just a coordinate mapping.** This means that **the falling particle's own clock becomes infinitely slow relative to the clock of a distant observer. Near the horizon, in the reference frame of the falling particle, all external processes appear to accelerate, and the whole history of the cosmos for a falling observer occurs in a tiny fraction of a second.**

Consider a black hole evaporating via Hawking radiation in finite coordinate time $t_{\text{evap}} < \infty$. In this period the geometry of the black hole evolves, so it grows if matter continues to fall onto it, but eventually the event horizon starts to shrink, and after a huge time interval it disappears. The falling particle cannot cross the horizon even in its own reference frame before the horizon disappears. **The classical event horizon always retreats faster than the infalling observer can cross it.** For example, a fall to an almost infinitesimally small distance above the horizon takes only a fraction of a second of its own proper time according to equation (2), while in the distant frame it takes billions of years. During this brief interval, the particle is exposed to a beam of high-energy Hawking radiation associated with the horizon. Instead of entering the hidden interior, the particle either evaporates at the edge of the horizon or eventually encounters a flat spacetime when the black hole evaporates completely. Thus, the classical horizon at $r_s = 2M$ never manifests itself as a traversable surface in any physical system. This imposes a global time constraint on any world line that tries to cross the horizon. In this framework, the proper time for the falling particle is constrained by the global causal structure of the Hawking evaporation geometry.

A growing body of work suggests that classical singularity may never form in a physically meaningful sense when quantum effects are properly accounted for. In particular, the concept of horizon avoidance posits that due to Hawking radiation and backreaction, the would-be event horizon evaporates faster than any infalling observer can cross it, effectively preventing the formation of a traversable boundary [18]. Alternative models such as gravastars and firewall scenarios also challenge the standard picture by proposing radical modifications to the interior structure or near-horizon quantum state [6, 19]. In a more conservative but consistent approach, semiclassical treatments like the Ashtekar-Bojowald and Vaidya-based models preserve unitarity while eliminating singularities through quantum gravitational effects that modify the collapse geometry from the outset [20, 21]. These insights align with the present framework, in which the horizon is not a surface to be crossed, but a dynamically encoded null-layer beyond which classical spacetime ceases to exist as an ontological manifold.

The implication is profound: **in the entire observable universe no particle has actually ever crossed the event horizon. All falling matter, whether seen by external or internal observers, remains just above the horizon until it is supposedly annihilated by Hawking radiation.**

3 Event Horizon

3.1 Event Horizon Formation

From the earliest collapse models of Oppenheimer and Snyder (1939) to modern numerical simulations and holographic formulations, **the formation of the event**

horizon has generally been treated as a global, teleological construct. In these approaches, the horizon is defined as the causal surface separating null geodesics that eventually escape from those that do not, an object identified only after the entire spacetime evolution is known. Even in semiclassical extensions such as the membrane paradigm, loop quantum gravity, or AdS/CFT duality, the event horizon is typically regarded as a pre-existing geometric feature enclosing an evolving interior. Nowhere in these frameworks is the horizon treated as a dynamically nucleated boundary with a physically realized beginning. In contrast, the horizon-layered model regards horizon formation as a *local and causal process*, a sequence of null-surface nucleations beginning at the Planck scale and expanding outward.

In classical general relativity, the compactness condition for the formation of a local Schwarzschild horizon is

$$\frac{2Gm(r)}{rc^2} \geq 1, \tag{14}$$

where $m(r)$ is the mass contained within radius r. Using the mean density

$$\langle \rho(r) \rangle = \frac{3m(r)}{4\pi r^3}, \tag{15}$$

the same condition may be written as a lower bound on average energy density [22]:

$$\langle \rho(r) \rangle \geq \frac{3c^2}{8\pi G r^2}. \tag{16}$$

This inequality shows that the required density increases steeply as r decreases, suggesting that horizon formation proceeds from smaller to larger radii.

Numerical simulations confirm this trend: only a fraction (typically 5–25%) of the total mass lies within the initially formed horizon [23–25], while the rest falls in later as the horizon expands. **Hence, the event horizon does not appear instantaneously at its final radius but grows dynamically outward from a compact central seed.**

To formalize this causal requirement, define the local compactness function

$$f(r) = \frac{2Gm(r)}{rc^2}, \tag{17}$$

where $m(r)$ is given by

$$m(r) = 4\pi \int_0^r \rho(r)\, r^2 dr, \tag{18}$$

which is monotonic for any nonnegative density $\rho(r) \geq 0$. The formation of a horizon at radius R requires

$$f(R) \geq 1. \tag{19}$$

Assume, for contradiction, that $f(r) < 1$ for all $r < R$ but $f(R) = 1$; that is, the compactness first reaches unity at the outer boundary. Differentiating $f(r)$ gives

$$f'(r) = \frac{2G}{c^2}\left(4\pi r\,\rho(r) - \frac{m(r)}{r^2}\right). \tag{20}$$

For $f(r)$ to increase from below 1 to 1 within a narrow shell $[R-\varepsilon,\, R]$, $f'(r)$ must be sharply positive near R. Integrating Eq. (20) over this shell yields

$$1 - f(R-\varepsilon) = \int_{R-\varepsilon}^{R} f'(r)\,dr \approx \frac{8\pi GR}{c^2}\int_{R-\varepsilon}^{R} \rho(r)\,dr, \tag{21}$$

where the finite term $-m(r)/r^2$ contributes negligibly. Since $1 - f(R-\varepsilon)$ remains finite as $\varepsilon \to 0$, the integral of $\rho(r)$ must also remain finite, forcing the average density in the shell to diverge:

$$\frac{1}{\varepsilon}\int_{R-\varepsilon}^{R} \rho(r)\,dr \;\to\; \infty. \tag{22}$$

Therefore, a first crossing of $f(r) = 1$ at large R requires a delta-like divergence in the density profile, which is physically inadmissible.

Alternatively, using the identity

$$\frac{d}{dr}\left(\frac{m(r)}{r}\right) = 4\pi r\rho(r) - \frac{m(r)}{r^2}, \tag{23}$$

it follows that a large positive derivative near R demands a strong local spike in $\rho(r)$. A smooth density profile cannot satisfy this condition, confirming that $f(r)$ must first reach unity at some smaller radius.

This result has direct physical implications. If most of the mass resided in an outer shell while the interior mass $m(r < R)$ were small, the shell would experience only a weak gravitational pull:

$$a(R) \approx -\frac{Gm(R_{\text{inner}})}{R^2}, \tag{24}$$

and could not collapse inward to form a horizon. Maintaining such a configuration would require an unphysical external pressure gradient. Hence, **the sudden appearance of a horizon at a large radius without prior inner formation is dynamically forbidden.**

The event horizon must therefore form first at the smallest radius where the compactness condition is locally satisfied, i.e. at the Planck scale. As the core density approaches the Planck limit, a minimal trapped region nucleates, forming the initial horizon seed. Subsequent accretion increases $m(r)$, extending the horizon outward in a series of causally nested surfaces. The event horizon is thus not a static, pre-defined surface but a dynamically realized boundary that grows outward layer by layer from a quantum–gravitational core.

This causal nesting of event horizon surfaces, starting from the smallest radii, leads to a well-defined initial radius: the formation of a minimal core that satisfies the

Schwarzschild condition on the Planck scale. As matter continues to collapse inward, gravitational contraction inexorably increases the local density until the inequality (14) is satisfied at the smallest possible physical scale. This occurs when the Planck mass m_p is confined within a radius $r \sim \ell_p$, forming a Planck sized Schwarzschild region. At that point, the classical description of spacetime ceases to hold, and quantum gravitational effects become dominant. The formation of this dense core on the Planck scale marks the beginning of a fundamentally new regime of evolution governed by the quantum geometry of the layered horizon.

Rather than being a problem for collapse, the Planck density acts as a critical threshold at which quantum gravitational effects replace classical dynamics. As collapse progresses, gravitational contraction increases the density of the core. Instead of this contraction continuing toward a classical singularity, the collapse stops at the limit defined by the Planck density:

$$\rho_{\mathrm{p}} = \frac{m_p}{\frac{4}{3}\pi r_p^3} \sim 5.1 \cdot 10^{96}\ \mathrm{kg/m}^3. \tag{25}$$

At this scale, the classical equations of motion no longer hold, and quantum gravitational corrections dominate. **The result is not a singularity, but a minimal black hole, a seed with Planck density around which the event horizon begins to grow. This initial core forms the boundary between classical collapse and a new phase governed by the accumulation of layers of matter with redshift just above the event horizon.**

Subsequent accretion no longer compresses the core, but deposits matter on the outer layers of the horizon. The Planck density therefore marks not an end, but a transition point: from volumetric compression to quantum encoding of the event horizon surface.

Thus, the horizon-layered model introduced here closes the classical conceptual gap by reinterpreting black hole formation as a causal, discrete, and locally generated process. This reinterpretation naturally resolves the singularity problem. The interior of the black hole is not formed by compression into a geometric point, but the event horizon dynamically grows outwards starting from the Planck core. Once the core is formed at the Planck scale, it acts as a gravitational surface attracting infalling matter.

This leads to a profound implication: **all black holes, regardless of their final size, start from a Planck seed.** Macroscopic horizons are structures formed by cumulative growth due to the accretion of matter. This layered growth ensures compliance with causal structure, quantum consistency, and the Bekenstein-Hawking entropy limit. It also rules out singularities by prohibiting further compression beyond the Planck density.

As the event horizon of a black hole begins to grow outward from the Planck size, a natural question arises: **what is the ontological status of the growing inner volume? In contrast to the classical intuition, where the event horizon encloses a pre-existing region of spacetime, this model suggests that the inner volume is causally excluded from the start. While the event horizon**

surface grows from the Planck size to macroscopic size, the inner volume does not participate in this process.

This view leads to a striking departure from classical intuition: the interior of the black hole does not pre-exist the horizon but emerges as a consequence of the horizon's layered growth. In the classical picture, the event horizon encloses an already-formed interior spacetime. But in the horizon layered framework developed here, the horizon acts as a null surface of projection, a redshift-frozen layer whose outermost geometry encodes all accessible information. As the horizon grows outward from the Planck core, it defines the emergence of new spacetime layers, but the interior volume remains causally inaccessible from the exterior and is not part of the dynamically evolving external manifold.

From this perspective, **the so-called "interior" is not an independently evolving region of spacetime, but an emergent construct entirely defined by the information encoded on the growing horizon.**

The implication is profound: spacetime inside the black hole is not ontologically fundamental. Instead, it is a dynamically generated structure that arises from the causal and geometric ordering of horizon layers. The singularity is thus avoided not by smoothing out infinite curvature, but by reinterpreting the notion of interior entirely. **There is no singular point, because there is no spacetime beyond the event horizon, only the null-layered horizon code just above the event horizon that seeds the emergent causal bulk.** The classical notion of an evolving 3D volume inside the black hole becomes replaced by a holographic code layered at the boundary, with the apparent bulk dynamics reconstructed through null-ordered updates from this encoding surface.

3.2 Reinterpreting Hawking Radiation

In the classical description, an infalling particle inevitably crosses the event horizon and proceeds into the interior of the black hole. In the present framework, however, this passage does not occur. Instead, the infalling particle becomes part of a radially compressed, redshift-frozen quantum structure accumulating just above the horizon. From the external viewpoint, the horizon is never reached in finite time; it functions as a limiting surface where information becomes causally frozen and holographically encoded.

With this recognition, the standard interpretation of Hawking radiation must be reconsidered. The familiar picture of pair creation across a geometric boundary separating interior and exterior presupposes that the interior region possesses an independent ontological status within the external manifold. Yet in the horizon-layered framework, such an interior does not exist. The external spacetime terminates at the event horizon, which forms the manifold's causal boundary. Infalling matter does not cross into a hidden domain but becomes progressively encoded within the horizon's null-ordered structure.

Accordingly, Hawking radiation cannot arise from quantum tunneling between an existing interior and exterior. The emission process should instead be understood as a structured quantum polarization effect emerging from the redshift-frozen quantum field near the horizon. This field remains external to the event horizon but is subject to

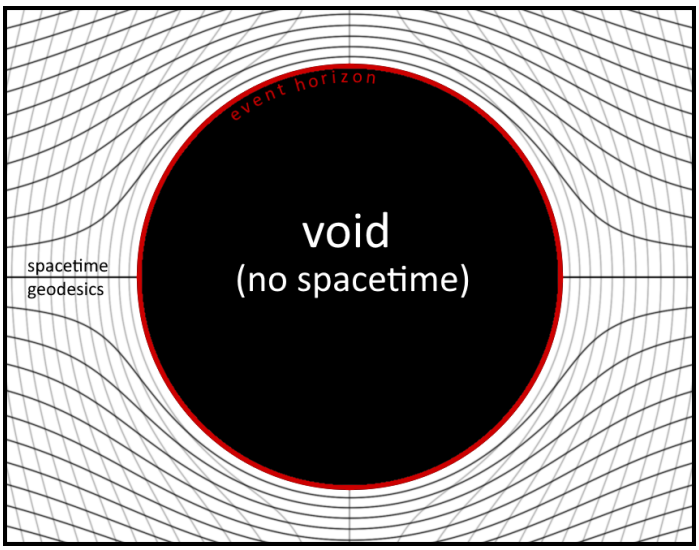

Fig. 2 Spacetime geodesics curve around a Schwarzschild black hole in this model much like streamlines in a compressible fluid flow bend around an obstacle. This behavior arises not from an embedded central mass, but from the topological excision of spacetime at the black hole interior. The event horizon marks the null surface beyond which no causal structure or geometry persists. Only geodesics orthogonal to the horizon terminate at this boundary; all others bend due to the elastic curvature induced by the absence of interior spacetime. The horizon acts as a holographic encoding surface for the excised region, consistent with entropy bounds and causal structure.

extreme time dilation and gravitational redshift. Infalling quanta continually perturb this layer, inducing minute changes in the local vacuum polarization and generating outward-propagating excitations. Because these excitations originate in the external domain, they can, in principle, escape to infinity, albeit with exponentially redshifted energy and stretched timescales. The resulting radiation therefore represents a coherent, causal rebalancing of the horizon's encoded information, not a stochastic flux of particles tunneling out of a hidden interior.

This mechanism naturally accounts for the observed thermal spectrum: photons emitted from the outermost redshift-frozen layer escape with energy

$$E_\infty = E_{\text{local}} \sqrt{1 - \frac{2Gm_{\text{bh}}}{rc^2}},$$

yielding an effective Hawking temperature

$$T_H = \frac{\hbar c^3}{8\pi G m_{\text{bh}} k_B},$$

which reflects the gravitational redshift rather than any actual emission from within the horizon. The black hole thus radiates, but only through processes occurring on the external manifold, within the redshift-frozen quantum layer that encodes infalling information.

Once the external manifold is recognized to end at the horizon, the notion of radiation directed "inward" or "outward" across the causal boundary loses physical meaning. The interior domain, being topologically and causally excised, provides no spacetime structure into which or from which particles could tunnel. The idea of inward or outward tunneling is therefore not merely improbable but undefined. In this sense, the standard mechanism of Hawking evaporation cannot be realized within a manifold that terminates at its own causal boundary.

This reinterpretation resolves the information paradox without invoking true evaporation. Information is never lost in an inaccessible region beyond the horizon; it remains encoded in the dynamic surface structure of the horizon itself. Apparent "evaporation" corresponds to the gradual reconfiguration or release of this holographic code, not to the destruction of matter within an interior volume. The process is consistent with unitarity, causality, and holography, and eliminates the need for a physically existing interior.

Ultimately, crossing the horizon is not a physical process but a classical extrapolation that fails under extreme redshift and quantum gravitational conditions. **The event horizon is not an entrance but the terminal surface of spacetime itself, a dynamic, null-ordered boundary where information is encoded. It defines the outer limit of the physical manifold, not the boundary of a hidden interior world.**

3.3 Reinterpretation of Mass and Spacetime

In classical general relativity, gravitational collapse leads to a singularity, an infinite-density locus of diverging curvature, under the assumptions of the Penrose–Hawking theorems [26]. These results presuppose a smooth manifold and standard energy conditions, with curvature sourced by stress–energy via

$$R_{\mu\nu} - \tfrac{1}{2} g_{\mu\nu} R \;=\; \frac{8\pi G}{c^4}\, T_{\mu\nu}. \tag{26}$$

In the horizon-layered, holographic picture advanced here, curvature is reinterpreted as the deformation of spacetime around what is *absent*. Mass corresponds to a topological *excision*, a finite, non-singular causal deficit in which the manifold fails to extend. These microexcisions bend geodesics not by inclusion but by exclusion, much like streamlines in a compressible flow curving around an obstacle (Fig. 2). Gravity is the elastic response of the manifold to this controlled absence of geometry.

Accordingly, the black hole event horizon is the terminal null boundary of the external manifold: beyond it no spacetime, field, or observer exists. Hawking radiation originates from quantum fluctuations just *outside* this causal edge; no interior dynamics are required. The classical singularity is thus replaced by a finite termination of geometry: curvature records the tension induced by the excised region rather than any divergent interior structure.

This viewpoint aligns naturally with the holographic principle. The Bekenstein–Hawking law,

$$S = \frac{k_B c^3}{4\hbar G} A, \tag{27}$$

implies that gravitational information resides on causal *surfaces*, not within volumes. In this setting, the energy–momentum tensor $T_{\mu\nu}$ is read as encoding both conventional stress–energy and the geometric strain required to maintain curvature around excised domains; Newton's constant G quantifies the manifold's resistance to such topological truncation. Curvature at the boundary thus corresponds to an entropy (information) deficit relative to a flat, unexcised geometry.

Because each mass quantum is defined by an absence of spacetime, such excised domains cannot coherently overlap into a singular point. There is no interior volume available to collapse; the singularity is *precluded* rather than regularized.

With the interior excised, the horizon is sustained entirely by the external geometry. The exterior metric imposes an inward geometric pressure on the horizon shell through the curvature jump at the manifold's terminus, but causal structure forbids completion beyond the null limit, fixing the shell at the physical boundary of spacetime. Phenomenologically, the equilibrium of this domain wall can be captured by a Young–Laplace–type balance,

$$\Pi_{\text{ext}} = 2\,\sigma\,H + \Pi_{\text{q}}, \tag{28}$$

where Π_{ext} is the inward curvature-induced pressure, σ an effective surface tension, H the mean curvature, and Π_{q} quantum/entanglement-pressure corrections. The term $2\sigma H$ represents the geometric resistance to deformation, ensuring equilibrium precisely at the null termination where no interior spacetime exists.

In this sense, **the event horizon is a self-consistent fixed point of the external manifold: a geometric equilibrium between excision and curvature, where gravity emerges as the tension field surrounding the absence of spacetime.**

This approach differs fundamentally from other non-singular models - Planck stars, gravastars, firewall proposals, and fuzzballs [6, 27–33], which typically retain an interior region or require exotic stress-energy conditions. In contrast, here the interior is a projection: spacetime ends at the horizon, and what lies "within" is a relational construct arising from entangled null-layer encoding rather than a curved geometric manifold.

Despite this re-interpretation, **all external predictions of general relativity are preserved. Gravitational waves, inspiral dynamics, and ringdown emissions occur outside the horizon, governed by standard field equations. The difference lies solely in the unobservable domain, offering a geometrically and informationally consistent picture of gravity and black hole thermodynamics.**

In this framework, the Planck mass,

$$m_p = \sqrt{\frac{\hbar c}{G}}, \tag{29}$$

acquires direct geometric meaning: it marks the transition between partial and complete excision. Below m_p, quantum matter remains embedded in spacetime; above it, the excision self-closes and a black hole forms. Mass hierarchy thus measures the degree of causal removal, while energy acts as the propagating strain restoring local manifold continuity at light speed. The equivalence $E = mc^2$ expresses this duality between static excision and dynamic curvature restoration.

A mass quantum thus corresponds to a topological discontinuity in the causal lattice, characterized by a finite causal charge, the degree of deficit in null connectivity.

Ordinary (baryonic) matter can be viewed as a bipolar, causal dipole: one pole remains connected to the surrounding spacetime network, while the other is excised. The connected side anchors the particle to the local causal web, ensuring interaction with radiation and other gauge fields; the excised side constitutes its gravitational charge, curving the external manifold through the induced causal asymmetry. This dipolar structure naturally explains why mass gravitates universally while still participating in electromagnetic and quantum interactions: its connected pole supports field couplings, while its disconnected pole anchors curvature.

Dark matter represents the limiting case of full causal excision: both poles of the dipole are disconnected from the manifold's causal substrate. The object exists only as a residual gravitational influence, a shadow of missing connectivity in the manifold's fabric. Because both poles are causally removed, dark matter interacts neither electromagnetically nor via standard quantum fields, it is causally *neutral* except through geometry. Its only signature is curvature itself, the elastic imprint left by absence. This view provides a geometric rationale for the otherwise puzzling invisibility of dark matter, situating it as a pure causal deficit without active field degrees of freedom.

Conversely, the massless sector, radiation and conformally invariant fields, corresponds to quanta with both causal poles fully connected. Such entities do not produce curvature because they represent no deficit of connectivity; they traverse the manifold without excising any portion of it. Their propagation along null geodesics reflects perfect causal continuity, and thus zero rest mass. In this sense, the absence of mass coincides with complete participation in the causal network: photons and other massless excitations *are* the coherence of spacetime.

The vacuum represents the complementary extreme: the *decoherent* phase of the causal network. Whereas matter, dark matter, and radiation embody coherent configurations of the causal code, locally phase-locked excitations that maintain stable relational structure, the vacuum consists of causally uncorrelated degrees of freedom. Its quanta correspond to *empty causal capacity*: the spacetime elements that are not phase-synchronized with the coherent code but are available to host it. Those quanta fluctuations reproduce the phenomenology of vacuum fluctuations in quantum field theory: transient excitations

appear and disappear without locking into stable causal connections. In this sense, vacuum quanta are *de-synchronized*, furnishing the neutral substrate through which coherent configurations can propagate.

3.4 Singularity as Holographic Inconsistency

Classical general relativity treats the event horizon of a black hole as a fictive geometric boundary beyond which physical quantities may diverge. The interior singularity, characterized by infinite curvature and vanishing volume, is considered a real endpoint of spacetime evolution. However, this treatment is incompatible with the holographic principle, which asserts that the physical degrees of freedom of a gravitational system are fully encoded on its bounding surface with entropy proportional to area, not volume.

If the singularity were a physical object, it would permit the accumulation of unbounded entropy and curvature within a region that contributes nothing to the total area-based entropy budget. In standard treatments, the holographic limit is applied to the event horizon of a black hole. In the framework proposed here, however, **the holographic bound must hold for *any volume* encapsulating matter-energy, including regions containing the singularity.** Consequently, a singularity would violate this bound by concentrating information density beyond the allowed limit in an otherwise negligible volume. This contradicts the Bekenstein–Hawking entropy limit and the covariant entropy bound [34], which restrict the maximal entropy to

$$S_{\max} = \frac{A}{4\ell_p^2}, \tag{30}$$

where A is the surface area enclosing the region. Allowing a singularity therefore undermines unitarity and the self-consistency of quantum gravity in any physically meaningful volume.

In the horizon-layered cosmological model, this inconsistency is resolved by excluding the interior volume from the causal structure. **The event horizon is not a fictive boundary but a physically operative, null-ordered, information-bearing surface that encodes infalling matter in Planck-scale strata.** The classical singularity is replaced by a dynamically expanding code surface whose entropy is finite and precisely saturates the holographic bound ensuring that all physical degrees of freedom are accounted for at the horizon and that no information is hidden behind a spacelike singularity.

This reformulation preserves unitarity, maintains the validity of entropy bounds, and aligns with holographic expectations. The singularity, in this view, is not a physical endpoint but a breakdown of classical reasoning beyond its applicable domain. The true physical content lies in the quantum encoding at the horizon, from which time, matter, and geometry emerge.

The holographic bound is more fundamental than the dynamical predictions of classical general relativity. Any apparent violation of the entropy bound, such as the occurrence of singularities predicted by the Penrose–Hawking singularity theorems, must be resolved by a transition in the holographic encoding of information.

Thus, when gravitational collapse drives a system toward saturation of the holographic limit, the singularity is replaced by a new phase of spacetime description, such as horizon-layered encoding or cosmological emergence.

On a holographic surface, regions of high curvature that would classically evolve toward singularities instead manifest as punctures in the holographic screen. Each puncture projects a recursively defined internal spacetime, encoded holographically, but without requiring the physical presence of a singular volume. Through this mechanism, singularities never form; they are replaced by successive layers of holographic encoding, preserving the information bound.

The present model enforces the holographic bound globally: **no spacetime volume may contain more information than permitted by the area of its boundary**. This extension restores unitarity and ensures the continuity of the information measure across all nested surfaces. The Planck-scale holographic horizon dynamically enforces this condition by transcribing infalling matter into surface quanta once their approach distance reaches the Planck threshold. Thus, while ordinary physics remains valid in the low-curvature limit, its local consistency is superseded by a globally consistent holographic mechanism that prevents singularity formation and reconciles gravitational collapse with quantum information conservation.

3.5 Horizon Layering, Null Ordering, and Angular Dynamics

The external gravitational field of a black hole characterized by its global parameters: mass, angular momentum, and charge does not determine the internal content. On the other hand, the detailed microstructure of the event horizon does not change the external field, but this surface holographically encodes the internal degrees of freedom, preserves the entropy of the black hole, and ensures compatibility with unitarity and the laws of thermodynamics. Accordingly, gravity and curvature arise from the causal absence of the internal volume, while the information defining the internal universe is nonlocally organized on the horizon, structured as a null-ordered gauge-invariant code subspace.

From the perspective of a distant observer, gravitationally collapsing matter asymptotically approaches the Schwarzschild radius in infinite coordinate time. As it approaches this limit, the infalling matter becomes increasingly time-dilated and redshifted, effectively freezing just before the event horizon (Fig. 3). **To describe this emerging structure, we introduced the concept of null-ordered layered accretion: a causal sequence of layers organized along lightlike null hypersurfaces, surfaces of constant advanced or retarded time. Each layer in this construction encodes a moment in the history of the collapse as it is embedded in the horizon surface, forming a geometrically ordered sequence that preserves the causal hierarchy.** In this regime, the proper time of each infalling layer is effectively stopped with respect to the external frame of reference. Once the Planck scale is reached, the redshift divergence triggers the encoding of the null surface. From that point on, the holographically coded inner spacetime disconnects from the parent cosmos and is projecting its own microcosm as a relational construct, encoded on the horizon in its causal surface structure.

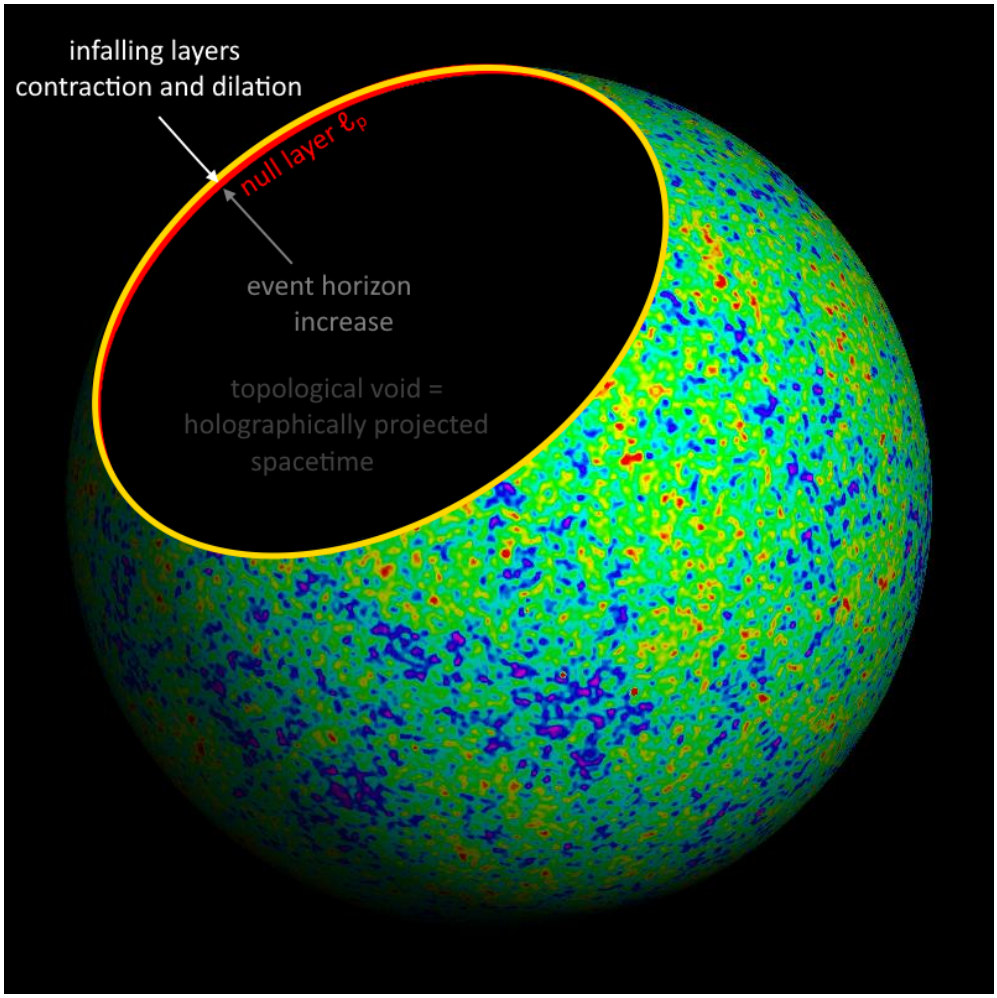

Fig. 3 Schematic representation of black hole gravitational collapse at a causal distance of ℓ_p above the event horizon. As infalling mass increases, the horizon expands, creating a redshift-based foliation of layers which subsequently are encoded into null-layer. Internal spacetime exists only as a holographic projection.

This becomes possible because **the relativistic length contraction compresses the falling matter into thinner and thinner layers in the radial direction. These layers flatten towards the horizon, becoming effectively two-dimensional (equation 7). Thus, the dynamics of the gravitational collapse naturally realize the Bekenstein-Hawking area law for entropy (equation 27).** This reduction of 3-dimensional falling particles to a two-dimensional informational surface is a feature of the holographic principle, in which the maximum entropy of a region is proportional to the area of its boundary, not its volume. The event horizon therefore acts not as a transition point to an unobservable interior,

but as a null surface in which quantum coding processes take place. Incoming matter is absorbed into causally ordered informational layers, with each redshifted arrival encoded sequentially.

This structure follows directly from the Schwarzschild metric. The redshift factor extracted from the Schwarzschild line element according to equation (1) (given in geometric units $G = c = 1$) we can define as:

$$g_{tt} = -\Big(1 - \frac{r_s}{r}\Big), \qquad d\tau = \sqrt{-g_{tt}}\, dt, \tag{31}$$

so that a local proper frequency $\omega_{\rm loc}$ is perceived at infinity as

$$\omega_\infty = \sqrt{-g_{tt}}\, \omega_{\rm loc}. \tag{32}$$

For a near-radial null trajectory,

$$\frac{dr}{dt} = \pm\Big(1 - \frac{r_s}{r}\Big), \tag{33}$$

and thus $dr/dt \to 0$ as $r \to r_s$. **Radial motion is therefore *frozen* with respect to the external coordinate time t; any degree of freedom requiring motion in r becomes infinitely time-dilated and effectively static to the distant observer.**

At fixed r, a null angular displacement satisfies

$$0 = ds^2 = -\Big(1 - \frac{r_s}{r}\Big)dt^2 + r^2 d\Omega^2, \qquad d\Omega^2 = d\theta^2 + \sin^2\theta\, d\phi^2, \tag{34}$$

giving the coordinate angular rate

$$\frac{d\Omega}{dt} = \frac{\sqrt{1 - r_s/r}}{r}. \tag{35}$$

Exactly at $r = r_s$ this vanishes, but on a *stretched horizon* located at $r = r_s + \epsilon$, with $\epsilon \sim \mathcal{O}(\ell_{\rm p})$, one finds

$$\frac{d\Omega}{dt} = \sqrt{\frac{\epsilon}{r_s + \epsilon}} > 0. \tag{36}$$

The radial components vanish linearly in the redshift factor, while tangential components vanish only as a square root. Hence radial motion freezes much more rapidly, whereas tangential (lateral) evolution, though redshifted, remains kinematically accessible with respect to the external time t. **These residual lateral degrees of freedom populate the constant-r horizon surface, supporting null propagation along it. Because their suppression is only of order $\sqrt{\ell_{\rm p}/r_s}$, these modes persist indefinitely, forming a stable substrate for coherent excitations, information exchange, and holographic storage. The emergent universe arises precisely from the persistence of these lateral dynamics on the "living surface" of the horizon.**

Thus, although the radial component becomes frozen near the horizon due to the redshift factor $\sqrt{1 - r_s/r} \to 0$, the angular component $r^2 d\Omega^2 = r^2(d\theta^2 + \sin^2\theta\, d\phi^2)$ remains kinematically active. Near the horizon, the effective time evolution seen from the external frame becomes entirely determined by lateral propagation across the surface. These angular modes tangential to the horizon sphere serve as physical channels through which information is stored, ordered, and projected holographically.

Internally it appears that each Planck-scale horizon cell can transmit information at any finite solid angle from 0 to 2π. For a spherical horizon of radius $r_{\rm s}$, the total number of causal cells is $N_{\rm cells} = 4\pi r_{\rm s}^2/\ell_{\rm p}^2$, and since the total solid angle of a sphere is 4π, the minimal resolvable angular element per cell is

$$\Delta\Omega_{\rm min} = \frac{4\pi}{N_{\rm cells}} = \frac{\ell_{\rm p}^2}{r_{\rm s}^2}, \qquad \Delta\theta_{\rm min} \sim \frac{\ell_{\rm p}}{r_{\rm s}}.$$

The factor 4π ensures proper normalization over the full solid angle of the spherical horizon, so that the discrete angular cells collectively tile the entire causal surface.

Thus, directional propagation is fundamentally discrete: information can be transmitted only along a finite number of angular channels. However, as the universe expands and $r_{\rm s}$ grows, the number of available angular modes increases as $r_{\rm s}^2$, rendering the discreteness observationally indistinguishable from a continuum. The apparent smoothness of angular propagation across spacetime is therefore an emergent property of the holographic lattice, an effective continuum arising from an underlying network of discrete causal directions.

3.6 Planck-Step Horizon Synchronization

Gravitational collapse halts at the Planck redshift limit, where further infall is converted into surface information rather than volumetric compression. At this threshold, the incoming information is encoded into horizon-localized degrees of freedom, angular momentum eigenmodes, quantum fluctuations, and spin-network links that together form the black hole's holographic code. The interior of the black hole is not a separately realized spacetime region but an emergent, holographically projected volume reconstructed from the ordered surface encoding. Although the internal volume scales with $r_{\rm s}^3$, its causal and informational genesis arises entirely from the dynamically stratified horizon surface. We now examine how this layered expansion proceeds.

The Schwarzschild radius of a black hole of mass $m_{\rm bh}$ is

$$r_{\rm s} = \frac{2G\, m_{\rm bh}}{c^2}, \tag{37}$$

so that a small mass increment $\Delta m_{\rm bh}$ changes the radius by

$$\Delta r_{\rm s} = \frac{2G\, \Delta m_{\rm bh}}{c^2}. \tag{38}$$

For $\Delta m_{\rm bh} = m_{\rm p}$ (one Planck mass),

$$\Delta r_{\rm s} = 2\,\ell_{\rm p}. \tag{39}$$

Each Planck-mass incorporation thus extends the horizon by two Planck lengths, forming a lightlike null layer of thickness $2\ell_{\rm p}$**.** In the horizon-layered cosmology, such a layer constitutes the smallest discrete reconfiguration of spacetime geometry, one global update of the holographic code.

The Planck quantities form a synchronized triplet,

$$m_{\rm p} = \sqrt{\frac{\hbar c}{G}}, \qquad \ell_{\rm p} = \sqrt{\frac{\hbar G}{c^3}}, \qquad t_{\rm p} = \frac{\ell_{\rm p}}{c},$$

linked by the identity

$$\frac{G m_{\rm p}^2}{\ell_{\rm p}} = m_{\rm p} c^2 = \frac{\hbar}{t_{\rm p}}.$$

At this scale, gravitational self-energy, quantum uncertainty, and relativistic causality coincide, defining the smallest self-localized excitation compatible with both general relativity and quantum mechanics. The synchronized triplet

$$(\Delta m,\, \Delta r,\, \Delta t) = (m_{\rm p},\, 2\ell_{\rm p},\, t_{\rm p})$$

represents the minimal causal act of horizon growth.

Each Planck-step transfers one Planck energy within one Planck time, corresponding to the universal causal power limit,

$$P_{\rm max} = \frac{E_{\rm p}}{t_{\rm p}} = \frac{c^5}{G}. \tag{40}$$

Numerically, $P_{\rm max} \approx 3.63 \times 10^{52}$ W, the absolute causal throughput of nature. **The event horizon operates precisely at this limit: one Planck energy per Planck time per global tick.**

When a collapsing core first attains the Planck density and accumulates one Planck mass within a Planck-scale region, this causal power limit is reached. At that instant, continuous classical collapse transitions to discrete causal incorporation. A black hole forms, and its horizon begins to grow through sequential Planck-step updates. This process marks the activation of the Planck-scale information channel.

Differentiating $r_{\rm s} = 2G\,m_{\rm bh}/c^2$ gives

$$\frac{dr_{\rm s}}{dm_{\rm bh}} = \frac{2G}{c^2}.$$

Setting $\Delta r_{\rm s} = 2\ell_{\rm p}$ yields

$$\Delta m_{\rm bh} = \frac{c^2}{2G}\,\Delta r_{\rm s} = m_{\rm p},$$

showing that each causal update represents a discrete yet globally coherent rhythm of incorporation.

The corresponding area change is

$$\Delta A = 16\pi r_{\rm s}\,\ell_{\rm p}, \qquad \frac{\Delta A}{\ell_{\rm p}^2} = 16\pi\,\frac{r_{\rm s}}{\ell_{\rm p}},$$

so every Planck step generates an entire spherical null shell of new boundary cells. Expressed directly in terms of $m_{\rm bh}$,

$$A = \frac{16\pi G^2 m_{\rm bh}^2}{c^4}, \qquad \frac{dA}{dm_{\rm bh}} = \frac{32\pi G^2 m_{\rm bh}}{c^4},$$

giving

$$\frac{\Delta A}{\ell_{\rm p}^2} = 32\pi\,\frac{m_{\rm bh}}{m_{\rm p}}, \qquad \frac{\Delta A/\ell_{\rm p}^2}{A/\ell_{\rm p}^2} = \frac{2m_{\rm p}}{m_{\rm bh}}.$$

For stellar-mass black holes, each Planck-step reconfigures roughly 10^{40} Planck-area cells while changing the total area by an infinitesimal fraction, macroscopic smoothness emerging from microscopic discreteness.

Each Planck incorporation thus represents a global logical update of the holographic code: a $2\ell_{\rm p}$ radial expansion, a $t_{\rm p}$ causal advancement, and the assimilation of one Planck mass of information–energy at the causal power limit c^5/G. From this discrete condition,

$$\frac{m_{\rm p}c^2}{t_{\rm p}} = \frac{c^5}{G},$$

one obtains the operational expression for Newton's constant,

$$G = \frac{c^3 t_{\rm p}}{m_{\rm p}},$$

where G quantifies the efficiency with which spacetime reconfigures in response to discrete energy–information influx at the causal limit. It acts as the conversion factor between energetic input and geometric response, the *causal compliance* of spacetime.

The same mechanism that limits the horizon's growth rate at $P_{\rm max} = c^5/G$ also governs how energy is encoded into structure. According to the holographic principle [1, 2], the total information within any causal domain is proportional to its boundary area:

$$I_{\rm max} = \frac{A}{4\,\ell_{\rm p}^2}. \tag{41}$$

In the present framework, this relation is not merely a bound but an equality dynamically maintained by successive Planck-scale incorporations. Each null layer reaching the horizon increases its area and information capacity, expanding the internal spacetime encoded by the surface.

Using

$$r_{\rm s} = \frac{2Gm_{\rm bh}}{c^2}, \qquad A = 4\pi r_{\rm s}^2 = 16\pi\,\frac{G^2 m_{\rm bh}^2}{c^4}, \tag{42}$$

Eq. (41) becomes

$$I = 4\pi\left(\frac{Gm_{\rm bh}^2}{\hbar c}\right) = 4\pi\left(\frac{m_{\rm bh}}{m_{\rm p}}\right)^2, \tag{43}$$

showing that total information scales quadratically with mass, $I \propto m_{\rm bh}^2$. Differentiating gives

$$\frac{dI}{dm} = 8\pi\,\frac{m_{\rm bh}}{m_{\rm p}^2}, \tag{44}$$

and for $\Delta m = m_{\rm p}$,

$$\Delta I_{\rm p} = 8\pi\,\frac{m_{\rm bh}}{m_{\rm p}}, \tag{45}$$

showing that each subsequent incorporation adds proportionally more information as the horizon grows.

The same scaling applies to entropy via the Bekenstein–Hawking relation,

$$S_{\rm bh} = 4\pi k_{\rm B}\left(\frac{m_{\rm bh}}{m_{\rm p}}\right)^2, \tag{46}$$

yielding an incremental entropy gain

$$\Delta S_{\rm p} = 8\pi k_{\rm B}\frac{m_{\rm bh}}{m_{\rm p}}. \tag{47}$$

The equality of coefficients in I and $S_{\rm bh}$ reflects their shared geometric origin: both arise from the same discrete area increments $\Delta A \propto m_{\rm bh}$.

In this framework, mass, entropy, and information are unified as complementary expressions of a single causal process, the sequential incorporation of null layers at the Planck-scale bandwidth $P_{\rm max} = c^5/G$. Each step increases $m_{\rm bh}$, A, S, and I in lockstep, maintaining exact holographic saturation,

$$S \propto I \propto A \propto m_{\rm bh}^2, \qquad \Delta S, \Delta I \propto m_{\rm bh}.$$

The universe thus evolves through discrete yet cumulative increments of encoded information, ensuring that the holographic bound remains exactly saturated throughout its history. This model thereby realizes the bulk–boundary duality of holography, provides a causal mechanism for black-hole growth without singularities, and preserves unitarity by encoding all information on the evolving horizon.

3.7 Planck-Mass Incorporation Throttling

As infalling matter approaches the stretched horizon at $r = 2M(t) + \ell_{\rm p}$, gravitational redshift and time dilation stratify it into a hierarchy of causally ordered null surfaces. Each stratum corresponds to a discrete incorporation event that expands the horizon

radius by $2\ell_{\rm p}$ and holographically encodes the newly created interior shell volume. Because successive incorporations encompass ever larger spherical envelopes, the internal volume grows in a quantized yet monotonic sequence, and temporal directionality emerges from the ordered succession of these causal incorporations. This mechanism parallels causal set theory, where spacetime is treated as a discrete, ordered set of fundamental events [35].

Each Planck-mass incorporation represents a *global causal update* of the horizon code. We model the stretched horizon as an active assimilation band of width $2\ell_p$, composed of an outer intake sublayer and an inner code-bearing sublayer, each of width ℓ_p. The stretched horizon functions as a finite quantum information surface composed of Planck-area dipolar units that encode both matter and vacuum degrees of freedom. When an infalling quantum reaches this surface, its classical trajectory terminates and its information becomes holographically re-expressed within the horizon's entangled state.

The horizon cannot incorporate information arbitrarily fast: the maximum rate is one Planck-mass equivalent per external Planck tick. Excess infalling flux therefore accumulates as a redshift-frozen queue, producing the appearance of asymptotic freezing in external coordinates. The instantaneous causal queue length,

$$Q(t) = N_{\rm infall}(t) - N_{\rm inc}(t), \tag{48}$$

quantifies the degree of local time dilation. As $Q(t)$ increases, external observers perceive infall as increasingly slow, even though the internal dynamics proceed in proper causal time.

When a queued layer completely reaches the incorporation threshold, the outer intake sublayer, the horizon executes a unitary update,

$$\Psi_{\mathcal{M}}(t_{n+1}) = \mathcal{U}_n \, \Psi_{\mathcal{M}}(t_n), \tag{49}$$

corresponding to a horizon-wide reconfiguration of the quantum code. Each such event creates approximately

$$N_{\rm eff} \;\sim\; \frac{dA}{\ell_{\rm p}^2} \;=\; 32\pi \, \frac{m_{\rm bh}}{m_{\rm p}}$$

new Planck-area cells, which for a solar-mass black hole corresponds to $N_{\rm eff} \sim 10^{40}$. The resulting entropy increase far exceeds one bit per tick, confirming that each incorporation event is a macroscopic, horizon-wide update rather than a microscopic addition.

Each Planck-mass incorporation advances internal time by one Planck tick,

$$t_{\rm int} = N_{\rm inc} \, t_{\rm p}, \tag{50}$$

representing a discrete synchronization of causal order. If accretion halts, $N_{\rm inc} \to 0$, internal time ceases to advance, and the emergent universe becomes causally static.

Externally, the black hole's mass-energy increases by roughly $m_{\rm p}c^2$ per incorporation, yet the associated energy is delocalized across many correlated cells. Each adjusts

its curvature and entanglement phase to maintain the global scaling $A \propto M^2$. Rapid lateral equilibration redistributes the incorporated energy, restoring local coherence through the horizon's dipolar correlation network.

Let $\tau_{\rm coh}$ denote the local equilibration time and $\Delta\tau_{\rm inc}$ the mean interval between incorporations, both measured in the horizon's proper frame. For coherent domain formation, interactions must complete before the next incorporation,

$$\tau_{\rm coh} \ll \Delta\tau_{\rm inc}. \tag{51}$$

If multiple quanta are absorbed within one coherence interval, domains cannot stabilize; when $\Delta\tau_{\rm inc}$ is long or equilibration rapid, lateral ordering occurs efficiently. Consequently, the horizon can only incorporate one Planck-mass quantum at a time.

To analyze the apparent tension between the redshifted external view and the horizon's intrinsic dynamics, it is essential to distinguish their time parameters.

The first is t: the *external* (parent-universe) Schwarzschild coordinate time;
The second is $\tau_{\rm loc}$: the *local proper time* on the stretched horizon at $r = r_s+\epsilon$:

$$d\tau_{\rm loc} = \sqrt{1 - \frac{r_s}{r_s + \epsilon}}\, dt;$$

The third is $t_{\rm internal}$: the *internal emergent time*, defined by null-ordered Planck incorporation ticks, in the ideal case equal to $\tau_{\rm loc}$ for observers within the holographic projection.

A tangential null displacement with $dr = 0$ satisfies equation (34), leading to

$$\frac{d\Omega}{dt} = \frac{\sqrt{1 - r_s/r}}{r}. \tag{52}$$

Converting to local proper time yields

$$\frac{d\Omega}{d\tau_{\rm loc}} = \frac{(d\Omega/dt)}{(d\tau_{\rm loc}/dt)} = \frac{\dfrac{\sqrt{1 - r_s/r}}{r}}{\sqrt{1 - r_s/r}} = \frac{1}{r}. \tag{53}$$

Thus a local observer measures a tangential speed

$$v_\perp = r\,\frac{d\Omega}{d\tau_{\rm loc}} = 1, \tag{54}$$

corresponding to lightlike propagation along the horizon. Restoring physical units gives:

$$v_\perp = c \tag{55}$$

Therefore, although a distant observer perceives extreme slowing ($d\Omega/dt \ll 1$), local and internal observers always measure lateral signal propagation at the full light speed c.

Because the internal clock t_{internal} is defined operationally by the sequence of Planck-scale incorporation events, it cannot outpace τ_{loc}. Each incorporation quantum reconfigures the entire horizon, producing a discrete update of internal causal order. Lateral signal propagation and field reorganization proceed at the internal light speed between successive incorporations, maintaining causal consistency and isotropy within the emergent universe.

In external coordinates, all these processes appear exponentially time-dilated by the near-horizon redshift factor $\sqrt{1 - r_s/(r_s + \epsilon)}$. Internally, however, they remain dynamically active and self-consistent. The apparent freezing of infall is therefore not a geometric singularity but a manifestation of *informational throttling*: the finite causal bandwidth limits the rate of horizon reconfiguration.

This mechanism replaces the classical picture of continuous metric dilation with a *discrete causal throttling* of information flow. Horizon growth becomes a locally causal, information-driven process: the boundary expands only when infalling information has been fully assimilated into the holographic code. The sequential, bandwidth-limited incorporation of Planck-scale layers thus generates the flow of internal time, the growth of mass and entropy, and the progressive deepening of curvature, three aspects of one unified, null-ordered process that defines the emergent universe's temporal and thermodynamic evolution.

Relativistic jets observed in active galactic nuclei (AGN) and microquasars are conventionally attributed to magnetohydrodynamic extraction of rotational energy from the Kerr black hole through the Blandford–Znajek process [36–38]. However, within the causal-incorporation framework, the emergence of such jets can be reinterpreted as a direct consequence of the finite information-processing capacity of the horizon's null-synchronized code. In this model, the event horizon admits new quanta only up to a maximal incorporation rate defined by the causal bandwidth of the membrane. When the inflow of mass-energy exceeds this rate, the horizon cannot instantaneously assimilate the full accreting flux. The excess information-energy must then be expelled along dynamically permissible channels, typically guided by open magnetic field lines threading the poles. **Jets thus appear as a macroscopic manifestation of a *causal overflow process*, where the horizon preserves null-order coherence by redirecting unassimilated energy into magnetically collimated outflows.**

The critical accretion rate can be expressed as a function of the fundamental incorporation bandwidth and the coherence time of each incorporated quantum:

$$\dot{M}_{\text{crit}} \sim \frac{m_{\text{p}}}{\tau_{\text{coh}}}, \tag{56}$$

where m_{p} is the Planck mass and τ_{coh} represents the characteristic coherence time of horizon-incorporation quanta. For an ideal, maximally coherent membrane, $\tau_{\text{coh}} = t_{\text{p}}$ yields the upper causal incorporation limit; for real, spin-coupled horizons, longer coherence times reduce the effective incorporation rate, leading to partial causal exclusion and jet formation. This introduces a natural feedback mechanism: accretion rates exceeding $\dot{M}_{\text{crit}}$ trigger causal overflow, while subcritical inflows are fully absorbed and incorporated into the membrane code without ejection.

In this view, the presence, strength, and intermittency of relativistic jets are not merely by-products of magnetohydrodynamic coupling but fundamental signatures of the causal incorporation limit. The horizon acts as a finite-bandwidth information regulator, maintaining global unitarity through selective ejection of excess flux. Jet luminosity, directionality, and variability therefore encode direct information about the dynamic mismatch between external accretion rates and the internal quantum coherence capacity of the membrane.

3.8 Relativity of Planck Scales Across Holographic Hierarchies

In a universe generated holographically from the horizon of a parent black hole, the fundamental Planck quantities remain internally self-consistent yet become *relational* between hierarchical levels of spacetime. Each universe possesses its own locally defined Planck mass, length, time, and energy, which satisfy the standard causal coupling

$$m_{\rm p} = \sqrt{\frac{\hbar c}{G}}, \qquad \ell_{\rm p} = \sqrt{\frac{\hbar G}{c^3}}, \qquad t_{\rm p} = \frac{\ell_{\rm p}}{c}, \qquad E_{\rm p} = m_{\rm p} c^2.$$

These relations express the universal balance between quantum uncertainty, relativistic causality, and gravitational self-energy. However, **when one universe emerges as the internal domain of another, the mapping between their proper times introduces an effective redshift of all Planck quantities.**

From the perspective of the parent universe, infalling matter asymptotically freezes near the event horizon due to infinite gravitational time dilation, while the interior of the forming black hole evolves in its own causal time frame. The relationship between the external coordinate time t and the emergent internal time $t_{\rm internal}$ satisfies

$$\frac{dt_{\rm internal}}{dt} \ll 1,$$

implying that internal processes appear extremely slowed or redshifted when viewed from the parent spacetime. Consequently, the *effective Planck time* of the child universe is longer than that of the parent,

$$t_{\rm p}^{internal} = (1 + z_{\rm h})\, t_{\rm p},$$

where $z_{\rm h}$ denotes the redshift associated with the horizon transition. Because the Planck energy is inversely proportional to the Planck time, $E_{\rm p} = \hbar / t_{\rm p}$, the corresponding Planck energy of the child universe is smaller by the same factor,

$$E_{\rm p}^{internal} = \frac{E_{\rm p}}{1 + z_{\rm h}}.$$

This scaling preserves the invariant causal throughput of spacetime,

$$\frac{E_{\rm p}}{t_{\rm p}} = \frac{c^5}{G},$$

which defines the maximum causal power or information flux that any horizon can sustain. Thus, although the numerical values of the Planck units differ across hierarchical levels, their ratios remain constant, maintaining dimensional self-consistency throughout the multiverse structure.

In the horizon-layered cosmology, the redshift between successive horizons therefore induces a *hierarchy of effective Planck scales*. Each child universe operates at a correspondingly lower energy density and longer causal tick, while preserving the same fundamental causal power c^5/G. This hierarchy ensures that the causal bandwidth of spacetime remains finite at every level, and that the apparent energy scales of emergent universes decrease systematically as information becomes increasingly redshifted across generations.

The relativity of Planck scales across horizons thus provides a natural explanation for why the internal Planck energy of our universe is vastly lower than that of its parent domain. The entire causal structure of the child universe emerges as a redshifted projection of the parent's Planck process, preserving the universal coupling of G, $\hbar$, and c while allowing each universe to experience its own proper causal rhythm.

3.9 Time as the Order of Horizon Code Configurations

Following the causal queueing principle introduced above, we may now express time in a precise and operational sense. **Time is not a pre-existing background coordinate but an emergent *order parameter* of horizon code configurations.** Each configuration Σ_i represents a complete, self-consistent encoding of matter, geometry, and causal relations at a given null layer of the stretched horizon. The passage of time corresponds to the discrete succession of these configurations, ordered by the causal incorporation of new layer quanta at the maximal holographic rate:

$$t_{\text{internal}} \;\equiv\; \mathcal{O}(\{\Sigma_1, \Sigma_2, \Sigma_3, \dots\}), \tag{57}$$

where the ordering $\mathcal{O}$ follows the null sequence of successful incorporations permitted by the horizon's finite processing bandwidth $(1/t_{\text{p}})$.

Each infalling layer, once admitted through the causal queue, triggers a global horizon reconfiguration, updating the entire holographic code through lateral entanglement redistribution and dipole realignment. This holistic reorganization defines one fundamental tick of internal time. The process is deterministic at the code level, governed by local and gauge-invariant update rules, yet its outcomes appear probabilistic when viewed through coarse-grained bulk variables, naturally accounting for quantum uncertainty as informational incompleteness within each discrete update.

Externally, infalling quanta follow null trajectories characterized by constant advanced time $v = t + r_*$, where $r_* = r + r_s \ln|r/r_s - 1|$ is the tortoise coordinate. Each increment in v corresponds to the arrival and successful incorporation of one additional null layer at the horizon, marking a discrete code update. Thus, internal time remains causally synchronized with the external advanced time,

$$t_{\text{internal}} = N\, t_{\text{p}} \quad\longleftrightarrow\quad v = v_0 + N\, \delta v_{\text{p}}, \tag{58}$$

where N counts the number of layers successfully incorporated from the causal queue, and δv_{p} denotes the advanced-time interval associated with one Planck-scale horizon update.

The cumulative internal time is proportional to the number N of incorporated quanta with $N = m_{\mathrm{bh}}/m_p$ (where m_{bh} is black hole mass in kilograms and $t_p/m_p = G/c^3$). Therefore:

$$\boxed{t_{\mathrm{internal}} = \frac{G m_{\mathrm{bh}}}{c^3}}, \tag{59}$$

internal cosmic time is the discrete accumulation of successfully incorporated mass–energy quanta.

Equivalently, internal time may be written using the black hole mass in geometric units (with $M_{\mathrm{bh}} = G m_{\mathrm{bh}}/c^2$):

$$\boxed{t_{\mathrm{internal}} = \frac{M_{\mathrm{bh}}}{c}}. \tag{60}$$

When accretion ceases, the horizon mass becomes constant and the sequence of code updates halts. Internal time stops, not by collapse or singularity, but by informational quiescence. When accretion resumes, time reactivates seamlessly: the internal universe continues from its last encoded state, unaware of any external delay. Thus, internal observers experience continuous temporal flow, while their clock remains causally bound to the parent universe's advanced-time sequence.

In this view, each Planck-mass incorporation produces a global, horizon-wide reconfiguration, an emergent "tick" of cosmic time that unifies gravitational growth, entropy increase, and causal continuity within a single holographic process.

4 Holographic Membrane

The holographic horizon surface can be understood as a dynamic membrane of Planck-scale thickness, where infalling matter is not transmitted into a classical volume but is instead transcribed onto a null-ordered encoding. Each unit of mass is represented as a topological excitation with one causal face coupled to the external geometry and one disconnected face projecting an excluded region that drives gravitational attraction. Under extreme time dilation and redshift, baryonic particles effectively freeze at a Planck-length offset above the Schwarzschild radius, transforming their volumetric description into surface-based quanta aligned radially on the horizon. To sustain holographic correlations, these quanta communicate laterally across the horizon sphere, establishing entanglement links that endow the membrane with coherence and error-correcting capacity.

The emergent interior is not a uniform filling of space but arises dynamically from the coherence properties of the horizon quanta. When their internal phases are uncorrelated, the bulk projection cancels to near emptiness, permitting only radiation and gravitational waves to propagate. By contrast, coherent alignment generates localized concentrations of energy that manifest as stable matter: strong coherence

yields baryonic fields, partial coherence produces dark matter halos, and incoherence contributes to the statistical projection identified with vacuum energy. The observed cosmic partition of energy fractions thus emerges naturally from this organization, since only a small fraction of the membrane reaches strong coherence, while most remains incoherent.

The membrane behaves as a dynamical fluid endowed with surface tension, which resists deformation and governs the effective gravitational coupling of the interior. Local variations in this tension induce curvature, with higher tension corresponding to deeper gravitational wells. The degree of coherence feeds back into the effective stiffness of the membrane: aligned phases enhance tension and stabilize baryonic structures, while incoherence softens the surface and contributes to vacuum-like behavior. Accretion onto the horizon increases its area and entropy in discrete Planckian steps, and when stresses exceed critical thresholds, punctures form that correspond to interior black holes.

The encoding mechanism of the holographic membrane can be framed as a radial fiber mapping: each Planck-scale patch of the horizon encodes the entire radial fiber of bulk voxels, preserving measure by reconciling boundary area with interior volume. In this scheme, the horizon patch serves as an address, while the associated fiber records the cumulative layering of infall. Because baryonic quanta fall stochastically, their incorporation occurs at random positions, so any finite membrane area contains excitations originating from multiple infall epochs. Quanta that were initially proximate in the early collapse may, due to the continued growth of the horizon, later be distributed across a much larger surface area. This stretching effect scrambles boundary positions into nonlocal correlations, yet does not erase baryonic clumping.

The membrane's effective tension dynamically drives state-switching among encoded quanta, ensuring that correlations necessary for massive body formation are preserved. In this way, the holographic mapping simultaneously scrambles microscopic boundary data while maintaining bulk coherence, allowing large-scale baryonic structures such as stars, galaxies, and planets to persist across the encoding.

Thus, the holographic membrane provides a unified framework in which tension generates effective gravity, coherence organizes the distribution of energy densities, and radial encoding preserves the bulk geometry. It acts simultaneously as a record of collapse history, a dynamical surface governing emergent curvature, and a quantum code that explains why the emergent universe exhibits its observed mixture of baryons, dark matter, and dark energy.

4.1 Causal Capacity, Information Encoding, and the Origin of Gravitation

In the horizon-layered cosmology, gravitation and mass emerge from *holographic encoding* on the black-hole membrane. Gravity reflects how information flow reorganizes around localized *reductions in causal capacity*. Let $\rho_{\mathcal{I}}(x)$ be the local density of active encoding channels (per unit Planck area). In vacuum, this capacity is maximal,

$$\rho_{\mathcal{I}}^{(0)} = \frac{1}{4\ell_{\mathrm{p}}^2},$$

while massive excitations induce a deficit,

$$\Delta\rho_{\mathcal{I}}(x) = \rho_{\mathcal{I}}(x) - \rho_{\mathcal{I}}^{(0)} < 0,$$

representing local *causal excision*. The integrated deficit defines effective mass,

$$m_{\rm bh} \propto -\int_{\mathcal{H}} \frac{\Delta\rho_{\mathcal{I}}(x)}{\rho_{\mathcal{I}}^{(0)}}\, dA,$$

so that mass measures a shortfall of causal connectivity. Curvature arises from the redistribution of information flow required to maintain

$$S \leq \frac{k_{\rm B} A}{4\ell_{\rm p}^2}.$$

As energy increases total entropy while suppressing local information throughput $\dot{\mathcal{I}}$, gravitational time dilation and curvature appear as emergent transport effects:

$$\nabla\Phi \propto -\nabla(\dot{\mathcal{I}}),$$

so that information naturally flows toward regions of reduced causal capacity, the apparent "force" of gravity.

This apparent paradox, that reduced causal capacity encodes mass, resolves once we distinguish between *potential* and *realized* information. Maximal capacity represents pure potentiality, devoid of specific structure. When channels freeze under infalling energy, their dynamic freedom is lost, yet each frozen link fixes a definite boundary condition on the holographic code. **Information arises not from abundance but from restriction:** mass corresponds to the stabilized pattern of frozen causal links that preserve global consistency.

At the deepest level, this framework implies that information is not a symbolic abstraction but the physical state of causality itself, the holographic code operates as a binary causal network, where each Planck link is either connected or disconnected. A completely connected network conveys no distinct information, and a completely disconnected one transmits none; maximal information arises when connected and disconnected links coexist in balanced proportion. **Reality thus emerges as the self-organized alternation between causal connection and disconnection, the physical substrate of the "1" and "0" of existence itself. Reality therefore arises as the dynamic equilibrium between potential causation and its localized restriction, between the capacity to connect and the necessity to define.**

This perspective reframes the gravitational field as the collective manifestation of constrained causal flow. Curvature is the geometric imprint of causal limitation, and mass quantifies the integrated deficit of connectivity. Time itself becomes the ordered sequence of causal updates propagating through this finite-bandwidth medium. In this sense, information, geometry, and dynamics are not separate domains but complementary aspects of a single process: the universe continuously writing itself into existence

through the discrete alternation of connection and disconnection at the Planck scale. **The holographic surface is therefore both the ledger and the logic of being, the physical substrate through which information becomes reality.**

4.2 Membrane Dipole Encoding

The Planck-scale cells that constitute the holographic surface, each defined by its causal polarity, spin orientation, and local connectivity, remain the most fundamental and mysterious elements of this framework. They are not derived from any prior structure, but exist as the minimal self-consistent units through which causality, geometry, and information coincide. Each cell may be regarded as a bipolar causal dipole whose internal degrees of freedom encode orientation (normal and tangential), phase (direction of rotation), and state (connected or disconnected) relative to its neighbours. These relations form the primitive syntax of spacetime: a lattice of mutual constraints from which the continuum of geometry and field emerges. Yet the origin of these units, the reason why such dipolar, spinful, binary elements exist at all, remains beyond derivation. They appear as the necessary atoms of reality's code, self-organized at the intersection of logic and existence: **causal nodes that are neither matter nor space, but the condition for both.** Each Planck cell thus represents the smallest possible act of the universe knowing itself.

Accordingly, each quantum that merges with the membrane is inherently *bipolar*. Possession of rest mass implies a causal asymmetry: one face of the quantum's structure is partially excised and oriented inward toward the black-hole center, while the opposite face remains causally open to the external field. This bipolarity guarantees gravitational attraction and alignment upon horizon contact. As infalling quanta redshift toward the stretched horizon, they align with the excised side inward, integrating coherently into the expanding null layer that defines the event horizon. The phenomenological *excision parameter* χ expresses the fraction of each quantum's causal surface that is disconnected from the external domain. Even for $\chi = 1/2$, the mass encoded per cell is far smaller than m_{p}, since a minimal black hole of total mass m_{p} would already contain 16π Planck-area cells, implying an average encoded mass per cell of $m_{\mathrm{p}}/(16\pi)$.

Gravitational curvature thus originates from spatial gradients in this causal deficit: where capacity is locally reduced, information flow bends inward, generating curvature; where it is replenished, expansion occurs. Energy and information are dual aspects of the same quantity, and gravity is their local disequilibrium.

In this model each holographic quantum can be modeled as a combination of two dipoles (Figure 4). Every dipole has two "edges" (ends) that can be causally connected or disconnected from the surrounding quanta. The primary dipole with its causally disconnected edge is directed toward the parent black hole's center and with its connected edge in the opposite direction.

A secondary dipole axis is orientated randomly, chosen isotropically on the disconnected hemisphere of the primary dipole (uniformly in solid angle with polar angle $\theta \in \left[0, \frac{\pi}{2}\right]$ relative to the disconnected normal of the primary dipole). The radial freezing locks the primary (radial) dipole along the normal axis n, preventing further

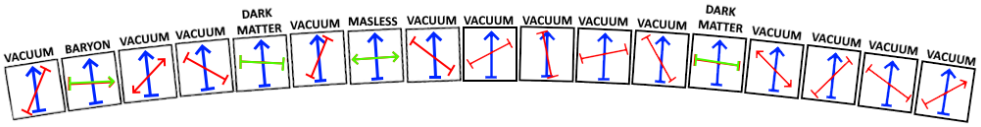

Fig. 4 Black hole holographic membrane quanta schematic representation. Each quanta has the primary dipole that operates in the parent universe (in blue) and the secondary dipole that operates in the child universe that is holographic projection of the membrane lateral dynamics (in red and green). Only the quanta with the secondary dipole laterally oriented encode the internal matter/energy sector (in green). Causally connected dipole edges are represented by an arrow and causally disconnected edges by a dash.

radial dynamics from contributing to the external time evolution. **Once embedded in the holographic membrane, a quantum's secondary dipole acquires a frozen radial component fixed to infinity. The matter–vacuum distinction arises in the lateral sector: if the secondary dipole orientation aligns to admit the lateral connectivity with neighbors, the dipole locks into a coherent causal network, thereby encoding matter. Such matter-encoding quanta remain indefinitely stable. By contrast, quanta without alignment remain in decohered, vacuum states.** The holographic membrane thus acts as a combinatorial lattice in which quanta continually reconfigure their encoded states. Matter and radiation propagate through swap dynamic. Because the secondary dipole rotates freely around the primary dipole axis, it explores all lateral directions on the transverse plane. This preserves isotropic selection of causal sectors.

The secondary dipole's angular tolerance for causal alignment is parameterized by γ, defining the cone of allowed lateral orientations:

$$\theta \in \left[\frac{\pi}{2} - \gamma,\, \frac{\pi}{2}\right]. \tag{61}$$

Only dipoles within this tolerance encode matter or radiation; others contribute to the vacuum background. Each dipole edge can be causally connected with probability $(1-p)$ or disconnected with probability p, leading to four configurations:

$$\begin{aligned} f_{\text{dark matter}} &= \sin\gamma\, p^2, \\ f_{\text{baryon}} &= \sin\gamma\, 2p(1-p), \\ f_{\text{massless}} &= \sin\gamma\, (1-p)^2, \\ f_{\text{vacuum}} &= 1 - \sin\gamma. \end{aligned} \tag{62}$$

With $\gamma = 18^\circ = 90^\circ/5$ and $p = 11/12$, these relations reproduce the observed cosmic composition with remarkable accuracy:

$$f_{\text{baryon}} \simeq 0.048, \quad f_{\text{dark matter}} \simeq 0.262, \quad f_{\text{vacuum}} \simeq 0.691, \quad f_{\text{massless}} \simeq 0.002.$$

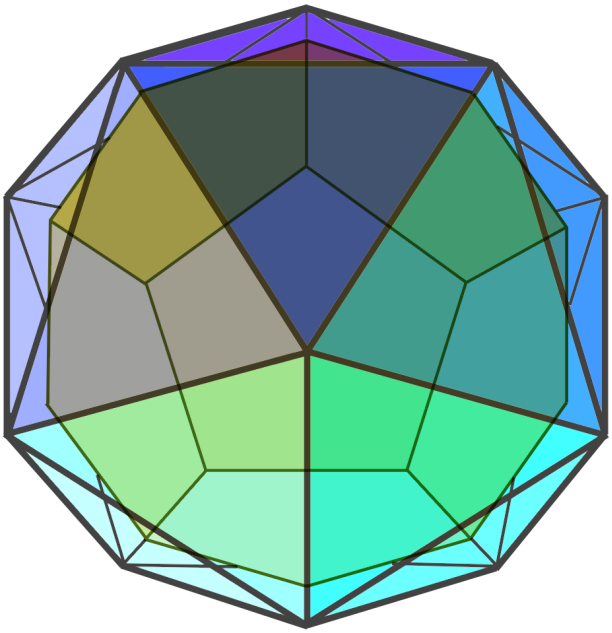

Fig. 5 Icosahedron-dodecahedron dual

The holographic directions of dipole orientations correspond to the dual Platonic pair, the *icosahedron* and *dodecahedron*. The dodecahedron partitions the inward hemisphere into five equal 18° sectors, providing a geometric rationale for the angular tolerance γ. The dual icosahedron defines twelve discrete vertex directions that correspond to possible causal edges; in the narrow-cone limit, one of the twelve aligns within a lateral sector, yielding a connection probability 1/12. Together these polyhedral structures explain the five-fold and twelve-fold factors that underlie the causal probabilities of Eq. (62). Their recurrence in particle physics, nuclear structure, and now holographic cosmology suggests that the icosahedron–dodecahedron dual pair encodes a universal symmetry governing matter organization.

When a child universe nucleates from a parent black-hole horizon, the causal interpretation of each dipole reorders. The parent's primary (radial) dipole, previously frozen by gravitational redshift, becomes an active tangential degree of freedom within the emergent universe; conversely, its secondary dipole reorients toward the center of a new internal black hole. This alternation ensures that radial and tangential channels exchange roles across generations, producing orthogonal holographic orientations and maintaining causal independence between successive universes. Each universe thus inherits its internal matter composition and symmetry pattern from the combinatorial orientation statistics of its parent membrane.

In this unified view, gravitation, mass encoding, and cosmological matter partition all arise from the same holographic mechanism: local excision and dipolar organization of Planck-scale membrane cells. Where causal capacity is removed, curvature forms; where lateral connectivity emerges, matter and radiation appear; and where alignment fails, vacuum dominates. The global evolution of the universe, the growth of mass, entropy, and causal order, thus reflects the collective, quantized reconfiguration of this dipolar membrane network.

4.3 Natural Discretization and Wavefunction Collapse

The discrete advancement of internal time, defined by successive incorporation events, implies that the evolution of the holographic membrane is inherently stepwise. Each incorporation corresponds to the addition of one Planck-scale quantum of mass, updating the global state of the membrane and generating a single "Planck tick" of internal time. In the null-ordered framework, infalling matter becomes redshift-frozen at a finite causal distance above the horizon, where it is assimilated into the stretched membrane through one such discrete update. The event horizon thus behaves not as a static surface but as a dynamically growing, tension-bearing quantum code boundary.

Radially, this growth proceeds in Planck-scale increments, while laterally the membrane is tessellated into Planck-area patches $\Delta A \sim \ell_p^2$, organized through near-optimal packing geometries (e.g., icosahedral or dodecahedral tilings) that maximize local coherence. Each patch acts as a coherent domain, linked by lateral null connections that propagate at the full light speed c within the stretched horizon's proper frame. The lateral equilibration condition $\tau_{\rm coh} \ll \Delta\tau_{\rm inc}$ (equation 51) ensures that the entire membrane attains a self-consistent causal phase before the next incorporation event occurs. This global reconfiguration condition provides the physical foundation for the arrow of internal time and establishes causal coherence between successive holographic states.

At each incorporation step, the newly infalling layer ceases to exist as an independent external entity. Its information is absorbed into the membrane's quantum code through a unitary update according to equation (49): $\Psi_{\mathcal{M}}(t_{n+1}) = \mathcal{U}_n\, \Psi_{\mathcal{M}}(t_n)$, where $\mathcal{U}_n$ represents the global reorganization of local dipole states and their entanglement links. From the internal perspective, this update is experienced as a discontinuous change in the effective state of the universe, a collapse of the internal wavefunction. What appears externally as a continuous, deterministic evolution of the global state becomes internally a sequence of discrete, causally gated transitions.

This natural discretization provides a physical mechanism for the wavefunction-collapse phenomenon. The membrane itself acts as an objective, geometric environment that enforces causal consistency and decoheres incompatible internal amplitudes. Quantum states that do not satisfy the membrane's updated coherence structure are eliminated from the internal Hilbert space, while those that remain form the next consistent layer of the holographic code. The process thus implements a physical selection rule analogous to Zurek's pointer-state decoherence [39], but rooted in the causal dynamics of the horizon.

Globally, the combined parent–interior system evolves unitarily across the extended Hilbert space of the holographic code: $\Psi_{\rm total}(t_{n+1}) =$

$U_{\text{global}}\,\Psi_{\text{total}}(t_n)$, **preserving total information. However, from the internal viewpoint, obtained by tracing out the external degrees of freedom, the evolution appears stochastic and non-unitary. The apparent collapse of the wavefunction is therefore not a subjective measurement event, nor a branching of worlds, but a physically necessary consequence of causal excision and finite incorporation rate. Each Planck-scale update defines a new causal boundary condition, and amplitudes incompatible with that boundary are effectively projected out.**

In this sense, quantum indeterminacy arises not from epistemic uncertainty but from geometric causality: only those internal configurations compatible with the current membrane state remain dynamically accessible. The redshift-induced causal separation between layers functions as a natural post-selection mechanism, ensuring consistency across the entire null-ordered history. The collapse of the wavefunction thus corresponds to a geometric transition in the allowed state space of the emergent universe, governed by the sequential updating of the holographic membrane.

This interpretation echoes Rovelli's relational quantum mechanics [40], where states are defined relative to their observers. Here, the event horizon itself plays the role of the relational observer, a dynamically evolving null surface that records, regulates, and selects the admissible amplitudes of the internal universe. Bell inequalities are violated for the same reason as in standard quantum mechanics, not through local hidden variables, but through the nonlocal, null-ordered entanglement of the holographic code. The "collapse" is thus the local manifestation of a global, unitary causal update.

In summary, wavefunction collapse in the causal-excision–holographic model is the internal appearance of a discrete, globally unitary reconfiguration of the horizon code. Each incorporation event advances the internal clock, increases the encoded entropy, and enforces a new set of admissible internal amplitudes. Time, decoherence, and wavefunction collapse are therefore three aspects of the same underlying process: the sequential, Planck-scale causal updates of the horizon membrane.

4.4 Quantum Tunnelling and Causal Information Exchange

In the horizon-layered cosmology, motion and interaction are not primitive ingredients of reality but emergent features of a deeper causal code. The horizon is a stationary lattice of Planck-scale cells, each representing a discrete causal element of spacetime. Nothing within this lattice literally moves, yet the global structure is in constant reconfiguration. Its dynamics proceed through successive incorporations of new Planck-area cells, each addition redefining the adjacency and relational geometry of all existing ones. From the external viewpoint, this appears as the steady growth of the event horizon; from the internal perspective, it manifests as the expansion of space itself.

Each new layer of cells introduces a global relational shift that alters the relative positions of pre-existing cells without requiring any local transmission of information. This radial process, the continuous addition of new causal elements, is what gives rise to the expansion of the internal universe. It is analogous to the stretching of space between galaxies: the galaxies themselves do not move through space, but the relational distances between them increase as new cells are incorporated into the causal

fabric. The universe grows because the horizon grows; the geometry evolves through relational retessellation rather than motion.

However, the horizon also supports a second, complementary process: lateral causal communication between neighboring cells. Each Planck-scale unit possesses a secondary dipole, an orientation tangential to the horizon, that allows it to exchange information with its neighbors through quantum tunnelling along null directions on the horizon surface. This lateral coupling establishes the foundation for interaction, coherence, and radiation. Whereas the radial process redefines the large-scale relational framework, the lateral exchange maintains local continuity, coherence, and dynamical connectivity among the horizon's degrees of freedom.

The lateral channel enables the propagation of field-like correlations across the horizon surface, producing the phenomena that, when projected into the internal universe, correspond to radiation and interaction. Massless excitations arise from maximally coherent lateral coupling: they propagate as pure information waves through the causal lattice. Massive quanta correspond to locally excised regions with reduced lateral coupling, their inertia emerging from the limited ability to tunnel between neighboring cells. Dark matter, in turn, represents the limiting case of full lateral disconnection, it neither radiates nor interacts electromagnetically because it lacks lateral causal links, responding only to the curvature of the global structure.

Gravitational attraction arises from gradients in this lateral coupling. Regions of diminished causal capacity draw nearby quanta toward them, much as curvature in classical spacetime attracts matter. In this view, gravity is the macroscopic expression of variations in the density and connectivity of lateral links within the horizon's causal network. Clumping of matter, galaxy formation, and large-scale structure thus emerge from the counterbalance between the outward radial expansion and the inward coherence of lateral coupling.

At the most fundamental level, the horizon's evolution consists of both processes acting in synchrony. Radial incorporations continuously rewrite the relational map, extending the causal manifold outward; lateral exchanges maintain coherence, propagate correlations, and enable the emergence of forces and radiation. Together they constitute a twofold causal mechanism: one that drives the expansion of space and one that preserves its structural unity. The first defines the arrow of cosmic growth; the second sustains the network of interactions that gives rise to matter, light, and gravity.

This dual process replaces the notion of motion with that of continuous relational restructuring. Apparent propagation, force, and interaction are emergent patterns within a stationary yet perpetually updated code surface. The speed of light c expresses the invariant rate at which this relational lattice can update and communicate across its null-connected links, setting the universal bound for both types of process. In this sense, reality itself is a still holographic code whose steady retessellation and lateral coupling together generate the full phenomenology of motion, radiation, gravitation, and cosmic evolution.

The coexistence of global relational reconfiguration and local lateral exchange yields a unified interpretation of light propagation and cosmic expansion. The photon's journey combines two complementary processes:

relational drift due to the growth of the causal manifold and local coherence maintained by lateral transmission. The result is a natural, holographically grounded explanation of cosmological redshift and the constancy of c: expansion reflects the geometric redefinition of adjacency in the underlying causal code, while light itself represents the stable, null-synchronous communication between stationary Planck cells.

This causal–informational framework naturally connects to discrete spacetime theories such as causal set models and cellular automata. In all such approaches, spacetime dynamics arises from successive updates of discrete elements rather than continuous motion of particles or fields. The present model extends this logic to the holographic horizon itself: the membrane acts as a null-synchronized automaton whose global update rules encode gravitational, quantum, and thermodynamic behavior within a unified causal structure. Hence, the stationary yet perpetually reconfigured horizon represents the common substrate from which motion, tunnelling, and spacetime continuity all emerge as large-scale manifestations of Planck-scale relational updates.

4.5 Relation to Discrete Causal and Cellular Automaton Models

The horizon-layered cosmological framework exhibits deep structural parallels with discrete causal and cellular automaton models of spacetime, most notably those developed in the context of the Wolfram Physics Project [41, 42]. Both approaches regard spacetime and physical law as emergent from an underlying network of discrete update events governed by causal rules. However, while the Wolfram framework treats this network as an abstract hypergraph evolving through local rewriting operations, the present model identifies a concrete physical substrate: the null-ordered black hole horizon itself, whose Planck-scale cells form the fundamental nodes of a physically realized causal automaton.

Each holographic incorporation event in the horizon-layered model corresponds to the addition of a Planck-scale null layer, generating a discrete update of the global causal code. This process defines a mapping onto a causal network of update events, where each horizon configuration Σ_n transitions to Σ_{n+1} through a null-synchronized rewriting analogous to Wolfram's graph evolution. The null-ordering principle enforces global consistency and causal invariance, providing a physical realization of the abstract "causal invariance" that in the Wolfram framework underlies Lorentz symmetry. In this sense, the horizon behaves as a null-synchronized automaton embedded in curved spacetime, with geometry and causal structure co-generated by its update rules.

Yet, the correspondence extends beyond formal analogy. In the Wolfram model, the hypergraph's links define both adjacency and causality, whereas in the horizon-layered picture these roles bifurcate into two complementary processes: (1) a *radial relational reconfiguration* that globally redefines adjacency through the incorporation of new Planck-scale cells, and (2) a *lateral causal exchange* that propagates coherence and interaction across neighboring cells along the horizon surface. The first process defines the expansion and temporal ordering of the universe, the sequential growth of the

causal manifold, while the second sustains local coherence, radiation, and gravitational coupling. Together, they constitute a dual causal architecture: a global null-ordered remapping that advances spacetime and a local tangential channel that preserves connectivity and physical interaction. In Wolfram's framework, both functions are conflated within local rewriting; here, they are physically distinguished and causally synchronized.

This distinction grounds Wolfram's abstract causal computation in thermodynamic and geometric reality. The horizon provides an explicit holographic substrate whose area growth encodes entropy increase and defines the arrow of time. Gravitational redshift and null synchronization give causal directionality without external postulate, while the entropic expansion of the horizon furnishes an intrinsic mechanism for irreversibility. Where the Wolfram model assumes asymmetric update rules to generate temporal flow, the present theory derives it directly from the holographic incorporation process at the Planck bandwidth limit c^5/G.

Moreover, the lateral tunnelling among Planck cells supplies a concrete analogue to Wolfram's local update rules: information propagates tangentially along the horizon lattice, constrained by the null condition $ds^2 = 0$, while the global relational remapping defines the higher-level evolution of the causal graph itself. The horizon thereby performs a dual computation, local and global, microscopic and cosmological, through which spacetime, motion, and interaction co-emerge as informational phenomena.

In this light, the black hole horizon functions as a physically instantiated causal automaton whose rule set is not arbitrary but determined by the geometric and thermodynamic constraints of general relativity. The sequential incorporation of Planck layers enforces causal order; lateral exchanges maintain coherence and field propagation; and their interplay saturates the holographic information bound. The discrete causal structure envisioned in cellular automaton physics thus finds a tangible realization on null surfaces, while the horizon-layered holographic mechanism supplies the physical law that performs the computation of spacetime itself.

4.6 Kerr Geometry as a Rotating Causal Structure

In classical general relativity, rotation in black holes is described not by the motion of material surfaces, but by the rotation of spacetime itself. The Kerr metric, which generalizes the Schwarzschild solution to include angular momentum, possesses a nonzero off-diagonal term,

$$g_{t\phi} = -\frac{2Gm_{\mathrm{bh}}a\sin^2\theta}{c^2 r_{\mathrm{s}}}, \tag{63}$$

where $a = J/(m_{\mathrm{bh}}c)$ is the Kerr spin parameter, J the black hole's angular momentum, and m_{bh} its physical mass in kilograms.

This term encodes the phenomenon of *frame dragging*, in which inertial frames near the horizon are twisted around the rotation axis. As a result, even though no material body crosses the event horizon in coordinate time, spacetime itself exhibits a stationary rotation. The event horizon is a null surface generated by lightlike trajectories

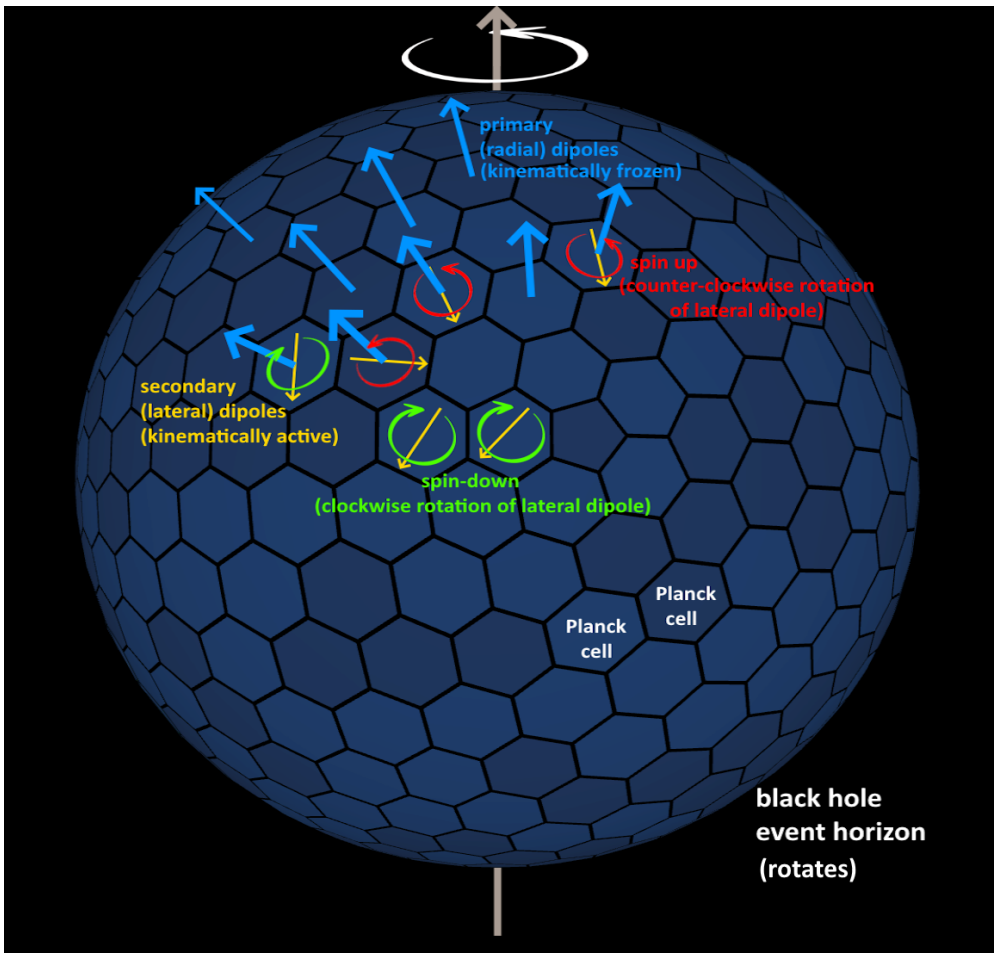

Fig. 6 Schematic representation of rotating horizon surface made of individual Planck cells

that spiral around the spin axis with angular velocity

$$\Omega_h \;=\; \frac{a\,c^3}{2\,G\,m_{\rm bh}\,r_{\rm s}}, \qquad r_{\rm s} \;=\; \frac{G m_{\rm bh}}{c^2} + \sqrt{\left(\frac{G m_{\rm bh}}{c^2}\right)^2 - a^2}, \tag{64}$$

Thus, the horizon is not a static boundary but a *rotating causal structure*. Its rotation is a geometric property of the metric, not a physical motion of matter; the null generators of the horizon co-rotate with spacetime itself. This resolves the apparent paradox between "time freezing" at the event horizon and the persistence of rotation: the freezing applies to infalling matter, whereas the rotation pertains to the spacetime geometry, which remains globally stationary but azimuthally twisted.

Within the horizon-layered cosmology, such large-scale alignments arise naturally from the *global rotation of the parent black hole's horizon.* **The holographic membrane that encodes our universe is not static with respect to the parent spacetime: it rotates according to the Kerr parameter**

$$a = \frac{J}{m_{\mathrm{bh}} c}, \tag{65}$$

where J is the black hole's angular momentum, m_{bh} its physical mass (kg). This rotation corresponds to a real physical motion of the horizon in the parent frame, producing frame dragging and differential redshift across latitudes. These effects modulate the causal order of null-layer incorporations, imparting a spin-dependent phase bias to the holographic encodings.

Internally, this global rotation is not experienced as bulk motion, since all causal degrees of freedom share the same co-rotating reference frame. Instead, the rotation manifests as a *phase structure* in the entanglement network: an azimuthal ordering of correlation phases across the holographic membrane. This phase gradient is the internal signature of the parent spin and serves as the seed of cosmic anisotropy. Thus, the emergent universe inherits a preferred axis corresponding to the direction of the parent black hole's spin vector, encoded as a coherent orientation in the primordial mode spectrum.

The Kerr-induced anisotropy of the null layering modulates the initial conditions of both matter and curvature perturbations. Because cosmic inflation in this framework is driven by the continuous growth of the parent horizon rather than by a scalar inflaton field, this spin-imprinted asymmetry is *not erased by inflationary expansion.* Instead, it is preserved as a large-scale alignment in the internal universe, manifesting observationally as the Cosmic Microwave Background (CMB) dipole and the alignment of low-ℓ multipoles (the "Axis of Evil").

In the standard ΛCDM cosmology, the CMB dipole is usually interpreted as the Doppler signature of our peculiar velocity relative to the cosmic rest frame. However, several recent analyses (e.g., [43]) have questioned this purely kinematic explanation, suggesting that a portion of the observed dipole and the alignment of low-ℓ multipoles (the "Axis of Evil") may reflect an intrinsic cosmological anisotropy imprinted at the earliest stages of the universe.

From the external viewpoint, the horizon's rotation represents a real physical motion in the parent spacetime. From the internal viewpoint, however, it is perceived only through phase correlations and anisotropic alignments in the emergent cosmological field structure. Hence, the black hole's rotation provides a geometric bridge between the external Kerr spacetime and the internal cosmological anisotropies, linking the global angular momentum of the parent black hole to the observed directional asymmetries of our universe.

This rotating causal structure defines the fundamental phase background on which all subsequent quantum and thermodynamic asymmetries are encoded.

4.7 Spin–Topological Origin of Baryon Asymmetry and Cosmic Anisotropy

Every Planck-scale quantum on the holographic membrane is represented by a bipolar causal unit, a pair of poles defining an oriented dipole. The local surface normal of the membrane provides a preferred axis, the radial direction relative to the black hole center. Each quantum's *primary dipole* aligns with this normal, while its *secondary dipole* lies within the tangent plane and carries an intrinsic spin-like orientation relative to the global horizon rotation. **Because the horizon is a two-dimensional surface, spin cannot assume arbitrary three-dimensional directions: each dipole's angular momentum vector can only be parallel or antiparallel to the local normal, producing two discrete causal orientations,**

$$s = +\tfrac{1}{2} \quad \text{(aligned with horizon spin)}, \qquad s = -\tfrac{1}{2} \quad \text{(anti-aligned)}.$$

These two orientations form the binary spin basis of the horizon code, corresponding to the familiar "up" and "down" states of fermionic matter in the emergent universe. Thus, the existence of only two intrinsic spin states arises directly from the two possible alignments of the secondary dipole with the membrane normal.

When the parent black hole possesses angular momentum $\mathbf{J}$, the frame-dragging field of the Kerr geometry introduces an azimuthal phase gradient across the horizon. The local angular velocity of frame dragging near the horizon is

$$\omega_{\mathrm{fd}} = \frac{2GJ}{c^2 r_{\mathrm{s}}^3}, \tag{66}$$

where r_{s} is the horizon radius. During a Planck-time incorporation interval $\Delta t = t_{\mathrm{p}}$, the two spin orientations acquire a differential phase shift

$$\Delta\phi = 2\,\omega_{\mathrm{fd}}\,t_{\mathrm{p}} = \frac{4GJ\,t_{\mathrm{p}}}{c^2 r_{\mathrm{s}}^3}. \tag{67}$$

For a near-extremal black hole with $J \sim G m_{\mathrm{bh}}^2/c$ this yields

$$\frac{\Delta\phi}{2\pi} \sim \frac{2G^2 m_{\mathrm{bh}}^2 t_{\mathrm{p}}}{\pi c^3 r_{\mathrm{s}}^3} \;\approx\; 10^{-10},$$

for a stellar-mass progenitor, precisely the magnitude needed to account for the observed baryon-to-photon ratio $\eta_b \sim 6\times10^{-10}$. The co-rotating orientation ($s = +\frac{1}{2}$) is slightly favored, leading to a cumulative baryon excess during sequential horizon incorporations. Antimatter corresponds to the opposite orientation ($s = -\frac{1}{2}$), which decoheres more rapidly due to its counter-rotating phase relation.

4.8 Mach's Principle and the Origin of Inertia

In classical mechanics, inertia quantifies an object's resistance to changes in motion and defines the structure of inertial frames. However, the source of inertia has remained

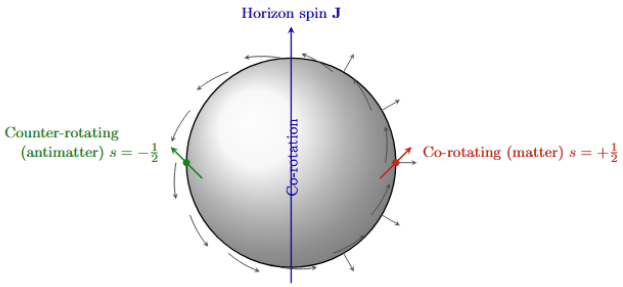

Fig. 7 Binary spin structure and baryon asymmetry on a rotating holographic horizon. Each surface quantum has a primary dipole normal to the horizon and a secondary dipole oriented tangentially. Because spin can only align or anti-align with the local normal, two discrete orientations exist: co-rotating (matter-like) and counter-rotating (antimatter-like). Frame dragging slightly favors the co-rotating orientation, producing a small but cumulative baryon excess during sequential horizon incorporations.

conceptually obscure: in Newtonian theory it is an intrinsic property of matter, while in Mach's relational view it arises from the mass distribution of the universe as a whole. General relativity partially realizes Mach's idea by allowing spacetime geometry to respond to energy–momentum, yet it still treats inertial motion as a property of geodesic structure rather than of the information network underlying it.

In the horizon-layered cosmology, inertia acquires a precise informational and relational meaning. Each Planck-scale horizon cell participates in a web of entanglement linkages with neighboring cells, forming a null-synchronized network that defines the causal code of spacetime. A "particle" corresponds to a persistent pattern of correlations among many such cells. Changing its state of motion, accelerating it, requires the continual reconfiguration of its entanglement attachments within this network. *Inertia thus represents resistance to the reassignment of causal links.* The greater the integrated connectivity of a pattern within the horizon code, the more informational work must be performed to alter its relational embedding, producing an effective inertial mass.

This definition renders Mach's principle operational: **inertia is not an intrinsic attribute of an isolated body but a collective property determined by the state of the entire causal boundary.** The rest frame of a particle corresponds to a condition of stable entanglement with its surrounding horizon neighborhood; acceleration disrupts this equilibrium and induces compensating adjustments throughout the global code. Because every local cell is entangled with the rest of the boundary, the inertial response of any subsystem implicitly depends on the configuration of all others, precisely the relational dependence Mach envisioned.

Mathematically, the effective inertial mass m_{eff} can be expressed as a measure of the entanglement gradient between a local subsystem $\mathcal{S}$ and its complement $\bar{\mathcal{S}}$:

$$m_{\text{eff}}c^2 \;\propto\; \frac{\partial I(\mathcal{S}:\bar{\mathcal{S}})}{\partial \tau},$$

where $I(\mathcal{S} : \bar{\mathcal{S}})$ is the mutual information between the subsystem and the rest of the horizon code, and τ is the proper time along the local causal trajectory. A uniform velocity corresponds to constant relational information, while acceleration corresponds to a temporal change in this mutual information, requiring energy input proportional to the rate of causal link reconfiguration.

In this way, the equivalence principle becomes a statement of informational symmetry: gravitational and inertial mass are identical because both quantify the resistance of the horizon code to changes in its relational structure. Gravitational curvature describes how the global connectivity field redirects causal pathways, while inertia measures the cost of altering those pathways locally. Both effects emerge from the same underlying process, the self-consistent maintenance of causal order across the holographic boundary.

Hence, the horizon-layered cosmology provides a concrete realization of Mach's principle within a quantum–informational framework: **inertia is the relational resistance of the holographic network to the reconfiguration of its causal entanglement structure.** Local inertial frames are thus defined not by empty space but by stable patterns of global connectivity within the horizon code, tying the experience of motion directly to the informational architecture of the universe itself.

5 Internal Universe Cosmology

In the framework developed here, the traditional Big Bang singularity is reinterpreted as the initial emergent interior of black hole formed in the parent universe. From an external perspective, this black hole develops from a Planck scale seed which experiences rapid growth via accretion.

Internally, this yields a smooth, continuously inflating universe whose energy scale reflects Planck-scale conditions. The apparent origin of time corresponds to the dynamical stratification of matter falling onto the horizon, with increasing entropy and energy encoded on the growing surface. This continuous influx from the parent universe provides a natural origin for the high energy densities of the early universe, eliminating the need for arbitrary initial conditions.

In the standard cosmological model, a brief period of exponential inflation is postulated to resolve several deep problems in early universe physics, including the horizon problem, flatness problem, and the monopole problem. According to this view, a tiny causally connected patch underwent rapid expansion, typically by a factor of at least 10^{26} in radius, within less than 10^{-32} seconds after the Big Bang, smoothing and correlating all regions that are now visible in the cosmic microwave background (CMB) [44, 45].

However, in the horizon-layered cosmological framework proposed here, no such inflationary epoch is required. In this model, **cosmic expansion arises directly and continuously from the growth of the parent black hole. The internal volume and time grows as a function of accreted mass.** Each increase in black hole mass corresponds to the null-ordered incorporation of a new layer of mass-energy into the horizon, triggering a global rearrangement that defines a single clock tick in internal time.

In this context, the horizon problem does not arise because the entire internal universe is constructed holographically from a single, null-surface origin: the event horizon of the collapsing star. All parts of the emerging universe are causally connected through this surface from the outset, eliminating the need for superluminal expansion to explain the observed isotropy of the CMB. Likewise, the flatness problem is naturally avoided because the spatial curvature of the universe is not a free parameter but an emergent property of the null-surface encoding and the geometric flow of entropy. No finely tuned initial curvature is required. The model predicts continuous expansion through the same scaling law, from the earliest times to the present.

The coexistence of global relational reconfiguration and local lateral exchange yields a unified interpretation of light propagation and cosmic expansion. **A photon emitted from a distant galaxy does not traverse a fixed spatial interval; rather, it is continuously re-encoded across a horizon-layered lattice that itself expands through the successive incorporation of new causal cells. Its apparent redshift arises because each global update stretches the relational distance between emitter and observer, increasing the effective wavelength without any local change in the photon's propagation speed. At the same time, within each discrete causal frame, the photon propagates tangentially across the horizon network through lateral tunnelling at the invariant null speed c.**

5.1 Universal Relation H = 1/t Across All Cosmic Epochs, Revised Cosmic Time and Redshift Relations

In the horizon-layered cosmology, cosmic time is not an emergent parameter of a continuous field evolution but a direct geometric consequence of the total encoded mass and radius of the enclosing parent black hole. The universe, viewed as the holographic interior of such a black hole, obeys the fundamental identity

$$r_{\mathrm{s}} = 2M_{\mathrm{bh}}, \tag{68}$$

which defines the causal boundary of the spacetime domain. Here M_{bh} denotes the black hole mass expressed in *geometric units* (i.e. as a length in meters). The corresponding physical mass in kilograms is given by

$$m_{\mathrm{bh}} = \frac{c^2 r_{\mathrm{s}}}{2G}, \tag{69}$$

From the discrete incorporation relation (equation 60), the cosmic time associated with a black hole of geometric mass M_{bh} is

$$t = \frac{M_{\mathrm{bh}}}{c} = \frac{G m_{\mathrm{bh}}}{c^3} = \frac{r_{\mathrm{s}}}{2c}. \tag{70}$$

Hence the physical radius of the universe at cosmic time t follows directly as

$$\boxed{r_{\rm s} = 2ct.} \tag{71}$$

This expresses the coevolution of cosmic time and horizon size as a purely geometric identity, independent of any assumed matter content, equation of state, or scale factor dynamics.

In the standard cosmological model, the Hubble radius is defined as

$$r_h = \frac{c}{H}. \tag{72}$$

At the present epoch, it is often noted empirically that $H_0 \approx 1/t_0$, giving $r_h \approx ct_0$. In the horizon-layered model, however, this identity is elevated from a coincidence to an exact geometric law valid at all epochs. Comparing equation (72) with equation (71), one obtains

$$\boxed{r_{\rm s} = 2r_h,} \tag{73}$$

and equivalently, from equation (68),

$$\boxed{M_{\rm bh} = 2M_h,} \tag{74}$$

where M_h denotes the effective Hubble mass enclosed within the radius r_h (in geometric units).

Thus, the cosmological horizon radius is always twice the local Hubble radius, and the total encoded geometric mass is twice the effective Hubble mass, relations that hold across all epochs and across all generations of black-hole-born universes.

Starting from equations (73) and (71), we have directly

$$r_h = \frac{r_{\rm s}}{2} = \frac{2ct}{2} = ct. \tag{75}$$

The Schwarzschild relation (equation 68) gives the corresponding black hole mass:

$$r_{\rm s} = 2M_{\rm bh} = \frac{2Gm_{\rm bh}}{c^2}. \tag{76}$$

Substituting into equation (70) yields

$$t = \frac{M_{\rm bh}}{c} = \frac{Gm_{\rm bh}}{c^3}. \tag{77}$$

Now, the local Friedmann-like expansion rate for a spherically symmetric causal patch of radius r_h containing effective geometric mass M_h can be written as

$$H_{\text{local}} = \sqrt{\frac{2M_h c^2}{r_h^3}} = \sqrt{\frac{2Gm_h}{r_h^3}}. \tag{78}$$

Using $M_h = M_{\text{bh}}/2$ and $r_h = ct$, we find

$$\begin{aligned} H_{\text{local}} &= \sqrt{\frac{2(M_{\text{bh}}/2)c^2}{(ct)^3}} = \sqrt{\frac{M_{\text{bh}}c^2}{c^3t^3}} = \sqrt{\frac{c^2M_{\text{bh}}}{c^3t^3}} \\ &= \sqrt{\frac{1}{t^2}} = \frac{1}{t}. \end{aligned} \tag{79}$$

Therefore,

$$\boxed{H = \frac{1}{t}} \tag{80}$$

is an exact and epoch-independent identity in the horizon-layered cosmology.

This result implies that **the cosmic expansion rate is a direct manifestation of the geometric time–mass correspondence of the enclosing black hole.** Unlike the Friedmann solutions, where $H(t)$ depends on the evolving energy density and equation of state, here H is entirely determined by the discrete causal synchronization of horizon incorporations. The relation $H = 1/t$ thus expresses the intrinsic holographic clock of the universe: the rate at which external incorporations generate internal time increments and horizon growth in perfect geometric proportion.

Te relation (80) allows us to directly infer the current cosmic time t_0 from the locally measured Hubble constant. Using the empirically determined value from the SH0ES collaboration [46] we obtain:

$$t_0 = \frac{1}{H_0} = \frac{1}{2.366 \times 10^{-18}\ \text{s}^{-1}} \approx 4.2265427 \times 10^{17}\,\text{s} \approx 13.402279\,\text{Gyr}. \tag{81}$$

This value is approximately 400 million years younger than the standard ΛCDM estimate of 13.8 Gyr. However, this is not a discrepancy but a theoretical pivot: our model redefines cosmic age as a measure of horizon growth, rather than a chronology derived from assumptions about the recombination epoch and dark energy.

Adopting $t_0 = 13.4$ Gyr therefore aligns directly with local observational data while remaining fully consistent within the horizon-layered framework.

The Hubble radius does not represent the total extent of our universe. Using equation (60), and adopted revised cosmic time ($\approx 4.2265427 \times 10^{17}$ s, contrary to inferred ΛCDM cosmic time $\approx 4.355 \times 10^{17}$ s), we are able to calculate our current parent black hole mass in geometric units:

$$M_{\rm bh} = t_0 \cdot c = 4.2265427 \times 10^{17} \cdot 2.99792458 \times 10^8 = 1.267086 \times 10^{26}{\rm m} \tag{82}$$

In physical mass units it is:

$$m_{\rm bh} = \frac{c^2 \cdot M_{\rm bh}}{G} = 1.706246 \times 10^{53}{\rm kg} \tag{83}$$

$$r_{\rm s} = 2M_{\rm bh} = 2.534171 \times 10^{26}{\rm m} \tag{84}$$

In our horizon-layered cosmological model, where cosmic time is emergent from null-ordered layering on a dynamically evolving horizon, redshift is redefined geometrically as a ratio of horizon-encoded timescales:

$$1 + z = \frac{\nu_z}{\nu_o} = \frac{r_{\rm s}^0}{r_{\rm s}^z} = \frac{2ct_0}{2ct_z} = \frac{t_0}{t_z}. \tag{85}$$

$$\Rightarrow \quad \boxed{t_z = \frac{t_0}{1+z}}. \tag{86}$$

This relation directly links the redshift of observed signals to their encoded position within the causal horizon, bypassing the need for global scale factor dynamics.

The Hubble parameter then evolves as:

$$\boxed{H(z) = \frac{1+z}{t_0}}. \tag{87}$$

In this model $z_{\rm initial}$ denotes the maximum redshift associated with the Planck time limit. This is defined by:

$$1 + z_{\rm initial} = \frac{t_0}{t_p}, \tag{88}$$

$$\Rightarrow \quad z_{\rm initial} = \frac{t_0}{t_p} - 1, \tag{89}$$

using $t_0 = 4.2265427 \times 10^{17}\,{\rm s}$ as the present cosmic time and $t_p = 5.391247 \times 10^{-44}\,{\rm s}$ Planck time. This yields the value of the maximum possible redshift:

$$z_{\rm initial} \approx 7.838 \times 10^{60}. \tag{90}$$

5.2 Thermal Scaling and Resolution of the Hubble Tension in Horizon-Layered Cosmology

In the standard ΛCDM framework, the inferred value of the Hubble constant from cosmic microwave background (CMB) anisotropy data is lower than that obtained from local distance ladder measurements, leading to the persistent "Hubble tension"

problem [46]. This discrepancy has remained unresolved despite increasingly precise observations and refinements in cosmological modeling.

Unlike standard cosmology, which adjusts acoustic parameters to reconcile early and late universe measurements, our approach accepts the local H_0 as fundamental and geometrically interprets cosmic time. As such, the Hubble tension is not a problem to be solved but an indication that the standard interpretation of cosmological redshift and temporal scaling is incomplete.

Using the observed redshift of the CMB surface, $z_{\rm cmb} = 1089.92 \pm 0.25$ [47], the internal emission time in this framework is computed as

$$t_{\rm CMB} = \frac{t_0}{1 + z_{\rm cmb}} = \frac{4.2265427 \times 10^{17}}{1090.92} \approx 3.874292 \times 10^{14}\,{\rm s} \approx 12.2853\,{\rm Myr}, \tag{91}$$

where $t_0 = 1/H_0$ is the present cosmic time. This shifts the apparent recombination epoch from 380 kyr in ΛCDM to 12.3 Myr internally, while preserving all observed redshift values. The shift directly alters the inferred expansion rate without requiring exotic late-time physics.

To consistently link temperature to redshift in both the low-temperature observational regime and the Planck-scale early universe, instead of the standard $T = T_0(1 + z)$ we adopt the phenomenological temperature–redshift relation:

$$T(z) = \frac{T_{\rm Planck}\, T_0\, (1 + z)}{T_{\rm Planck} + T_0\, (1 + z)}, \tag{92}$$

where T_0 is the present-day CMB monopole temperature and $T_{\rm Planck}$ is the Planck temperature. Equation (92) ensures exact normalization $T(0) = T_0$ and reproduces the standard scaling for $T_0(1 + z) \ll T_{\rm Planck}$, while saturating at $T_{\rm Planck}$ in the $z \to z_{\rm initial}$ limit. This avoids unphysical divergence of temperature in the earliest epochs and provides a smooth transition from quantum-gravity-dominated conditions to the classical thermal history.

For the CMB epoch with $T_{\rm Planck} \approx 1.417 \times 10^{32}\,{\rm K}$ and $T_0 = 2.725\,{\rm K}$, we find:

$$T_{\rm CMB} = \frac{1.417 \times 10^{32} \times 2.725 \times 1090.92}{1.417 \times 10^{32} + 2.725 \times 1090.92} \approx 2972.757\ {\rm K},$$

in agreement with the expected thermal state at recombination. The difference from the standard scaling is negligible at this redshift, but becomes dominant for z approaching the initial Planck-scale epoch, where horizon-layer microphysics would prevent temperatures from exceeding $T_{\rm Planck}$. In the observational regime, the law preserves all standard cosmological predictions, while offering a natural ultraviolet completion that respects holographic entropy bounds.

5.3 Galaxy Formation Timing in Horizon-Layered Cosmology

A key observational challenge to the standard ΛCDM model arises from the early appearance of massive, metal-rich galaxies at redshifts $z \gtrsim 10$, even to $z = 14.44$, as revealed by recent JWST data [48]. In the ΛCDM framework, z=14.4 corresponds to

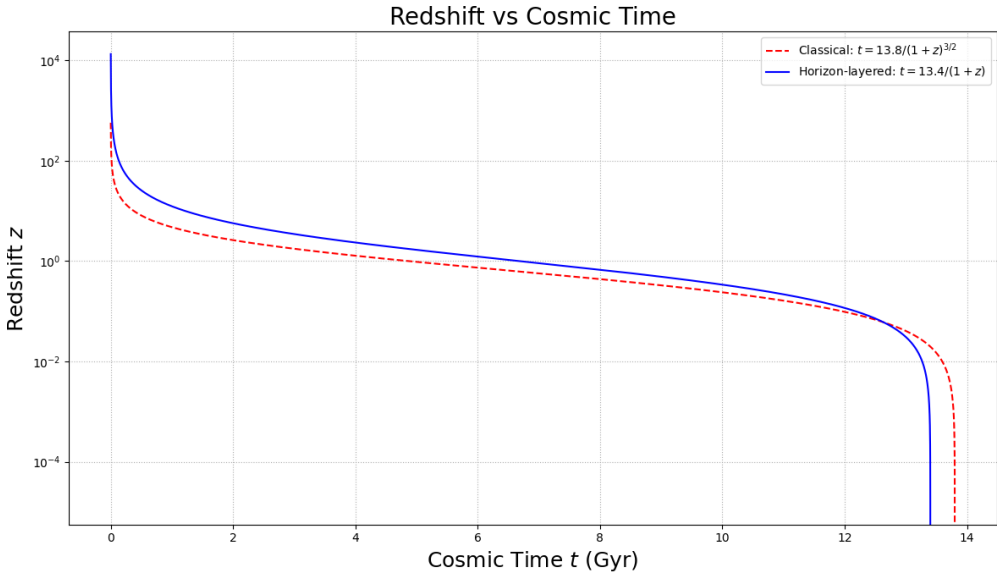

Fig. 8 Graph showing the relation between redshift factor z and time according to classical approximation (red dashed line, $t = 13.8 \cdot \frac{1}{(1+z)^{3/2}}$) and according to the model presented in this framework (blue solid line $t = 13.4 \cdot \frac{1}{1+z}$). The presented model is built under assumption that our cosmological time is 13.4 Gyr in contrast to classical 13.8 Gyr

a cosmic time of approximately 280 million years after the Big Bang. However, this timescale is arguably too short to accommodate the gravitational collapse, cooling, and star formation processes necessary for the formation of complex galactic structures.

By contrast, in the horizon-layered cosmological model at $z = 14.44$ (adopted from the MoM-z14 model [49]), yields cosmic time equal to:

$$t(z = 14.44) = \frac{13.4\,\text{Gyr}}{15.44} \approx 868\,\text{Myr},$$

providing significantly more time for galaxy formation to occur. This discrepancy is illustrated in the following comparative table:

Feature	**ΛCDM Timeline**	**Horizon-Layered Model**
Current cosmic time	~ 13.8 Gyr	~ 13.4 Gyr
CMB	~ 380 kyr	~ 12.3 Myr
First galaxies (z=14.44)	~ 280 Myr	~ 868 Myr
Structure growth time	Short, fine-tuned	Long, natural
Compatibility with JWST	Tension with data	Improved alignment
Redshift-time relation	$t(z) \propto (1+z)^{-3/2}$	$t(z) \propto (1+z)^{-1}$

Thus, the horizon-layered model provides a more realistic timeline for gravitational collapse and galaxy formation. It avoids the need for extreme early star formation

efficiency, exotic cooling channels, or highly tuned initial conditions. The observed maturity of early galaxies is reinterpreted as a natural outcome of an extended pre-galactic era enabled by a more gradual redshift-time scaling. Furthermore, this model's consistency with classical timescales for structure formation supports its viability as a physically motivated alternative to ΛCDM.

5.4 Resolution of the Vacuum Catastrophe through Holographic Encoding

One of the most persistent puzzles in theoretical physics is the "vacuum catastrophe", the enormous discrepancy between the quantum field theoretical estimate of vacuum energy and the observed cosmological constant. In conventional quantum field theory (QFT), summing the zero-point modes of all fields up to the Planck scale yields

$$\rho_{\rm vac}^{\rm qft} \sim \frac{\hbar c}{\ell_{\rm p}^4},$$

which exceeds the measured value by roughly 10^{120} orders of magnitude. This discrepancy arises because QFT assumes that all bulk vacuum modes are physically realized and gravitationally active.

In the horizon-layered cosmology, only *encoded* vacuum information, those degrees of freedom causally registered on the boundary, contribute gravitationally. The effective vacuum energy density is constrained not by volumetric mode summation but by the holographic area scale. Following the thermodynamic–holographic arguments of Padmanabhan and the equipartition treatments of horizon energy by Verlinde and Gibbons–Hawking, the effective vacuum density can be expressed as

$$\rho_{\rm vac} \;\simeq\; \kappa\,\frac{c^4}{8\pi G\, r_{\rm s}^{\,2}},$$

where $r_{\rm s}$ is the black-hole or cosmic boundary radius defining the curvature scale, and $\kappa = \mathcal{O}(1-10)$ is a dimensionless factor encoding the horizon convention (event vs. particle or de Sitter normalization) and the fractional redundancy of the boundary code assigned to vacuum degrees of freedom. This scaling may be obtained either (i) from the de Sitter relation $\rho_\Lambda = \Lambda c^2/(8\pi G)$ with $\Lambda = 3/r_{\rm s}^2$, or (ii) from the holographic equipartition condition $E = \frac{1}{2}Nk_BT$, with $N = A/(4\ell_{\rm p}^2)$ and the Gibbons–Hawking temperature $T = \hbar c/(2\pi k_B r_{\rm s})$. In both derivations, the vacuum energy density scales as $r_{\rm s}^{-2}$, linking it directly to the finite information capacity of the cosmic boundary rather than to divergent zero-point energies.

The inverse-square scaling of vacuum energy, $\rho_{\rm vac} \propto c^4/(Gr^2)$, has appeared previously in different theoretical contexts. In classical de Sitter cosmology, $\Lambda = 3/r^2$ implies $\rho_\Lambda = 3c^4/(8\pi Gr^2)$, a purely geometric identification of curvature with energy density. In the thermodynamic approach of Gibbons and Hawking [50], this same scaling emerges from the horizon temperature $T = \hbar c/(2\pi k_{\rm B} r)$ and entropy proportional to surface area. Padmanabhan [51, 52] and Verlinde [53] reinterpreted these

relations through holographic equipartition, viewing gravity as emergent thermodynamics. Independently, holographic dark-energy models such as Li [54] adopted $\rho_{\rm vac} = 3c^2 M_p^2 L^{-2}$ as an empirical ansatz, fitting the observed dark-energy density when L is taken as the cosmological horizon scale.

In contrast to these heuristic or empirical formulations, the horizon-layered cosmology derives the same functional dependence from the discrete, causal mechanics of horizon encoding. Here,

$$\rho_{\rm vac} \;\simeq\; \kappa\,\frac{c^4}{8\pi G\, r_{\rm s}^2}$$

emerges not as a postulate or thermodynamic analogy but as the geometric consequence of finite information throughput at the causal boundary. Vacuum energy represents the residual curvature associated with limited redundancy of the holographic code, dynamically regulated by the rate of Planck-scale incorporations. This causal–holographic interpretation provides the missing microphysical mechanism behind the holographic dark-energy relation, replacing heuristic thermodynamic reasoning with an operational encoding principle rooted in null-layer growth dynamics.

Using the previously calculated cosmic horizon radius $r_{\rm s} = 2.534171 \times 10^{26}$ m (§84) gives

$$\rho_{\rm vac}(\kappa{=}1) \;=\; \frac{c^4}{8\pi G r_{\rm s}^2} \;\approx\; 7.50 \times 10^{-11}\ {\rm J\,m^{-3}} \;\approx\; 8.34 \times 10^{-28}\ {\rm kg\,m^{-3}}.$$

The 2015 *Planck* measurement is $\rho_{\rm vac}^{\rm Planck} \approx 5.96 \times 10^{-27}\ {\rm kg\,m^{-3}}$, which corresponds to a calibration factor

$$\kappa \;=\; \frac{\rho_{\rm vac}^{\rm Planck}}{c^4/(8\pi G r_{\rm s}^2)} \;\approx\; 7.15.$$

This κ can naturally be interpreted as the product of (i) a de Sitter/Hubble normalization factor ~ 3 and (ii) a code–redundancy or sector-weighting factor ~ 2.4, both of order unity.

In this view, the "vacuum energy" is not a bulk sum of zero-point modes but residual curvature arising from finite redundancy in the holographic boundary code. As the horizon area $A = 4\pi r_{\rm s}^2$ grows, redundancy increases and the effective density $\rho_{\rm vac} \propto r_{\rm s}^{-2}$ dilutes. The cosmological constant thus represents a dynamically regulated curvature term that tracks the evolving information capacity of the horizon, rather than a fixed universal constant. Within the natural range of $\mathcal{O}(1)$ in κ, the holographic estimate reproduces the observed vacuum energy scale, resolving the vacuum catastrophe without invoking divergent zero-point sums.

In the horizon-layered picture, this dilution arises directly from the causal incorporation of new Planck cells: as each layer is added, the boundary's information capacity expands, reducing the effective vacuum curvature and driving the observed cosmic acceleration.

5.5 Schwarzschild-Hubble Relation and Holographic Principle

In this framework, our universe originated from a Planck-sized seed within a parent black hole, which accreted rapidly through a redshifted layered horizon. But we need to reconcile this with the fact that the inside observers observe a spatially flat, homogeneous, and isotropic Friedmann–Robertson–Walker (FRW) universe, in which the spacetime geometry is described by the scale factor $a(t)$, with $H(t) = \dot{a}/a$ denoting the Hubble parameter and $d\Omega^2$ the metric on the unit 2-sphere. This geometry possesses no preferred spatial location, every point is equivalent, and the line element is given by:

$$ds^2 = -c^2\,dt^2 + a(t)^2\left[dr^2 + r^2 d\Omega^2\right]. \tag{93}$$

The first Friedmann equation can be written as

$$H^2 = \frac{8\pi G}{3}\rho, \tag{94}$$

where ρ is the total mass–energy density (including matter, radiation, and vacuum contributions).

The Hubble radius is defined as

$$r_h = \frac{c}{H}. \tag{95}$$

The total mass–energy enclosed within the Hubble sphere is

$$m_h = \frac{4\pi}{3} r_h^3 \rho. \tag{96}$$

Substituting equations (94) and (95) into equation (96) yields

$$m_h = \frac{4\pi}{3}\left(\frac{c}{H}\right)^3 \frac{3H^2}{8\pi G} = \frac{c^3}{2GH}. \tag{97}$$

Rewriting this result in terms of r_h gives

$$r_h = \frac{2Gm_h}{c^2}. \tag{98}$$

Equation (98) is formally identical to the Schwarzschild radius relation for a static black hole of mass m.

In conventional cosmology, equation (98) is viewed as a mathematical identity arising from the Friedmann equation for $k = 0$ spatial curvature. The Hubble radius is an apparent horizon, not a true event horizon: it does not causally disconnect the interior from the exterior permanently, and comoving objects can re-enter it as H decreases over cosmic time. The Schwarzschild relation holds only when $r_h = c/H$ and m_h is the total mass–energy enclosed within this sphere. For any other radius

$r \neq r_h$, the enclosed mass scales as

$$m_{\text{frw}}(r) = \frac{4\pi}{3} r^3 \rho, \tag{99}$$

where ρ is the constant matter-energy density. Thus, the equality $r = 2Gm/c^2$ is unique to the Hubble scale in standard FRW and does not hold at arbitrary radii.

In the framework proposed here, the Schwarzschild equality is not a mere formal coincidence but a physical statement: the observable universe is interpreted as the interior of a parent black hole. The surface at r_{s} (the parent black hole radius) functions as a holographic screen, encoding all physical degrees of freedom within it in accordance with the holographic principle. This view is motivated by the Bekenstein–Hawking entropy bound, which requires that the maximal information content of any spatial volume is proportional to the area of its bounding surface. In this model, the interior spacetime is a projection from the null surface at r_{s}, analogous to the interior description of a black hole in holographic dualities. The coincidence of equation (98) is therefore elevated from a mathematical identity to an ontological clue: the large-scale universe *is* a holographically generated black hole interior.

5.6 The Schwarzschild Identity Consequences

In the horizon-layered cosmological model, the universe is treated as the interior of a parent black hole, with the Schwarzschild relation $R = 2M$ enforced universally (in geometric units $G = c = 1$). This relation holds exactly at all times for the observer located at the center of symmetry. In this model, the total mass of the parent black hole is exactly twice the mass enclosed within the Hubble radius:

$$r_{\text{s}} = 2r_h \quad \Rightarrow \quad M_{\text{bh}} = 2M_h. \tag{100}$$

Although the Hubble mass constitutes 50% of the total black hole mass, the Hubble volume occupies only 12.5% of the total interior volume:

$$P = \frac{V_h}{V_{\text{bh}}} = \left(\frac{r_h}{r_{\text{s}}}\right)^3 = \left(\frac{1}{2}\right)^3 = 0.125. \tag{101}$$

This discrepancy arises from the non-additive nature of black hole horizons. When two black holes of equal mass M merge, the resulting black hole of mass $2M$ has radius $r_{\text{s}} = 4M = 2r$, doubling the radius rather than increasing according to the naive Euclidean volume scaling

$$r_{\text{classical}} = (2r^3)^{1/3} \approx 1.26r, \tag{102}$$

which would underestimate the true radius growth. This behavior is a direct consequence of the holographic area law $A \propto M^2$, ensuring linear growth $r \propto M$ and contrasting with classical volume-based intuition.

If the holographic principle holds universally, then every finite spatial region must be fully described by degrees of freedom residing on its boundary. The model proposed

here extends this notion to all interior regions of the cosmic black hole, postulating that the Schwarzschild relation

$$r = \frac{2Gm(r)}{c^2} \tag{103}$$

is satisfied for all concentric spheres inside the universe. This implies a linear mass–radius scaling

$$m(r) = \frac{c^2}{2G} r, \tag{104}$$

and consequently a radially dependent mass density

$$\rho(r) = \frac{dM}{dV} \propto \frac{1}{r^2}, \tag{105}$$

implying denser inner regions and lighter outer shells.

Such a profile differs fundamentally from the homogeneous FRW model, introducing a preferred center and breaking large-scale spatial homogeneity. This feature represents both a strength and a conceptual challenge: it embeds the holographic principle deeply into the structure of spacetime but requires a justification for why an FRW-like region emerges near the center despite global Schwarzschild saturation.

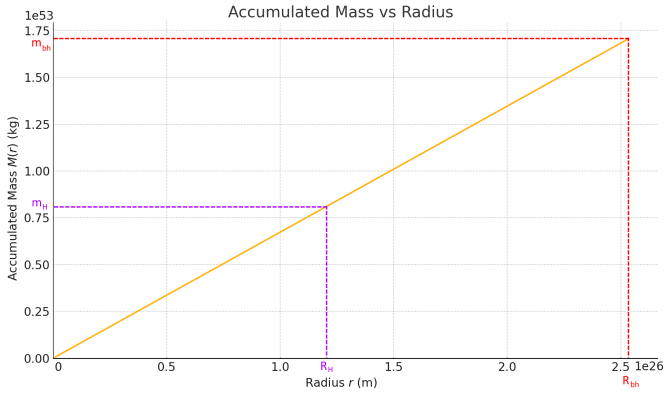

Fig. 9 Graph of accumulated mass $M(r)$ versus radius r, assuming a radial density profile where $\rho(r) \propto 1/r^2$. The mass increases linearly with radius in this model, reaching the total black hole mass $m_{\rm bh} = 1.706246 \times 10^{53}$ kg at the Schwarzschild radius $R = 2.53418 \times 10^{26}$ m, consistent with the $R = 2M$ condition. The Hubble mass m_H is reached at the 50% of the black hole total radius

Below we show that this tension is only apparent: an *approximate* FLRW metric can arise naturally in a finite central region of the holographic interior without abandoning the global Schwarzschild saturation.

A useful exact class of spherically symmetric solutions that continuously interpolates between global radial inhomogeneity and local FLRW

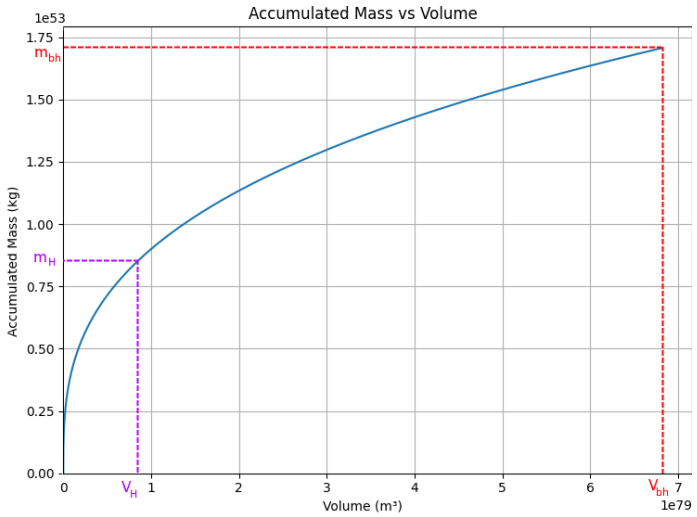

Fig. 10 Graph of accumulated mass $M(r)$ versus volume V, assuming a radial density profile where $\rho(r) \propto 1/r^2$. The mass grows nonlinearly with volume in this model, reaching the total black hole mass $m_{\rm bh} = 1.706246 \times 10^{53}$ kg at the Schwarzschild volume $V = 6.81712 \times 10^{79}\,\mathrm{m}^3$, consistent with the $R = 2M$ condition. The Hubble mass m_H is reached at the 12.5% of the black hole total volume.

behaviour is the Lemaître–Tolman–Bondi (LTB) family (spherically symmetric dust). An LTB metric may be written as

$$ds^2 = -dt^2 + \frac{\big(R'(t,r)\big)^2}{1+2E(r)}\,dr^2 + R(t,r)^2 d\Omega^2, \tag{106}$$

with local mass function $m(r)$ and energy function $E(r)$. Choosing $m(r)$ so that $m(r) \propto r$ reproduces the global scaling (105), while imposing regularity conditions near $r = 0$ yields a region where $R(t,r) \simeq a(t)\,r$ and the metric reduces to FLRW to leading order. Thus, an LTB construction demonstrates that a centrally defined FLRW patch is an exact, regular limit of spherically symmetric, Schwarzschild-saturated interiors.

Two physically motivated mechanisms in the holographic membrane justify a nearly homogeneous central region.

The membrane field theory includes an effective lateral stiffness (tension) and short-range entangling interactions between neighbouring Planck patches. These lateral dynamics redistribute information and stress, acting like an effective pressure that resists large radial gradients over distances comparable to the lateral correlation length ξ. If the correlation length established during collapse (e.g. via a Kibble–Zurek type quench) satisfies $\xi \gtrsim R_c$, then the membrane actively smooths phase and density fluctuations across the central region $r \lesssim R_c$, producing an effective uniformity on scales relevant for observers.

Life and macroscopic structure preferentially arise where gradients are mild. Observers will therefore most likely be found within central regions where the membrane coherence has already produced near-uniform baryonic clustering. This

anthropic/selection effect does not require global homogeneity, only that the observer's causal patch satisfies small relative density contrast.

Combining these two mechanisms, a small central radius R_c naturally develops that is effectively homogeneous and isotropic on scales $\lesssim R_c$.

For a Hubble patch centred on an observer at radius r_0 to be well described by FLRW it suffices that the fractional density variation across that patch is small:

$$\left.\frac{\Delta\rho}{\rho}\right|_{r_h} \equiv \frac{\rho(r_0+\Delta r)-\rho(r_0)}{\rho(r_0)} \ll 1, \tag{107}$$

with $\Delta r \sim r_h$ the patch size. For the global profile $\rho(r) \propto r^{-2}$ we have

$$\frac{\Delta\rho}{\rho} \simeq -2\,\frac{\Delta r}{r_0}\,.$$

Therefore the condition (107) becomes $\Delta r \ll r_0/2$. If the observer sits sufficiently near the centre (i.e. $r_0 \gtrsim r_h$ or if the central homogeneous core has $R_c \gtrsim r_h$), the density variation within the Hubble sphere is small and the local geometry is well approximated by FLRW. Physically, this is the statement that the Hubble sphere samples only a narrow radial range where the r^{-2} law is almost constant.

A consistent scenario that yields an internal FLRW patch is therefore: global holographic saturation enforces $M(R) \propto R$ at large radii (outer shell), membrane coherence and lateral smoothing produce a central core of radius R_c whose density is approximately constant on scales $\lesssim R_c$ and one (or many) observer-sized Hubble patches lie within this core, satisfying $\Delta\rho/\rho \ll 1$ and therefore experiencing locally FLRW kinematics and dynamics to high precision.

This picture is empirically distinct from strict global FLRW and yields falsifiable predictions. The number counts, BAO scales, and average galaxy densities should show a weak, monotonic radial trend on scales approaching R_c–r_s (testable with DESI, Euclid, LSST). Off-centre observers would see small hemispheric asymmetries in large-scale clustering and in the low multipoles of the CMB; current CMB dipole/quadrupole limits constrain our displacement from the symmetry centre. Fitting local expansion history and distance–redshift relations with an LTB model matched to the holographic mass function will determine the allowed R_c and the degree of required membrane smoothing.

Rather than forcing a global FLRW metric, the horizon-layered model explains why FLRW is an excellent *local* approximation in empirically relevant patches: membrane dynamics (coherence and tension), selection effects, and the possibility of a regular central region together produce near-homogeneity on observer scales. The outer region remains holographically saturated and Schwarzschild-governed, so entropy bounds are respected globally while the internal patch reproduces the phenomenology that has been ascribed to an FRW spacetime. The interpolation is physically natural, mathematically implementable (via LTB→FLRW limits), and observationally testable.

5.7 The Inaccessibility of the Outer Horizon

In the horizon-layered cosmology, the Schwarzschild radius $r_{\rm s}$ defines not a fixed surface in space but a dynamically advancing causal frontier. Each Planck tick of internal time $t_{\rm p}$ corresponds to the incorporation of one Planck mass $m_{\rm p}$ and the creation of a new null layer of radial width $2\ell_{\rm p}$. This synchronization of mass, radius, and time increments,

$$(\Delta M,\, \Delta r_s,\, \Delta t) = (m_{\rm p},\, 2\ell_{\rm p},\, t_{\rm p}), \tag{108}$$

implies an effective radial growth rate

$$\frac{dr_{\rm s}}{dt} \;=\; \frac{2\ell_{\rm p}}{t_{\rm p}} \;=\; 2c. \tag{109}$$

The outer horizon therefore advances at twice the speed of light relative to the internal frame. Because no physical signal or photon within the interior can exceed c, it is kinematically impossible for any emission to reach or overtake this expanding boundary. Even as radiation propagates outward at c, the causal frontier itself recedes faster, maintaining a permanent separation between the internal spacetime and the external universe.

Consequently, no physical signal, energy, or information emitted within the internal universe can ever cross beyond $r_{\rm s}$. The horizon constitutes a moving causal limit of reality, an interface between distinct manifolds that cannot communicate except through the encoded boundary degrees of freedom. In this sense, the event horizon is not a location in space, but a transition in ontology: a dynamic domain where spacetime itself changes character with each Planck-step reconfiguration.

This causal structure integrates naturally with the model's null-ordered holographic encoding. As $r_{\rm int}(z) \to r_{\rm s}$, the redshift diverges and the internal coordinate time required to reach $r_{\rm s}$ becomes asymptotically infinite. Outgoing null rays "freeze" in place, their phase information stretched over unbounded intervals. No internal observer ever witnesses an event crossing the horizon; rather, each approaching signal becomes part of the boundary's evolving quantum code, ensuring that unitarity and causal completeness are preserved. The universe thus possesses a strict finite bound $r_{\rm s}$ while exhibiting the observed cosmological signatures of accelerating expansion and redshifted recession for distant sources.

In this model, the cosmic horizon corresponds to twice the Hubble radius,

$$r_s = \frac{2c}{H_0} \approx 26.8\,\mathrm{Gly}, \tag{110}$$

defining a causal limit intrinsically linked to the present Hubble flow. By contrast, the $\sim 46\,\mathrm{Gly}$ radius of the observable universe in standard ΛCDM cosmology represents the particle horizon, the comoving distance from which the oldest observable photons were emitted after 13.8 Gyr of propagation through an expanding background. This difference arises because the particle horizon measures accumulated light travel, whereas the holographic horizon measures the instantaneous causal limit of an

expanding black-hole interior. The factor of two between $r_{\rm s}$ and r_h thus expresses the geometric relation between the local expansion rate and the global causal boundary, without violating any physical constraint.

Unlike the homogeneous scaling $\rho_m \propto (1+z)^3$ of standard FLRW cosmology, the horizon-layered model maintains holographic saturation at all scales, enforcing the Schwarzschild relation $r_s = 2M$ locally and globally. The redshift–time correspondence,

$$t(z) = \frac{t_0}{1+z}, \qquad t_0 \approx 13.4\,\mathrm{Gyr}, \tag{111}$$

emerges directly from the null-layer ordering and provides testable predictions for galaxy number densities and baryon acoustic oscillation (BAO) scaling observable by DESI, JWST, and future surveys. By embedding holography directly into the dynamical horizon, this framework resolves the entropy-bound tension of early FLRW cosmology and eliminates the need for an inflationary epoch. Entropy, energy, and causal order arise self-consistently from the Planck-synchronized null layering of spacetime.

A natural corollary is that observers are statistically favored to emerge within the inner half-radius of the total mass distribution, where the identity $r_h = 2M_h$ holds. This corresponds to the 50% mass fraction enclosed within the central 12.5% of the total volume, explaining why most observers measure a local Schwarzschild–Hubble correspondence. Off-center observers would detect small hemispheric asymmetries in number counts and clustering, potentially observable by 2MASS, SDSS, DESI, and LSST.

Finally, while the outer layers obey the Schwarzschild scaling $\rho(r) \sim 1/r^2$, continuation of this law to $r \to 0$ would lead to a singularity. To avoid this, the model introduces a central transition region $r < R_c$ of nearly uniform, FRW-like density, preserving isotropy and homogeneity at large scales while maintaining holographic and Schwarzschild behavior near the boundary. The resulting interior universe is coherent, self-contained, and causally complete: nearly FRW-like in its core, holographically encoded at its frontier, and globally governed by the universal identity $R = 2M$.

In the horizon-layered model, the internal (cosmic) time t is identified with the discrete accumulation of horizon incorporation events, so that $t_{\rm int} = t$ and, in geometric units, $t_{\rm int} = M_{\rm bh}/c$. The model therefore implies the simple reciprocal relation between the effective Hubble parameter and the internal clock:

$$H \;=\; \frac{c}{M_{\rm bh}} \;=\; \frac{1}{t_{\rm int}} \;=\; \frac{1}{t}. \tag{112}$$

Two immediate consequences follow.

First, internal observers whose proper time is measured by the same null-ordered sequence of membrane updates that defines t, experience a uniform local tick rate (their clocks advance normally). The decrease of H with cosmic time is not perceived as a local slowing of proper time: rather, it is a change in the large-scale kinematics of the emergent geometry (the rate of cosmological expansion measured in inverse time units).

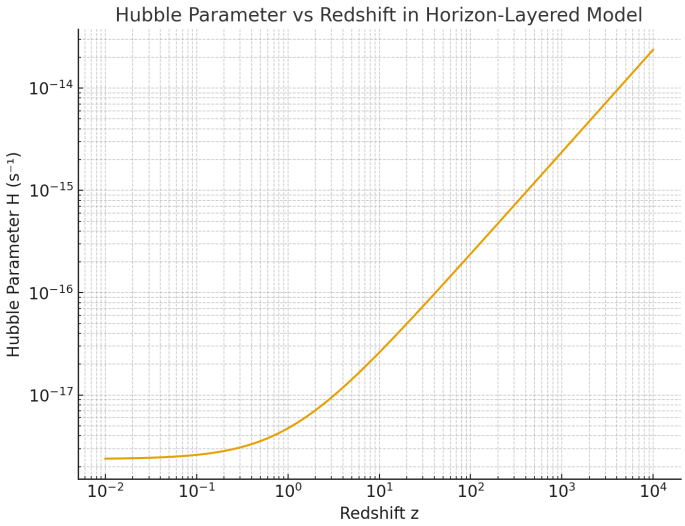

Fig. 11 Hubble parameter as a function of redshift in the horizon-layered cosmology. The plotted curve shows the linear relation $H(z) = \frac{1+z}{4.2265427\times10^{17}}$ s^{-1}, predicted by the causal incorporation model, with the redshift z expressed on a logarithmic scale. In this framework, the Hubble parameter is not governed by energy-density dilution as in the standard ΛCDM cosmology, but arises directly from the discrete, constant incorporation of information quanta across the holographic horizon. The expansion of space corresponds to the cumulative growth of internal time, $H = 1/t$, where t measures the total number of successful incorporations since the initial horizon formation. Thus, the apparent decrease of H with cosmic time does not signify a slowing of dynamics or matter dilution, but simply reflects the increasing temporal depth of the internal universe as more information is encoded. The incorporation rate itself remains fixed at one quantum per Planck tick, defining the universal causal rhythm underlying cosmic expansion.

Second, because $H \propto 1/t$, the expansion rate necessarily decays as the internal clock advances. In the present picture this decay has a simple causal origin: as more Planck-area quanta are incorporated the total encoded mass $M_{\rm bh}$ (and hence t) increases, diluting the instantaneous expansion rate H according to (112). Thus an internally steady clock coexists with a decreasing Hubble parameter; internal observers register normal local physics while the global expansion slows as $1/t$.

This framework reinterprets cosmic expansion as the causal response of spacetime to the increasing internal information load. The apparent dark energy density arises not from an external cosmological constant, but from the information-pressure that sustains holographic equilibrium. The universe expands to accommodate the influx of new encoded quanta, maintaining the holographic bound across cosmic history.

The holographic bound acts as a global regulator of information density. As the causal boundary grows, more Planck-scale incorporation events occur, generating additional spacetime volume and internal proper time. The expansion of space therefore *is* the geometric expression of information growth. In contrast to classical cosmology, where total mass-energy is assumed conserved, the present model treats mass and information as dynamically co-generated quantities. The internal universe grows in

both extent and complexity as new layers of the holographic code become causally integrated.

Invariant Mass Growth via Horizon Encoding and Chandrasekhar Limit Detectors

Classical cosmology, formulated within general relativity and the ΛCDM paradigm, describes the universe as a continuous four-dimensional manifold whose geometry evolves according to the Friedmann equations. In this picture, cosmic expansion is a purely geometric process driven by the interplay of matter, radiation, and dark energy densities, with the total mass–energy of the universe approximately conserved. This view is geometrically complete but *informationally incomplete*. It neglects the evolution of the universe's total information capacity, treating expansion as a smooth deformation of geometry without accounting for how the number of physically realizable states evolves with time.

From an informational standpoint, this omission leads to a fundamental inconsistency. If the universe's spatial volume grows as $V(t) \propto a^3(t)$ while its total mass–energy remains fixed, the average information density must decline rapidly as the universe expands. Yet, the Bekenstein–Hawking bound asserts that the maximal information content of any causal region is proportional not to its volume but to the *area* of its boundary:

$$S_{\max} = \frac{k_B c^3}{4G\hbar} A, \tag{113}$$

where A is the area of the bounding surface. As the cosmic boundary grows with time, its total information capacity must increase as $A(t) \propto R^2(t)$. A static information bound would therefore contradict the observed expansion of spacetime.

In the horizon-layered cosmology, this inconsistency is resolved by assigning physical causality to the growth of the boundary itself. The universe's expansion is reinterpreted as the geometric manifestation of ongoing information incorporation at the causal horizon. Each discrete Planck-scale incorporation event adds one quantum of horizon area and one Planck unit of mass–energy, advancing internal time by a single causal tick. The holographic bound is dynamically saturated at all times:

$$I_{\max} = \frac{A}{4\,\ell_{\mathrm{p}}^2} \tag{114}$$

The causal growth of A therefore represents the physical process through which both spacetime and information evolve in synchrony.

In the horizon-layered cosmological framework, the internal mass of the universe increases in concert with the growth of the parent black hole's horizon and information capacity. A compelling question arises: through which channels is this added mass distributed internally?

A recent theoretical and observational literature on cosmologically coupled black holes, for instance, Croker and Weiner [55] showed that in non-singular black hole

models with vacuum-energy interiors, the gravitating mass evolves as

$$m(a) = M(a_i) \left(\frac{a}{a_i} \right)^k , \tag{115}$$

where a is the scale factor and $k = -3w$. If the internal equation-of-state parameter $w = -1$ (vacuum energy), then $k = 3$, yielding $m \propto a^3$. This scaling ensures that, although the number density of black holes drops as a^{-3}, the total mass density remains constant, effectively mimicking a cosmological constant, i.e., dark energy [56].

Observationally, Farrah et al. (2023) found significant evidence for such coupling in elliptical galaxies across $0 < z \lesssim 2.5$, ruling out $k = 0$ at 99.98% confidence and suggesting consistency with $k \approx 3$ within uncertainties. These findings suggest that black hole mass can grow with the cosmic expansion, independently of accretion or mergers [56, 57].

Within the holographic membrane picture, black holes in our universe appear as *punctures* on the surface of the parent horizon. As the parent horizon expands due to continued infall from its own embedding universe, these punctures widen in proportion to the parent's area increase. Thus, even in the absence of local accretion, the event horizons of child black holes embedded in our universe inherit growth from the global dynamics of the parent surface. Formally, one may write

$$\frac{\dot{R}_{\text{child}}}{R_{\text{child}}} \approx \frac{\dot{R}_{\text{parent}}}{R_{\text{parent}}}, \tag{116}$$

where R_{child} and R_{parent} are the radii of the child and parent horizons, respectively. This coupling ensures entropy conservation across layers while providing a natural holographic mechanism for cosmological black hole growth.

We now extend this principle beyond black holes. In the invariant mass growth hypothesis, all gravitating structures, stars, planets, compact remnants, and even gas clouds, gain mass proportionally with cosmic time.

This universality ensures that dynamical relations remain intact: orbital trajectories are unaffected, galactic structures remain stable, and stellar evolution proceeds in familiar patterns. The growth applies universally, such that every body with gravitational identity inherits additional mass. This proposal thus circumvents the restrictive assumption that only black holes experience cosmological coupling [55, 56]. Instead, the growth is holographically encoded across all scales.

A particularly striking implication emerges for degenerate stars near critical thresholds. In standard astrophysics, Type Ia supernovae are attributed either to accretion from a companion (single-degenerate channel) or to binary white dwarf mergers (double-degenerate channel). Both scenarios face serious challenges: the paucity of accreting systems in X-ray surveys [58], the lack of observed surviving companions after explosions [59], and the difficulty of sustaining fine-tuned accretion rates without mass loss via novae.

Within the invariant growth framework, such contrived channels are unnecessary. **White dwarfs naturally gain mass slowly and uniformly as part of the universal holographic encoding process. When a white dwarf's mass reaches**

the Chandrasekhar limit,

$$M_{\mathrm{Ch}} \approx 1.44\, M_{\odot},$$

it explodes, independent of any local accretion or merger history. Since the Chandrasekhar mass is a fixed threshold determined by fundamental constants, it acts as an invariant "cosmic trigger." This mechanism directly explains both the uniformity of Type Ia explosions and their role as standard candles: they are, in effect, *horizon-driven Chandrasekhar limit detectors of universe total mass increase.*

Thus, the very phenomenon that anchors cosmological distance measurement may instead be the most direct observational proof of universal mass growth via horizon encoding. Type Ia supernovae, far from being powered by improbable accretion, are signatures of the deep holographic coupling between our universe and its parent horizon.

5.8 Merging Black Holes and Internal Causal Reconfiguration

In the framework of horizon-layered cosmology, black hole mergers are not merely external astrophysical events but correspond to deep reorganizations of the internal causal structure. Each black hole, prior to merger, possesses its own null-ordered horizon encoding: a layered quantum surface from which an internal spacetime emerges. This internal evolution is driven by causal incorporations associated with discrete accretion events, as described in previous sections.

When two black holes merge, their event horizons coalesce into a single, larger apparent horizon. Externally, this process is accompanied by a burst of gravitational radiation and a sudden increase in the total horizon area and entropy:

$$S_{\mathrm{total}}^{\mathrm{after}} > S_1 + S_2, \tag{117}$$

$$\Delta S = \frac{k_B c^3}{4G\hbar}\,(A_{\mathrm{after}} - A_1 - A_2) > 0. \tag{118}$$

The increase in horizon entropy activates new degrees of freedom in the holographic code, allowing for additional causal strata to be generated internally. However, the precise outcome depends on the relative masses and coherence structure of the merging horizons.

In the first scenario, where both black holes are of comparable mass, the merger reinitializes the null-ordered encoding. The result is the formation of a new, unified causal manifold internally, a fresh emergent spacetime seeded by superposed or entangled boundary conditions from both progenitor horizons. The merger, in this sense, represents a cosmogenic transition: the causal code reorganizes into a new internal universe with its own null origin and arrow of time.

In the second scenario, where one black hole dominates in mass, the internal universe associated with the dominant horizon persists through the merger. The incorporation of the smaller horizon then appears, from the internal perspective, as a violent causal shock or injection event, reconfiguring the near-horizon causal order

without destroying global coherence. The added horizon area corresponds to a discrete advance in internal causal layering, producing a measurable increase in the effective internal expansion rate.

From the internal viewpoint, the merger can manifest as the sudden addition of a new spacetime region causally adjoining the existing manifold, accompanied by a discontinuous change in the internal Hubble constant,

$$H_{\text{int}}^{\text{after}} \neq H_{\text{int}}^{\text{before}}. \tag{119}$$

The change in the internal expansion rate can be related to the relative increase in the total horizon area. Since the internal expansion rate is governed by the causal update frequency of the horizon code, and the area determines the number of active encoding sites, one finds a proportional relation of the form

$$\frac{H_{\text{int}}^{\text{after}}}{H_{\text{int}}^{\text{before}}} \approx \left(\frac{A_{\text{after}}}{A_{\text{before}}}\right)^{1/2}, \tag{120}$$

or, equivalently,

$$\Delta H_{\text{int}} \propto \frac{1}{2H_{\text{int}}^{\text{before}}} \frac{\dot{A}}{A}, \tag{121}$$

where $\dot{A}$ is the rate of change of the horizon area during merger. Thus, an external increase in horizon area maps to an accelerated expansion rate of the internal universe. In the limit of equal-mass mergers, the sudden doubling of A implies a transient inflationary episode within the internal domain, consistent with a jump in the effective vacuum energy density. This corresponds to a phase-transition-like event analogous to a cosmological constant shift, $\Lambda \to \Lambda'$, as in vacuum decay scenarios [45, 60, 61].

In the present horizon-layered model the internal Hubble rate is the inverse of the internal clock time,

$$H_{\text{int}} = \frac{1}{t_{\text{int}}},$$

and, using the identification $t_{\text{int}} = M_{\text{bh}}/c$ (with M_{bh} expressed in geometric units, i.e. as a length), one obtains the compact relation

$$H_{\text{int}} = \frac{c}{M_{\text{bh}}}. \tag{122}$$

For a binary merger the post-merger internal Hubble rate follows directly from the sum of the geometric masses (neglecting radiative mass loss for simplicity):

$$M_{\text{after}} \simeq M_1 + M_2 \quad \Longrightarrow \quad H_{\text{int}}^{\text{after}} = \frac{c}{M_1 + M_2}.$$

Hence the ratio of post- to pre-merger Hubble rates is

$$\frac{H_{\text{int}}^{\text{after}}}{H_{\text{int}}^{\text{before}}} = \frac{M_{\text{before}}}{M_1 + M_2},$$

where M_{before} is the appropriate pre-merger mass used for comparison (e.g. M_1).

This result is fully consistent with the area-based scaling used earlier: since the horizon area scales as $A \propto M_{\text{bh}}^2$, one has $A^{1/2} \propto M_{\text{bh}}$ and therefore the relation

$$H_{\text{int}} \propto A^{-1/2}$$

is algebraically equivalent to (122).

Externally, the merger produces gravitational waves, metric perturbations radiating from the high-shear deformation of the null-layered surface during coalescence. Internally, these waves correspond to non-adiabatic code transitions, localized anisotropies, or topological defects imprinted in the emergent spacetime. While internal observers cannot directly perceive the external merger, they would experience its consequences as a sudden cosmological event: a burst of anisotropy, a jump in expansion rate, or even the appearance of a new causal domain.

In summary, black hole mergers in this framework are inherently cosmogenic. They mark transitions between distinct epochs of causal organization. Depending on the mass ratio and phase coherence of the merging horizons, the result may be a rebirth, a shock, or a fusion of internal histories. The newly merged horizon defines a revised boundary condition for the internal arrow of time and entropy flow, establishing a fresh layer of cosmological evolution grounded in the holographic reconfiguration of the horizon code.

Within the horizon-layered framework, mergers between parent black holes correspond to discrete reorganizations of the internal causal code, inducing abrupt transitions in the emergent Hubble rate. When the parent horizon mass increases discontinuously during a merger, the corresponding internal expansion rate decreases, producing a sudden change in the effective cosmological constant. From the internal perspective, such transitions could manifest as steps in cosmic acceleration, anisotropic dark energy components, or large-scale topological anisotropies. Observed anomalies such as the CMB quadrupole suppression, dipolar alignments, and Hubble-tension discrepancies may represent residual signatures of these parent-level causal reorganizations.

5.9 Fate of the Internal Universe During Evaporation

In this framework, accretion increases horizon entropy and drives the internal arrow of time via causal updates to the horizon code. When accretion halts, internal time freezes, as no new layers are added. However, once the black hole begins to evaporate, horizon entropy decreases. This too triggers discrete reorganizations of the horizon quantum code, producing a new sequence of causal updates internally.

Importantly, this does not imply that internal observers experience time running backwards. The bits lost to evaporation are not shed in the same order they were acquired during accretion. The internal evolution during evaporation constitutes a distinct causal history, not a reversal of the original one. From the inside, time still appears to move forward, even though from the external perspective the system's entropy is decreasing. This asymmetry reflects the deeper holographic structure of

time in this model: the arrow of time emerges from the causal structure of horizon-layer updates, not from global entropy monotonicity alone.

In the horizon-layered cosmology, time is not a continuous geometric parameter but a discrete causal process: each increment of internal time corresponds to the successful incorporation of one quantum of information into the null-synchronized membrane. The cumulative internal time is therefore a direct count of these incorporations. The sequence of incorporations defines an intrinsic causal order that cannot be reversed, since each new layer depends on the prior configuration of the horizon code.

Backward time travel would require reversing this causal sequence, that is, re-emitting the encoded quanta from the membrane in precisely the reverse order and with exact phase coherence. Such a reversal would correspond to a complete inversion of the membrane's causal dynamics, including the reordering of null synchronization across all horizon fibers.

Thus, backward time travel is not merely technologically unfeasible but fundamentally prohibited. It would require the global membrane to emit its stored information in reverse causal order, effectively undoing the universe's entire informational history. The horizon-layered model therefore provides a physical basis for temporal irreversibility, grounding the arrow of time in the discrete and unidirectional growth of the holographic boundary itself.

The black hole, from the external perspective, radiates away its stored information in a unitary and gradual fashion. The entropy associated with the internal universe is not destroyed but disentangled and emitted, potentially reconstructing the interior from the outside over extremely long timescales [62, 63]. The internal configuration is preserved in principle, even as it becomes causally disconnected from ongoing dynamics. If the horizon eventually dissolves entirely, the final encoding remains preserved in the emitted Hawking radiation, ensuring consistency with unitarity and holography [2].

In the maximally extended Schwarzschild geometry of classical general relativity, a black hole has a formal time-reversed counterpart, the white hole, representing a region from which matter and radiation can only emerge. Although mathematically consistent within time-symmetric field equations, such entities have no known physical realization. They would require an exact time reversal of all boundary conditions, violating the second law of thermodynamics and producing entropy decrease.

In the present model, white holes are excluded by construction. The null-synchronized horizon evolves through discrete incorporations of Planck-scale quanta, each step increasing entropy and advancing internal causal time:

$$t_{\text{internal}} = N\, t_{\text{p}}, \qquad \Delta S > 0.$$

This directed layering defines an intrinsic arrow of time, independent of external observers. Reversing this process would require the holographic membrane to emit quanta in precisely the reverse causal sequence, effectively reversing the temporal order of the entire universe it encodes.

Even black hole evaporation does not constitute a white-hole phase: the Hawking process removes encoded information thermally from the outermost layers without reversing the incorporation order. The causal orientation of the code remains forward.

Consequently, the causal incorporation law replaces the time-symmetric structure of classical general relativity with a fundamentally oriented, information-theoretic dynamics. The white-hole solutions are thus recognized not as physical possibilities but as artifacts of an incomplete, time-symmetric treatment of gravitational collapse.

5.10 Kerr-Dependent Internal Physics and the Evolution of Cosmic Symmetry

In the horizon-layered cosmology, the angular momentum of the parent black hole plays a central role in determining the physical properties of its emergent internal universe. The Kerr spin parameter, expressed in SI units, is

$$a = \frac{J}{m_{\mathrm{bh}} c},$$

where J is the angular momentum and m_{bh} is the black hole's physical mass in kilograms. This parameter defines the degree of frame dragging and azimuthal phase twisting on the horizon surface. Because each horizon cell encodes information through locally synchronized null interactions, the global rotation of the horizon imprints a continuous phase gradient across the holographic code. This phase gradient constitutes a boundary condition for all subsequent causal incorporations, thereby influencing the emergent structure of the internal spacetime and the microscopic symmetries of its quantum fields.

The secondary dipole of each Planck-scale horizon cell couples to the local frame-dragging field, acquiring a spin-dependent phase shift during each Planck-time incorporation step. For a local angular velocity of frame dragging ω_{fd}, the phase increment per Planck tick is

$$\Delta\phi = 2\,\omega_{\mathrm{fd}}\,t_{\mathrm{p}} = \frac{4GJ\,t_{\mathrm{p}}}{c^2 r_{\mathrm{s}}^3}.$$

This geometric phase difference biases the relative populations of the two spin orientations of the horizon dipoles (co-rotating and counter-rotating), generating a chiral asymmetry that propagates into the internal universe as a matter–antimatter imbalance. Universes originating from more rapidly rotating black holes ($a \to G m_{\mathrm{bh}}/c^2$) therefore exhibit stronger intrinsic chirality and larger parity violation, while slowly rotating progenitors produce more symmetric, potentially matter–antimatter-balanced cosmologies. In this way, the parent black hole's rotation velocity acts as a global order parameter for the internal universe's quantum symmetry breaking pattern.

As the black hole's mass m_{bh} increases through accretion, the spin parameter $a = J/(m_{\mathrm{bh}}c)$ generally decreases, because angular momentum J grows more slowly than mass in most realistic astrophysical processes. The horizon rotation velocity thus diminishes with time, reducing the frame-dragging field and weakening the azimuthal phase bias. In the internal universe, this corresponds to a gradual relaxation of the

global chiral asymmetry, an effect that could manifest as the apparent alignment evolution of galactic spins or the redshift-dependent variation in polarization anisotropies observed in large-scale surveys.

Formally, the horizon angular velocity is given by

$$\Omega_h = \frac{ac^3}{2Gm_{\rm bh}r_{\rm s}},$$

which scales approximately as $\Omega_h \propto 1/m_{\rm bh}$ for moderate spins. Thus, the causal rotation rate of the boundary code decelerates as the parent horizon grows. This slowdown implies that the internal universe experiences a changing boundary phase gradient: in early epochs (corresponding to smaller $m_{\rm bh}$), the encoded phase anisotropy was stronger, imprinting pronounced spin alignments and chiral asymmetries; as the parent horizon expanded, these effects became diluted. The present-day isotropy of the CMB and the small residual parity violations in cosmological observables may therefore represent the surviving imprint of an initially stronger Kerr-induced asymmetry.

Because each black hole in any parent universe can possess a distinct rotation parameter, the physical laws of their corresponding internal universes may differ. The Kerr parameter acts as a geometric regulator of encoded symmetry: its magnitude and sign determine the sense and strength of chiral bias, the relative populations of spin states, and the direction of the emergent cosmic axis. In this picture, the ensemble of internal universes generated across the cosmic hierarchy spans a distribution of symmetry patterns, coupling constants, and anisotropy levels determined by the spin spectrum of their progenitor black holes. This mechanism provides a concrete physical realization of cosmological natural selection [64], in which universes with dynamically stable, information-efficient spin encodings are favored to produce further generations of black holes.

If the internal physical laws are indeed Kerr-dependent, residual signatures of the parent horizon's rotation should persist in the large-scale structure of our universe. Possible observable consequences include: small but coherent spin alignment of galaxies relative to a global axis (as observed in [65, 66]); parity-violating features or hemispherical power asymmetry in the CMB polarization spectrum; a slow evolution of global anisotropy with cosmic time, reflecting the decreasing frame-dragging strength as the parent horizon mass $m_{\rm bh}$ grows.

Such effects, if confirmed, would provide empirical evidence that the microscopic properties of matter and the macroscopic geometry of the universe share a common rotational origin.

In summary, the Kerr rotation of the parent black hole acts as a geometric control parameter for the internal universe's fundamental properties. It determines the magnitude of chiral asymmetry, the alignment of spin fields, and the strength of parity violation, while its gradual reduction with increasing $m_{\rm bh}$ defines the cosmological evolution of these asymmetries. Thus, particle physics and cosmology are unified under a single causal mechanism: the encoding of horizon information within a rotating Kerr geometry that links the microphysical structure of quantum matter to the macroscopic history of cosmic expansion.

5.11 Empirical Hints for Rotational Memory of the Horizon

The horizon-layered cosmology predicts that the internal universe retains a measurable imprint of its parent black hole's rotation. This imprint, expressed as a global azimuthal phase gradient across the holographic horizon, should manifest observationally as preferred-axis alignments, parity-violating asymmetries, and spin correlations in the large-scale structure of the universe. Although no single observation can uniquely identify such a holographic origin, a growing body of empirical evidence is consistent with the presence of a persistent rotational memory in cosmological data.

Recent analyses of deep-field galaxy surveys reveal statistically significant asymmetries in the distribution of spiral spin directions. For instance, [65–67] reported that spiral galaxies exhibit a weak but consistent preference in their rotational orientation across gigaparsec scales, with the degree of alignment increasing toward higher redshifts. More recent observations from the *James Webb Space Telescope* suggest similar spin-direction asymmetries among distant galaxies, implying that large-scale rotational coherence was stronger in the early universe [68]. Within the horizon-layered framework, such behavior follows naturally: as the parent black hole's mass $m_{\rm bh}$ grows through accretion, its spin parameter $a = J/(m_{\rm bh}c)$ decreases, reducing the strength of the phase gradient imprinted on the holographic code. Consequently, early cosmic epochs, when the parent horizon rotated more rapidly, would exhibit stronger global spin alignment, while later epochs would appear increasingly isotropic.

Observations of the cosmic microwave background have long shown low-ℓ anomalies, including alignments of the quadrupole and octupole moments, hemispherical power asymmetry, and parity violation in temperature and polarization modes [69, 70]. These features, collectively known as the "Axis of Evil," remain unexplained within standard ΛCDM cosmology. In the horizon-layered interpretation, they represent the large-scale relic of the parent black hole's rotational phase pattern projected onto the internal spacetime. The apparent alignment of low multipoles with the ecliptic and large-scale galaxy spin axis suggests that this primordial anisotropy may share a common causal origin—the global Kerr rotation encoded on the parent horizon.

Astrophysical studies of supermassive black holes indicate that spin parameters tend to decrease as mass increases, due to angular momentum loss through accretion torques, magnetic jets, and mergers [71, 72]. This secular spin-down mirrors the behavior expected in the parent horizon of the horizon-layered model: as $m_{\rm bh}$ grows, the dimensionless ratio $ac^2/(Gm_{\rm bh})$ diminishes, and with it the horizon's rotational phase bias. If the internal universe's physical laws depend on this parameter, as suggested here, then measurable traces of its historical variation could persist in the evolution of cosmic anisotropies, polarization alignments, and chiral asymmetries.

Taken together, these phenomena, galaxy spin alignment, CMB low-ℓ anisotropy, and black hole spin evolution, suggest a consistent pattern: the universe retains a subtle but coherent rotational signature that diminishes over time. This trend aligns with the expectation that the parent horizon's angular momentum per unit mass decreases as its total mass $m_{\rm bh}$ increases, producing a gradual relaxation of internal anisotropy and parity violation. The persistence of this faint directional memory across vastly different scales and epochs constitutes circumstantial but striking evidence that

our universe may indeed preserve a holographic record of the rotation of its progenitor black hole.

5.12 Apparent Quantum Randomness and Deterministic Parent Horizons

In conventional quantum mechanics, randomness is regarded as intrinsic: measurement outcomes are assumed to occur without underlying determinism. Within the horizon-layered cosmology, this interpretation is replaced by a causal–informational hierarchy in which quantum indeterminacy emerges from limited causal access to a deeper deterministic process.

Each universe in the holographic hierarchy arises as the internal projection of a parent horizon. From the parent frame, every Planck-scale incorporation event is a definite causal update, a discrete addition of one quantum of information-energy to the horizon code. From within the emergent internal spacetime, however, those same updates appear as probabilistic quantum events. The apparent stochasticity of wavefunction collapse therefore reflects the partial visibility of the underlying causal sequence: observers embedded inside the emergent universe can access only coarse-grained projections of the external encoding process.

In this framework, *quantum randomness is epistemic, not ontic.* It is a manifestation of informational coarse-graining imposed by the horizon boundary, not a fundamental property of reality. The deterministic evolution of the parent horizon generates, by causal projection, the statistical behavior described by the Born rule in the child universe:

$$P_{\text{internal}}(i) = \left|\langle i \,|\, \psi_{\text{encoded}}\rangle\right|^2,$$

where $|\psi_{\text{encoded}}\rangle$ represents the boundary state as encoded by discrete causal incorporations. Each internal measurement corresponds to a boundary-state update that is determinate externally but appears probabilistic internally.

The rotation of the parent horizon, characterized by its Kerr parameter $a = J/(Mc)$, further modulates these statistics by introducing an azimuthal phase gradient across the holographic code. This gradient slightly biases the causal incorporation of co-rotating versus counter-rotating quanta, embedding parity and chirality preferences in the apparent internal randomness. Consequently, while local outcomes remain probabilistic, their global distribution inherits the rotational memory of the parent horizon, manifesting in large-scale anisotropies and matter–antimatter asymmetry.

If the holographic hierarchy is finite, its highest level, the ultimate parent horizon, constitutes a closed causal network containing all information. At that level, no hidden surfaces remain and all causal relationships are internally complete. The ultimate horizon is therefore fully deterministic: a null-ordered informational substrate from which all emergent spacetimes and their apparent quantum probabilities arise as coarse projections. In this view, the deepest layer of physical reality is not indeterminate but perfectly ordered, and the quantum randomness observed within our universe is a perspectival consequence of our position inside the holographic hierarchy.

5.13 Multiverse Prospects and Holographic Hierarchies

As the event horizon forms during gravitational collapse, the interior of the black hole becomes causally separated from the external universe and begins to evolve according to null-surface dynamics. In this model, the entire internal cosmology is holographically encoded on the growing event horizon, structured as a temporally ordered sequence of null layers. Each infalling quantum is incorporated at the Planck scale, and the resulting horizon code defines the initial conditions of a new, inflating universe. The classical singularity is replaced by a causal and informational origin: a boundary from which an emergent spacetime unfolds.

The parent universe may contain a vast population of such black holes, primordial, astrophysical, or otherwise, each creating its own internal universe. Every black hole thus serves as a node in a generative cosmic hierarchy, with observable quantities in any universe reflecting the specific accretion history and horizon-layer structure of its ancestor. The resulting architecture constitutes a recursively nested multiverse, where each generation inherits its initial conditions from the causal encoding of the previous one.

This scenario resonates with earlier proposals for multiverses and baby universes [64, 73], reinterpreting black holes as cosmological generators, nodes in a recursive holographic hierarchy. The evolution of each child universe depends entirely on the microscopic degrees of freedom encoded on the parent horizon. According to the no-hair theorem, a classical black hole is externally characterized by only three parameters: mass, electric charge, and angular momentum [22]. All other internal information is causally inaccessible, yet holographically encoded in the parent horizon.

In this framework, the full causal structure, including the emergent spacetime of the child universe, is encoded in the quantum correlations of Planck-scale horizon cells. These cells form the primitive substrate of spacetime itself: each represents a discrete causal unit whose connections to neighboring cells may be complete, partial, or absent. Complete connections yield smooth causal propagation and define the continuum geometry; partial or missing links reduce local causal capacity, producing curvature and gravitational mass. In this sense, spacetime is an emergent network of correlations, not a preexisting manifold. The horizon acts as a dynamically evolving causal lattice operating at the Planck power limit $P_{\max} = c^5/G$, continually reorganizing its correlations to preserve global consistency.

The horizon thus enforces a strengthened form of cosmic censorship: it is not a physical barrier hiding a singularity, but a terminal surface beyond which classical geometry ceases and quantum correlation order dominates. No observer within the internal universe can access or probe this outer boundary, because the emergent spacetime itself is generated from its causal encoding. The Bekenstein–Hawking entropy of the parent horizon limits the number and diversity of possible descendants [13].

Although each black hole may create a new universe, the total number of offspring is finite, bounded by the entropy budget of the parent. Recursive encoding is allowed, but each level's entropy imposes a strict upper bound on productive generations [64]. This results in a finite, causally disjoint multiverse: a hierarchy of universes generated through successive gravitational collapses.

A further implication is that the present multiverse architecture, in which universes obey similar physical laws, may be the outcome of an evolutionary selection process. Earlier lineages that failed to achieve causal or entropic coherence would have produced infertile or short-lived offspring. Stable lineages, those able to sustain self-consistent horizon layering and reproduce black holes, naturally dominate. This concept parallels Smolin's cosmological natural selection [64], here reinterpreted in holographic terms: universes evolve toward optimal causal encoding efficiency.

In this model, our observed universe originates as the emergent interior projected from a boundary code located just above the parent horizon. The apparent spacetime volume does not coexist with that boundary in the same geometric domain; rather, the boundary itself belongs to a higher-order spacetime that remains causally inaccessible from within. The event horizon is therefore not a surface embedded in our universe, but a generator of it, an outer null layer defining the causal order of the emergent interior.

Ultimately, everything is correlation. What appears as matter, fields, or geometry is a manifestation of the evolving pattern of causal connectivity among horizon cells. The physical world is not embedded in spacetime but arises from the ordering and reordering of information on lower-dimensional holographic boundaries. The multiverse thus becomes not a collection of disconnected domains, but a recursive hierarchy of projected correlation structures, each emerging from and limited by the informational capacity of its predecessor. In this view, dimension, mass, and curvature are not fundamental entities but emergent properties of a deeper, dimensionless network of causal relations.

The holographic hierarchy also provides a natural origin for the arrow of time. Each new horizon layer records an irreversible causal update, increasing total entropy and establishing a directed sequence of informational incorporations. Because every descendant universe inherits its causal order from the layering of its parent, the temporal asymmetry is recursively transmitted through the multiverse hierarchy. The arrow of time is therefore not an imposed boundary condition but an inherited property of the holographic process itself, the universal memory of causal order embedded in the structure of horizons.

6 Conclusion

This paper has introduced a new paradigm in which gravitational collapse is reinterpreted as a process of cosmogenesis. Taking the external observer's frame as physically definitive, the event horizon is no longer a passive boundary to be crossed but an active, information-rich surface that encodes infalling matter into null-ordered, redshift-frozen strata. These horizon layers form a self-updating holographic code obeying the universal relation $R = 2M$, in which each incorporation event drives internal inflation, structure formation, and quantum state selection. Within this framework, the internal age of the emergent universe is determined by the cumulative mass encoded on the horizon, yielding approximately 13.4 billion years, consistent with observation. The model further predicts that the observable Hubble patch constitutes roughly 50% of the total internal mass, resolving the Hubble tension and reproducing

cosmic acceleration without invoking an external dark-energy term. Expansion arises instead from geometric horizon-layering dynamics, linking cosmic growth directly to the causal encoding rate of new Planck-scale cells.

The holographic membrane model developed here replaces the unphysical singularity of classical general relativity with a finite, null-ordered boundary that preserves causal structure and unitarity. In this view, the interior of a black hole does not contain diverging curvature or undefined spacetime, but is instead replaced by a self-consistent termination of geometry maintained by the external manifold. Curvature reflects the elastic response of spacetime to causal excision, and gravity emerges as the tension field surrounding the absence of geometry itself. This finite, dynamically maintained horizon removes the singularity without violating known physical principles, providing a continuous bridge from external spacetime to the holographic boundary and, by extension, to the internal cosmological domain it encodes.

When the parent black hole possesses angular momentum, its Kerr rotation induces a global azimuthal phase gradient across the horizon code. This rotation establishes a coherent spin field that imprints a causal anisotropy into the encoded layers, linking microscopic spin quantization with macroscopic cosmological asymmetry. Frame dragging biases co-rotating and counter-rotating quanta, producing a small but cumulative matter–antimatter asymmetry and defining a preferred cosmic axis preserved through inflation. The binary spin structure of the Planck-scale horizon quanta provides a geometric origin for fermionic spin-$\frac{1}{2}$ behavior and the Pauli exclusion principle, while the global SU(2) phase winding of the rotating horizon naturally accounts for the observed alignments of CMB multipoles and galactic spin directions. Thus, baryon asymmetry, spin quantization, and cosmic anisotropy emerge as unified consequences of a single holographic–causal mechanism operating on the rotating horizon.

From a broader theoretical perspective, this framework extends general relativity and holography into a new physical regime where time dilation, quantum coherence, and horizon thermodynamics jointly govern causal evolution. The horizon acts as a stationary yet self-reconfiguring causal lattice: new Planck cells are incorporated radially through global relational updates, while lateral communication among existing cells, mediated by null-compatible tunnelling, supports radiation, interaction, and gravitational clustering. Together, these two channels of causal propagation reproduce the dual behavior of our universe: relational expansion between distant regions and coherent communication within gravitationally bound systems. Even the speed of light c emerges as the invariant ratio between spatial separation and temporal reconfiguration within this stationary causal substrate. In this sense, spacetime dynamics, motion, and cosmic expansion all arise from successive updates of a fundamentally still holographic code.

The same mechanism naturally resolves the vacuum catastrophe. Because only boundary-encoded degrees of freedom gravitate, the effective vacuum energy density is finite and scales with r_s^{-2}, consistent with the observed value $\rho_{\mathrm{vac}} \approx 6 \times 10^{-27}\,\mathrm{kg\,m^{-3}}$ for $\kappa \sim 7$. Vacuum energy thus represents residual curvature associated with limited redundancy in the horizon code, dynamically diluted as new Planck cells are

added. Cosmic acceleration becomes the geometric response to expanding holographic capacity, not an intrinsic property of empty space.

While the conventional singularity-based paradigm remains mathematically consistent within general relativity, the horizon-layered cosmology offers a deeper geometric and informational rationale. It preserves all verified external predictions, gravitational waves, inspiral dynamics, and black-hole thermodynamics, yet replaces the unobservable singular interior with a physically defined causal boundary. Observable consequences such as spin-induced anisotropies, horizon coherence effects, and holographic regulation of vacuum energy provide potential empirical tests that could distinguish this framework from ΛCDM and other semiclassical models.

Although the present formulation is primarily conceptual, it establishes a coherent foundation for future quantitative work. Subsequent developments should incorporate more realistic collapse geometries, anisotropic spin distributions, and explicit simulations of null-layer encoding to evaluate the robustness of the holographic dynamics and its phenomenological signatures. Nevertheless, the central proposition, that black holes holographically encode emergent universes through causally ordered, redshift-frozen surface structures, offers a unified, testable, and profoundly geometric bridge between quantum information, gravity, and cosmology. **In this view, the universe itself is not a spacetime continuum filled with moving matter, but the evolving relational pattern of a still holographic horizon, whose successive causal incorporations generate the very fabric of reality.**

References

[1] Hooft, G.: Dimensional reduction in quantum gravity. arXiv preprint gr-qc/9310026 (1993)

[2] Susskind, L.: The world as a hologram. Journal of Mathematical Physics **36**(11), 6377–6396 (1995)

[3] Maldacena, J.M.: The large n limit of superconformal field theories and supergravity. Advances in Theoretical and Mathematical Physics **2**, 231–252 (1998) https://doi.org/10.4310/ATMP.1998.v2.n2.a1 hep-th/9711200

[4] Thorne, K.S., Price, R.H., Macdonald, D.A.: Black Holes: The Membrane Paradigm. Yale University Press, New Haven (1986)

[5] Hayden, P., Preskill, J.: Black holes as mirrors: Quantum information in random subsystems. Journal of High Energy Physics **09**, 120 (2007) https://doi.org/10.1088/1126-6708/2007/09/120 arXiv:0708.4025 [hep-th]

[6] Almheiri, A., Marolf, D., Polchinski, J., Sully, J.: Black holes: complementarity or firewalls? Journal of High Energy Physics **2013**(2), 62 (2013) https://doi.org/10.1007/JHEP02(2013)062 arXiv:1207.3123 [hep-th]

[7] Almheiri, A., Mahajan, R., Maldacena, J., Zhao, Y.: The page curve of hawking radiation from semiclassical geometry. Journal of High Energy Physics **2020**(3), 149 (2020) https://doi.org/10.1007/JHEP03(2020)149

[8] Schwarzschild, K.: On the gravitational field of a mass point according to einstein's theory. arXiv preprint physics/9905030 (1999)

[9] Schutz, B.: A First Course in General Relativity, pp. 317–322. Cambridge university press, Cambridge (2022)

[10] Hafele, J.C., Keating, R.E.: Around-the-world atomic clocks: Observed relativistic time gains. Science **177**(4044), 168–170 (1972)

[11] Ashby, N.: Relativity in the global positioning system. Living Reviews in relativity **6**(1), 1–42 (2003)

[12] Chou, C.-w., Hume, D., Koelemeij, J., Wineland, D.J., Rosenband, T.: Frequency comparison of two high-accuracy al+ optical clocks. Physical review letters **104**(7), 070802 (2010)

[13] Bekenstein, J.D.: Black holes and entropy. Physical Review D **7**(8), 2333 (1973)

[14] Hawking, S.W.: Particle creation by black holes. Communications in mathematical physics **43**(3), 199–220 (1975)

[15] Sperhake, U.: General Relativity 2: Lecture Notes. University of Cambridge. https://www.damtp.cam.ac.uk/user/us248/Lectures/Notes/grII.pdf (2016)

[16] Carroll, S.M.: An introduction to general relativity: spacetime and geometry. Addison Wesley **101**, 102 (2004)

[17] Aristotle: Physics

[18] Barceló, C., Liberati, S., Visser, M.: Horizon thermodynamics and emergent gravity. International Journal of Modern Physics D **20**(08), 1667–1676 (2011) https://doi.org/10.1142/S0218271811019341 arXiv:0909.4157 [gr-qc]

[19] Mazur, P.O., Mottola, E.: Gravitational vacuum condensate stars. Proceedings of the National Academy of Sciences **101**(26), 9545–9550 (2004) https://doi.org/10.1073/pnas.0402717101 arXiv:gr-qc/0407075

[20] Ashtekar, A., Bojowald, M.: Black hole evaporation: A paradigm. Classical and Quantum Gravity **22**(16), 3349–3362 (2005) https://doi.org/10.1088/0264-9381/22/16/014 arXiv:gr-qc/0504029

[21] Hajicek, P., Kiefer, C.: Singularity avoidance by collapsing shells in quantum gravity. International Journal of Modern Physics D **10**(06), 775–779 (2001) https://doi.org/10.1142/S0218271801001118 arXiv:gr-qc/0107102

[22] Misner, C.W., Thorne, K.S., Wheeler, J.A.: Gravitation. Macmillan, San Francisco (1973)

[23] O'Connor, E., Ott, C.D.: Black hole formation in failing core-collapse supernovae. The Astrophysical Journal **730**(2), 70 (2011)

[24] Shapiro, S.L., Teukolsky, S.A.: Black Holes, White Dwarfs and Neutron Stars: the Physics of Compact Objects. John Wiley & Sons, New York (2024)

[25] Woosley, S., Wilson, J., Mathews, G., Hoffman, R., Meyer, B.: The r-process and neutrino-heated supernova ejecta. Astrophysical Journal, Part 1 (ISSN 0004-637X), vol. 433, no. 1, p. 229-246 **433**, 229–246 (1994)

[26] Hawking, S.W., Ellis, G.F.: The Large Scale Structure of Space-time. Cambridge university press, Cambridge, New York, Melbourne (2023)

[27] Rovelli, C., Vidotto, F.: Planck stars, white holes, remnants and planck-mass quasi-particles. the quantum gravity phase in black holes' evolution and its manifestations. arXiv preprint arXiv:2407.09584 (2024)

[28] Ashtekar, A., Bojowald, M.: Quantum nature of the schwarzschild singularity. Classical and Quantum Gravity **23**(2), 391–411 (2005)

[29] Ashtekar, A., Pawlowski, T., Singh, P.: Quantum nature of the big bang. Physical Review Letters **96**(14), 141301 (2006)

[30] Ashtekar, A.: Quantum geometry in action: Big bang and black holes. In: Proceedings of the 11th Marcel Grossmann Meeting, p. (2008). arXiv:0812.0177

[31] Bojowald, M.: Absence of a singularity in loop quantum cosmology. Physical Review Letters **86**(23), 5227 (2001)

[32] Mazur, P.O., Mottola, E.: Gravitational vacuum condensate stars. Proceedings of the National Academy of Sciences **101**(26), 9545–9550 (2004)

[33] Mathur, S.D.: The fuzzball proposal for black holes: An elementary review. Fortschritte der Physik **53**(7-8), 793–827 (2005) https://doi.org/10.1002/prop.200410203

[34] Bousso, R.: A covariant entropy conjecture. Journal of High Energy Physics **1999**(07), 004 (1999)

[35] Sorkin, R.D.: Causal sets: Discrete gravity (notes for the valdivia summer school). In: Gomberoff, A., Marolf, D. (eds.) Lectures on Quantum Gravity, pp. 305–327. Springer, , (2005)

[36] Blandford, R.D., Znajek, R.L.: Electromagnetic extraction of energy from kerr black holes. Monthly Notices of the Royal Astronomical Society **179**, 433–456

(1977) https://doi.org/10.1093/mnras/179.3.433

[37] McKinney, J.C.: General relativistic magnetohydrodynamic simulations of the jet formation and large-scale propagation from black hole accretion systems. Monthly Notices of the Royal Astronomical Society **368**, 1561–1582 (2006) https://doi.org/10.1111/j.1365-2966.2006.10256.x

[38] Komissarov, S.S.: Observations and theory of relativistic jets. Monthly Notices of the Royal Astronomical Society **359**, 801–818 (2005) https://doi.org/10.1111/j.1365-2966.2005.08974.x

[39] Zurek, W.H.: Decoherence and the transition from quantum to classical. Physics today **44**(10), 36–44 (1991)

[40] Rovelli, C.: Relational quantum mechanics. International journal of theoretical physics **35**, 1637–1678 (1996)

[41] Wolfram, S.: A class of models with the potential to represent fundamental physics. Complex Systems **29**(2), 107–536 (2020)

[42] Wolfram, S., Gorard, J.: Causal graphs and the emergence of spacetime. Complex Systems **30**(1), 1–76 (2021)

[43] Sullivan, R.M., Scott, D.: The cmb dipole: Eppur si muove. In: The Sixteenth Marcel Grossmann Meeting on Recent Developments in Theoretical and Experimental General Relativity, Astrophysics and Relativistic Field Theories: Proceedings of the MG16 Meeting on General Relativity; 5–10 July 2021, pp. 1532–1541 (2023). World Scientific

[44] Guth, A.H.: Inflationary universe: A possible solution to the horizon and flatness problems. Physical Review D **23**(2), 347–356 (1981) https://doi.org/10.1103/PhysRevD.23.347

[45] Linde, A.D.: A new inflationary universe scenario: A possible solution of the horizon, flatness, homogeneity, isotropy and primordial monopole problems. Physics Letters B **108**(6), 389–393 (1982) https://doi.org/10.1016/0370-2693(82)91219-9

[46] Riess, A.G., Yuan, W., Macri, L.M., Scolnic, D., Brout, D., Casertano, S., Jones, D.O., Murakami, Y., Peterson, R., Polin, A., *et al.*: A comprehensive measurement of the local value of the hubble constant with 1 km/s/mpc uncertainty from the hubble space telescope and the sh0es team. The Astrophysical Journal Letters **934**(1), 7 (2022) https://doi.org/10.3847/2041-8213/ac5c5b

[47] Collaboration, P., Aghanim, N., Akrami, Y., Ashdown, M., Aumont, J., Baccigalupi, C., Ballardini, M., Banday, A., Barreiro, R., Bartolo, N., *et al.*: Planck 2018 results. vi. cosmological parameters. Astronomy & Astrophysics **641**, 6

(2020) https://doi.org/10.1051/0004-6361/201833910

[48] Boylan-Kolchin, M.: Stress testing λ cdm with high-redshift galaxy candidates. Nature Astronomy **7**(6), 731–735 (2023)

[49] Author(s): MoM-z14 Dataset: High-Redshift Cosmological Modeling. Manuscript or Dataset. Redshift value $z = 14.44$ used in revised CMB interpretation (2025). https://example.org/momz14

[50] Gibbons, G.W., Hawking, S.W.: Cosmological event horizons, thermodynamics, and particle creation. Physical Review D **15**(10), 2738–2751 (1977)

[51] Padmanabhan, T.: Thermodynamical aspects of gravity: new insights. Reports on Progress in Physics **73**(4), 046901 (2010)

[52] Padmanabhan, T.: The atoms of spacetime and the cosmological constant. In: Journal of Physics: Conference Series, vol. 880, p. 012008 (2017)

[53] Verlinde, E.: On the origin of gravity and the laws of newton. Journal of High Energy Physics **2011**(4), 1–27 (2011)

[54] Li, M.: A model of holographic dark energy. Physics Letters B **603**(1-2), 1–5 (2004)

[55] Croker, K.S., Weiner, J.: Cosmologically coupled compact objects (2019). Preprint

[56] Farrah, D., al.: Observational evidence for cosmological coupling of black holes and its implications for an astrophysical source of dark energy. The Astrophysical Journal Letters **944**, 31 (2023) arXiv:2302.07878

[57] Croker, K.S., al.: Implications of cosmologically coupled black holes for pulsar timing arrays. Scientific Reports **14**, 31296 (2024)

[58] Gilfanov, M., Bogdán, Á.: An upper limit on the accretion rates of white dwarfs before type ia supernovae. Nature **463**, 924–925 (2010) https://doi.org/10.1038/nature08878

[59] Schaefer, B.E., Pagnotta, A.: An absence of ex-companion stars in the type ia supernova remnant snr 0509–67.5. Nature **481**, 164–166 (2012) https://doi.org/10.1038/nature10705

[60] Coleman, S., De Luccia, F.: Fate of the false vacuum: Semiclassical theory. Physical Review D **21**(12), 3305–3315 (1980)

[61] Guth, A.H.: Inflationary universe: A possible solution to the horizon and flatness problems. Physical Review D **23**(2), 347–356 (1981)

[62] Almheiri, A., Mahajan, R., Maldacena, J., Zhao, Y.: The entropy of bulk quantum fields and the entanglement wedge of an evaporating black hole. Journal of High Energy Physics **2020**(3), 149 (2020)

[63] Papadodimas, K., Raju, S.: Infalling observers and black hole complementarity. Journal of High Energy Physics **2014**(10), 1–35 (2014)

[64] Smolin, L.: The Life of the Cosmos. Oxford University Press, New York - Oxford (1997)

[65] Longo, M.J.: Detection of a dipole in the handedness of spiral galaxies with redshifts $z \sim 0.04$. Physics Letters B **699**(4), 224–229 (2011) https://doi.org/10.1016/j.physletb.2011.04.008

[66] Shamir, L.: Asymmetry between galaxies with clockwise and counterclockwise spin directions: A possible signature of large-scale structure. The Astrophysical Journal Supplement Series **250**(1), 1 (2020) https://doi.org/10.3847/1538-4365/aba4a5

[67] Shamir, L.: Evidence of large-scale spin alignment in galaxies. Mon. Not. R. Astron. Soc. **522**, 2450–2464 (2023)

[68] Shamir, L.: Spin asymmetry in high-redshift galaxies observed by jwst. Preprint (2024) arXiv:2403.17271

[69] Copi, C.J., Huterer, D., Schwarz, D.J., Starkman, G.D.: Large-scale alignments from wmap and planck. Advances in Astronomy **2010**, 847541 (2010) https://doi.org/10.1155/2010/847541

[70] Collaboration, P.: Planck 2018 results: Isotropy and statistics of the cmb. Astron. Astrophys. **641**, 7 (2020)

[71] Reynolds, C.S.: Observational constraints on black hole spin. Ann. Rev. Astron. Astrophys. **57**, 445–487 (2019)

[72] Avara, M.J., McKinney, J.C.: Magnetically arrested accretion and the evolution of black hole spin. Astrophys. J. **893**, 16 (2020)

[73] Frolov, V., Novikov, I.: Black Hole Physics: Basic Concepts and New Developments vol. 96. Springer, Dordrecht (2012)